

Highly oxygenated organic molecules (HOM) formation in the isoprene oxidation by NO₃ radical

Defeng Zhao^{1, 2, 3}, Iida Pullinen^{2, a}, Hendrik Fuchs², Stephanie Schrade², Rongrong Wu², Ismail-Hakki Acir^{2, b}, Ralf Tillmann², Franz Rohrer², Jürgen Wildt², Yindong Guo¹, Astrid Kiendler-Scharr², Andreas Wahner², Sungah Kang², Luc Vereecken², Thomas F. Mentel²

¹Department of Atmospheric and Oceanic Sciences & Institute of Atmospheric Sciences, Fudan University, Shanghai, 200438, China;

²Institute of Energy and Climate Research, IEK-8: Troposphere, Forschungszentrum Jülich, 52425, Jülich, Germany

³Big Data Institute for Carbon Emission and Environmental Pollution, Fudan University, Shanghai, 200438, China

^aNow at: Department of Applied Physics, University of Eastern Finland, Kuopio, 7021, Finland.

^bNow at: Institute of Nutrition and Food Sciences, University of Bonn, Bonn, 53115, Germany;

Correspondence to: Thomas F. Mentel (t.mentel@fz-juelich.de), Defeng Zhao (dfzhao@fudan.edu.cn)

Abstract

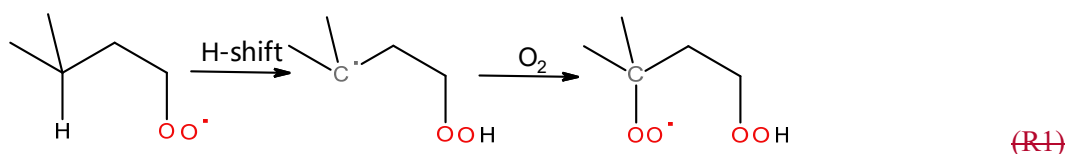
Highly oxygenated organic molecules (HOM) are found to play an important role in the formation and growth of secondary organic aerosol (SOA). SOA is an important type of aerosol with significant impact on air quality and climate. Compared with the oxidation of volatile organic compounds by O₃ and OH, HOM formation in the oxidation by NO₃ radical, an important oxidant at night-time and dawn, has received less attention. In this study, HOM formation in the reaction of isoprene with NO₃ was investigated in the SAPHIR chamber (Simulation of Atmospheric PHotochemistry In a large Reaction chamber). A large number of HOM including monomers (C₅), dimers (C₁₀), and trimers (C₁₅), both closed-shell compounds and open-shell peroxy radicals, were identified and were classified into various series according to their formula. Their formation pathways were proposed based on the peroxy radicals observed and known mechanisms in the literature, which were further constrained by the time profiles of HOM after sequential isoprene addition to differentiate first- and second-generation products. HOM monomers containing one to three N atoms (1-3N monomers) were formed, starting with NO₃ addition to carbon double bond, forming peroxy radicals (RO₂), followed by autoxidation. 1N monomers were formed by both the direct reaction of NO₃ with isoprene and of NO₃ with first-generation products. 2N-monomers (e.g. C₅H₈N₂O_n (n=7-13), C₅H₁₀N₂O_n (n=8-14)) were likely the termination products of C₅H₉N₂O_n•, which was formed by the addition of NO₃ to C₅-hydroxynitrate (C₅H₉NO₄), a first-generation product containing one carbon double bond. 2N-monomers, which were second-generation products, dominated in monomers and accounted for ~34% of all HOM, indicating the important role of second-generation oxidation in HOM formation in the isoprene+NO₃ reaction under our reaction experimental conditions. H-shift of alkoxy radicals to form peroxy radicals and subsequent autoxidation (“alkoxy-peroxy” pathway) was found to be an important pathway of HOM formation. HOM dimers were mostly formed by the accretion reaction of various HOM monomer RO₂ and via the termination reactions of dimer RO₂ formed by further reaction of closed-shell dimers with NO₃ and possibly by the reaction of C₅-RO₂ with isoprene. HOM trimers were likely formed by the accretion reaction of dimer RO₂ with monomer RO₂. The concentrations of different HOM showed distinct time profiles during the reaction, which was linked to their formation pathway. HOM concentrations either showed a typical time profile of first-generation products, or of second-generation products, or a combination of both, indicating multiple formation pathways and/or multiple isomers. Total HOM molar yield was estimated to be 1.2%^{+1.3%}_{-0.7%}, which corresponded to a SOA yield of ~3.6% assuming the molecular weight of C₅H₉NO₆ as the lower limit.

40 This yield suggests that HOM may contribute a significant fraction to SOA yield in the reaction of isoprene with
41 NO_3 .

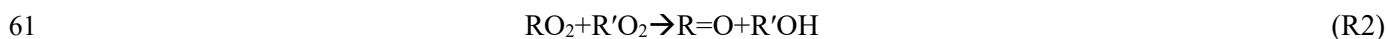
42 1 Introduction

43 Highly oxygenated organic molecules (HOM) are an important class of compounds formed in the oxidation
44 of volatile of organic compounds (VOC) including biogenic VOC (BVOC) and anthropogenic VOC (Crouse
45 et al., 2013; Ehn et al., 2014; Jokinen et al., 2014; Rissanen et al., 2014; Jokinen et al., 2015; Krechmer et al.,
46 2015; Mentel et al., 2015; Rissanen et al., 2015; Kenseth et al., 2018; Molteni et al., 2018; Garmash et al., 2019;
47 McFiggans et al., 2019; Molteni et al., 2019; Quelever et al., 2019). A number of recent studies have
48 demonstrated that HOM play a pivotal role in both nucleation and also particle growth of pre-existing particles,
49 thus contributing to growth of secondary organic aerosol (SOA) (Ehn et al., 2014; Kirkby et al., 2016; Tröstl et
50 al., 2016). Particularly, in the early stage of aerosol growth, HOM may contribute a significant fraction of SOA
51 mass (Tröstl et al., 2016).

52 HOM are formed by the autoxidation of peroxy radicals (RO₂), which means they undergo intraermolecular
53 H-shift forming alky radicals, followed by O₂ addition leading to formation of new RO₂ as shown in R1 below
54 (Vereecken et al., 2007; Crouse et al., 2013; Ehn et al., 2017; Bianchi et al., 2019; Møller et al., 2019; Nozière
55 and Vereecken, 2019; Vereecken and Nozière, 2020).



57 Besides autoxidation, the RO₂ can also react with HO₂, RO₂ and NO₃, either forming a series of termination
58 products (R1-3), including organic hydroxyperoxide, alcohol, and carbonyl, or forming alkoxy radicals (RO,
59 R4-5) via the following reactions.



66 The termination products are detected in the mass spectra at masses M+1, M-15, M-17 respectively with
67 M being the molecular mass of the parent RO₂ (Ehn et al., 2014; Mentel et al., 2015). In case that RO₂ is an acyl
68 peroxy radical, percarboxylic acids and carboxylic acids are formed instead of hydroperoxides and alcohols in
69 R3 and R1, respectively (Atkinson et al., 2006; Mentel et al., 2015). RO₂ can also form HOM dimers by the
70 accretion reaction of two RO₂ (R6) (Berndt et al., 2018a; Berndt et al., 2018b; Valiev et al., 2019). Additionally,
71 HOM can be formed via H-shift in RO followed by O₂ addition (referred to as “alkoxy-proxy” pathway)
72 (Finlayson-Pitts and Pitts, 2000; Vereecken and Peeters, 2010; Vereecken and Francisco, 2012; Mentel et al.,
73 2015). These pathways are summarized in a recent comprehensive review (Bianchi et al., 2019), which also
74 further clarifies HOM definition.

75 Currently, most laboratory studies of HOM formation focus on the VOC oxidation by OH and O₃ (Crouse
76 et al., 2013; Ehn et al., 2014; Jokinen et al., 2014; Rissanen et al., 2014; Jokinen et al., 2015; Krechmer et al.,
77 2015; Mentel et al., 2015; Rissanen et al., 2015; Kirkby et al., 2016; Tröstl et al., 2016; Kenseth et al., 2018;
78 Molteni et al., 2018; Garmash et al., 2019; McFiggans et al., 2019; Molteni et al., 2019; Quelever et al., 2019;
79 Wang et al., 2020; Yan et al., 2020). HOM formation in the oxidation of VOC with NO₃ has received much less
80 attention. NO₃ is another important oxidant of VOC mainly operating during nighttime. Particularly, NO₃ has
81 high reactivity with unsaturated BVOC such as monoterpene and isoprene. It is often the dominant oxidant of
82 these compounds at night, especially in regions where biogenic and anthropogenic emissions mix (Geyer et al.,
83 2001; Brown et al., 2009; Brown et al., 2011). The reaction products contribute to SOA formation (Xu et al.,
84 2015; Lee et al., 2016). Also, the organic nitrates produced in these reactions play an important role in nitrogen
85 chemistry by altering NO_x concentration, which further influences photochemical recycling and ozone
86 formation in the next day. Among these reaction products, HOM ~~may can~~ also be formed (Xu et al., 2015; Lee
87 et al., 2016; Yan et al., 2016). Despite the potential importance, studies of HOM formation in the oxidation of
88 BVOC by NO₃ are still limited compared with the HOM formation via oxidation by O₃ and OH. Although a
89 number of laboratory studies have investigated the reaction of NO₃ with BVOC (Ng et al., 2008; Fry et al., 2009;
90 Rollins et al., 2009; Fry et al., 2011; Kwan et al., 2012; Fry et al., 2014; Boyd et al., 2015; Schwantes et al.,
91 2015; Nah et al., 2016; Boyd et al., 2017; Clafin and Ziemann, 2018; Faxon et al., 2018; Draper et al., 2019;
92 Takeuchi and Ng, 2019; Novelli et al., 2021; Vereecken et al., 2021), these studies mostly focus on either SOA
93 yield and composition, or on the gas-phase chemistry mechanism mainly for “traditional” oxidation products
94 that stem from few oxidation steps.

95 Importantly, HOM formation in the reaction of NO₃ with isoprene, the most abundant BVOC accounting
96 for more than half of the global BVOC emissions, has not been explicitly addressed yet, to the best of our
97 knowledge. Although isoprene from plants are mainly emitted under light conditions, i.e., in the daytime, ~~and~~
98 ~~its chemical lifetime with respect to its reaction with OH is typically only a few hours, its concentration isoprene~~
99 ~~can remain high after sunset in significant concentrations (Starn et al., 1998; Stroud et al., 2002; Brown et al., 2009)~~
100 ~~because of the reduced consumption by OH and is found to decay rapidly~~. A substantial fraction of isoprene can
101 then be oxidized by NO₃ (Brown et al., 2009). Regarding the budget of NO₃, ~~the reaction of isoprene with NO₃~~
102 ~~can contribute to a significant or even dominant fraction of NO₃ loss at night in regions where VOC is dominated by~~
103 ~~isoprene such as Northeast US (Brown et al., 2009). Under some circumstances, the reaction of isoprene with NO₃~~
104 ~~can contribute to a significant fraction during the afternoon and afterwards (Ayres et al., 2015; Hamilton et al.,~~
105 ~~2021) the reaction of isoprene with NO₃ contributes to a significant fraction of NO₃ loss at night, and in some~~
106 ~~circumstances even during the day, especially in the afternoon and afterwards (Ayres et al., 2015)~~. The reaction
107 of isoprene with NO₃ is the subject of a number of studies (Ng et al., 2008; Perring et al., 2009; Rollins et al.,
108 2009; Kwan et al., 2012; Schwantes et al., 2015; Vereecken et al., 2021). These studies focus on the oxidation
109 mechanism and “traditional” oxidation products, as well as SOA yields. The initial step is the NO₃ addition to
110 one of the C=C double bonds, preferentially to the carbon C1 (Schwantes et al., 2015), followed by O₂ addition
111 forming a nitrooxyalkyl peroxy radical (RO₂). This RO₂ can undergo the reactions described above, forming a

112 series of products such as C5-nitrooxyhydroperoxide, C5-nitrooxycarbonyl, and C5-hydroxynitrate (Ng et al.,
113 2008; Kwan et al., 2012), as well as methyl vinyl ketone (MVK), potentially methacrolein (MACR),
114 formaldehyde, OH radical, and NO₂ as minor products (Schwantes et al., 2015). A high nitrate yield (57-95%)
115 was found (Perring et al., 2009; Rollins et al., 2009; Kwan et al., 2012; Schwantes et al., 2015). Products in the
116 particle phase such as C₁₀ dimers were also detected (Ng et al., 2008; Kwan et al., 2012; Schwantes et al., 2015).
117 The SOA yield varies from 2% to 23.8% depending on the organic aerosol concentration (Ng et al., 2008;
118 Rollins et al., 2009). These studies have provided valuable insights in oxidation mechanism, particle yield and
119 composition. However, because HOM formation was not the focus of these studies, only a limited number of
120 products, mainly moderately oxygenated ones (oxygen number ≤ 2 in addition to NO₃ functional groups), were
121 detected in the gas phase. The detailed mechanism of HOM formation and their yields in the reaction of
122 BVOC+NO₃ are still unclear.

123 In this study, we investigated the HOM formation in the oxidation of isoprene by NO₃. We report the
124 identification of HOM, including HOM monomers, dimers, and trimers. According to the reaction products and
125 literature, we discuss the formation mechanism of these HOM. The formation mechanism of various HOM is
126 further constrained with time series of HOM upon repeated isoprene additions. We also provide an estimate of
127 HOM yield in the isoprene+NO₃-reaction and assess their roles in SOA formation.

128 2 Experimental

129 2.1 Chamber setup and experiments

130 Experiments investigating the reaction of isoprene with NO₃ were conducted in the SAPHIR chamber
131 (Simulation of Atmospheric PHotochemistry In a large Reaction chamber) at Forschungszentrum Jülich,
132 Germany. The details of the chamber have been described before (Rohrer et al., 2005; Zhao et al., 2015a; Zhao
133 et al., 2015b; Zhao et al., 2018). Briefly, SAPHIR is a Teflon chamber with a volume of 270 m³. It can utilize
134 natural sunlight for illumination and is equipped with a louvre system to switch between light and dark
135 conditions. In this study, the experiments were conducted in the dark with the louvres closed.

136 Temperature and relative humidity were continuously measured. Gas and particle phase species were
137 characterized using a comprehensive set of instruments with the details described before (Zhao et al., 2015b).
138 VOC were characterized using a Proton Transfer Reaction Time-of-Flight Mass Spectrometer (PTR-ToF-MS,
139 Ionicon Analytik, Austria). NO_x and O₃ concentrations were measured using a chemiluminescence NO_x analyzer
140 (ECO PHYSICS TR480) and an UV photometer O₃ analyzer (ANSYCO, model O341M), respectively. OH,
141 HO₂ and RO₂ concentrations were measured using a laser induced fluorescence system (LIF) (Fuchs et al., 2012).
142 NO₃ and N₂O₅ were detected by a custom-built instrument based on cavity ring-down spectroscopy. The design
143 of the instrument is similar to that described by Wagner et al. (2011). NO₃ was directly detected in one cavity
144 by its absorption at 662 nm and the sum of NO₃ and N₂O₅ in a second, heated cavity, which had a heated inlet
145 to thermally decompose N₂O₅ to NO₃. The sampling flow rate was 3 to 4 liters per minute. The detection by
146 cavity ring-down spectroscopy was achieved by a diode laser that was periodically switched on and off with a

147 repetition rate of 200 Hz. Ring-down events were observed by a digital oscilloscope PC card during the time
148 when the laser was switched off and were averaged over 1s. The zero-decay time that is needed to calculate the
149 concentration of NO₃ was measured every 20 s by chemically removing NO₃ in the reaction with excess nitric
150 oxide (NO) in the inlet system. The accuracy of measurements was limited by the uncertainty in the correction
151 for inlet losses of NO₃ and N₂O₅. In the case of N₂O₅ a transmission of (85±10) % was achieved and in the case
152 of NO₃ of (50±30) %.

153 Before an experiment, the chamber was flushed with high purity synthetic air (purity>99.9999% O₂ and N₂).
154 Experiments were conducted under dry condition (RH<2 %) and temperature was at 302±3 K. NO₂ and O₃ were
155 added to the chamber first to form N₂O₅ and NO₃, reaching concentrations of ~60 ppb for NO₂ and ~100 ppb for O₃.
156 After around half an hour, isoprene was sequentially added into the chamber for three times at intervals of ~1 h.
157 Around 40 min after the third isoprene injection, NO₂ was added to compensate the loss of NO₃ and N₂O₅. Afterwards,
158 three isoprene additions were repeated in the same way as before. O₃ was added before the fifth and the sixth isoprene
159 addition to compensate for its loss by reaction. The schematic for the experimental procedure is shown in Fig. S1.
160 Experiments were designed such that the chemical system was dominated by the reaction of isoprene with NO₃ and
161 the reaction of isoprene with O₃ did not play a major role (<3% of the isoprene consumption). Figure S2 shows the
162 relative contributions of the reaction of O₃ and NO₃ with isoprene to the total chemical loss of isoprene using the
163 NO₃ and O₃ concentrations measured. The reaction with NO₃ accounted for >95% of the isoprene consumption at all
164 time for the whole experiments. The contribution of the reaction of isoprene with trace amount of OH, mainly
165 produced in the reaction of isoprene+O₃ via Criegee intermediates (Nguyen et al., 2016), is negligible as the OH yield
166 is less than one (Malkin et al., 2010) and thus its contribution is less than that of isoprene+O₃. This is consistent with
167 the contribution determined using measured OH concentration, despite some uncertainty in measured OH
168 concentration due to the interference from NO₃. In these experiments, RO₂ fate is estimated to be dominated by its
169 reaction with NO₃ according to the measured NO₃, RO₂, and HO₂ concentration and their rate constants for the
170 reactions with RO₂ (MCM v3.2(Jenkin et al., 1997; Jenkin et al., 2003; Saunders et al., 2003; Jenkin et al., 2015), via
171 website: <http://mcm.leeds.ac.uk/MCM>) despite uncertainties of the measured RO₂ and HO₂ concentration due to
172 interference from NO₃. As a large portion of RO₂ is not measured by LIF (Vereecken et al., 2021) and thus RO₂ is
173 underestimated, we expected the reaction of RO₂+RO₂ to be also important. Overall, we estimate that the RO₂ fate is
174 dominated the reaction RO₂+NO₃ with significant contribution of RO₂+RO₂.
175

176 2.2 Characterization of HOM

177 In this study we refer to similar definition for HOM by Bianchi et al. (2019)-, i.e., HOM typically contain six or
178 more oxygen atoms formed via autoxidation and related chemistry of peroxy radicals.- HOM were detected using a
179 Chemical Ionization time-of-flight Mass Spectrometer (Aerodyne Research Inc., USA) with nitrate as the reagent ion
180 (CIMS) (Eisele and Tanner, 1993; Jokinen et al., 2012). ¹⁵N nitric acid was used to produce ¹⁵NO₃⁻ in order to
181 distinguish the NO₃ group in target molecules formed in the reaction from the reagent ion. The details of the
182 instrument are described in our previous publications (Ehn et al., 2014; Mentel et al., 2015; Pullinen et al., 2020).
183 The CIMS has a mass resolution of ~4000 (m/dm). Examples of peak fitting are shown in Fig. S3. HOM

184 concentrations were estimated using the calibration coefficient of H₂SO₄ as described by Pullinen et al. (2020)
185 because the charge efficiency of HOM and H₂SO₄ can be assumed to be equal and close to the collision limit (Ehn et
186 al., 2014; Pullinen et al., 2020). The details of the calibration with H₂SO₄ are provided in the supplement S1. Since
187 HOM contain more than six oxygen atoms and their clusters with nitrate ions are quite stable (Ehn et al., 2014), the
188 charge efficiency of HOM is thus assumed to be equal to that of H₂SO₄, which is close to the collision limit (Viggiano
189 et al., 1997). If HOM do not charge with nitrate ions at their collision limit or the clusters formed break during the
190 short residence time in the charger, its concentration would be underestimated as pointed by Ehn et al. (2014). Thus,
191 our assumption provides a lower limit of the HOM concentration. The HOM yield was derived using the
192 concentration of the HOM produced, divided by the concentration of isoprene that was consumed by NO₃. The
193 uncertainty of HOM yield was estimated to -55%/+103%. The loss of HOM to the chamber was corrected using a
194 wall loss rate of 6×10⁻⁴ s⁻¹ as quantified previously (Zhao et al., 2018). HOM concentrations were also corrected for
195 dilution due to the replenishment flow needed to maintain a constant overpressure of the chamber (loss rate ~1×10⁻⁶
196 s⁻¹) (Zhao et al., 2015b). The influence of wall loss correction and dilution correction on HOM yield was ~12% and
197 <1%, respectively. Although the wall loss rate of vapors in this study might not be exactly the same as in our previous
198 photo-oxidation experiments (Zhao et al., 2018), HOM yield is not sensitive to the vapor wall loss rate. An increase
199 of wall loss rate by 100% or a decrease by 50% only changes the HOM yield by 11% and -6%, respectively.
200

201 3 Results and discussion

202 3.1 Overview of HOM

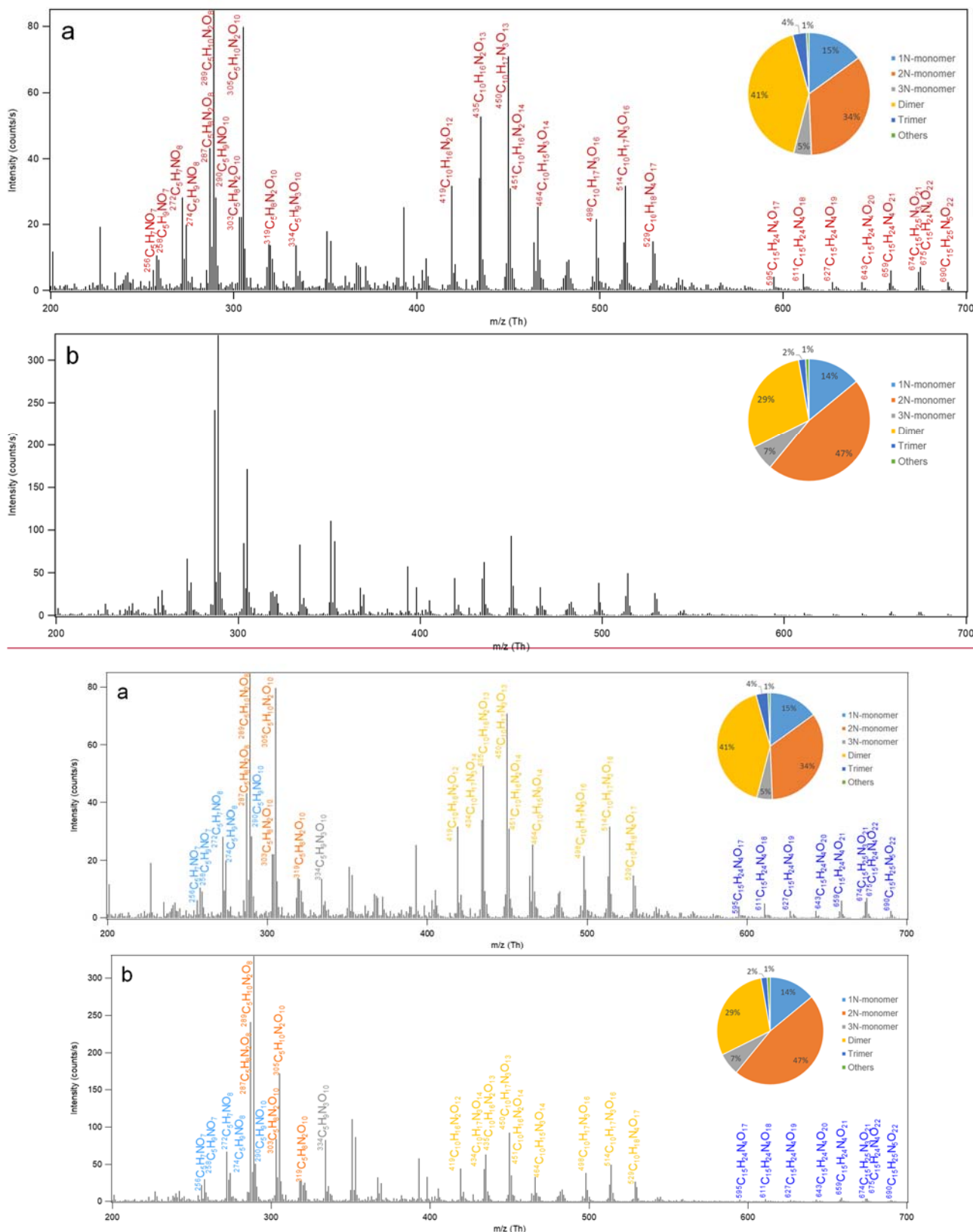
203 The mass spectra of HOM in the gas phase formed in the oxidation of isoprene by NO₃ are shown in
204 Fig. 1. A large number of HOM were detected. Almost all peaks are assigned HOM containing nitrogen atoms
205 with possibly few exceptions such as C₅H₁₀O₈ and C₅H₈O₁₁ with very minor peaks (<~1% of the maximum
206 peak). The reaction products can be roughly divided into three classes: monomers (C₅, ~200-400 Th), dimers
207 (C₁₀, ~400-600 Th), and trimers (C₁₅, ~>600 Th), according to their mass to charge ratio (m/z). The detailed
208 peak assignment of monomers, dimers, and trimers is discussed in the following sections.

209 3.2 HOM monomers and their formation

210 3.2.1 Overview of HOM monomers

211 HOM monomers showed a roughly repeating pattern in the mass spectrum at every 16 Th
212 (corresponding to the mass of oxygen) (Fig. 1a). Here a number of series of HOM monomers with continuously
213 increasing oxygenation were found, such as C₅H₉NO_n, C₅H₇NO_n, C₅H₈N₂O_n, C₅H₁₀N₂O_n (Table 1, Table S1-2
214 and Fig. 2). These monomers included both stable closed-shell molecules and open-shell radicals, such as
215 C₅H₈NO_n• and C₅H₉N₂O_n•. The open-shell molecules were likely RO₂ radicals because of their much longer life
216 time and hence higher concentrations compared with alkoxy radicals (RO) and alkyl radicals (R). Since the
217 observed stable products were mostly termination products of RO₂ reactions, we describe the stable products in

218 a RO₂-oriented approach. It is worth noting that some of the termination products may contain multiple isomers
 219 formed from different pathways.



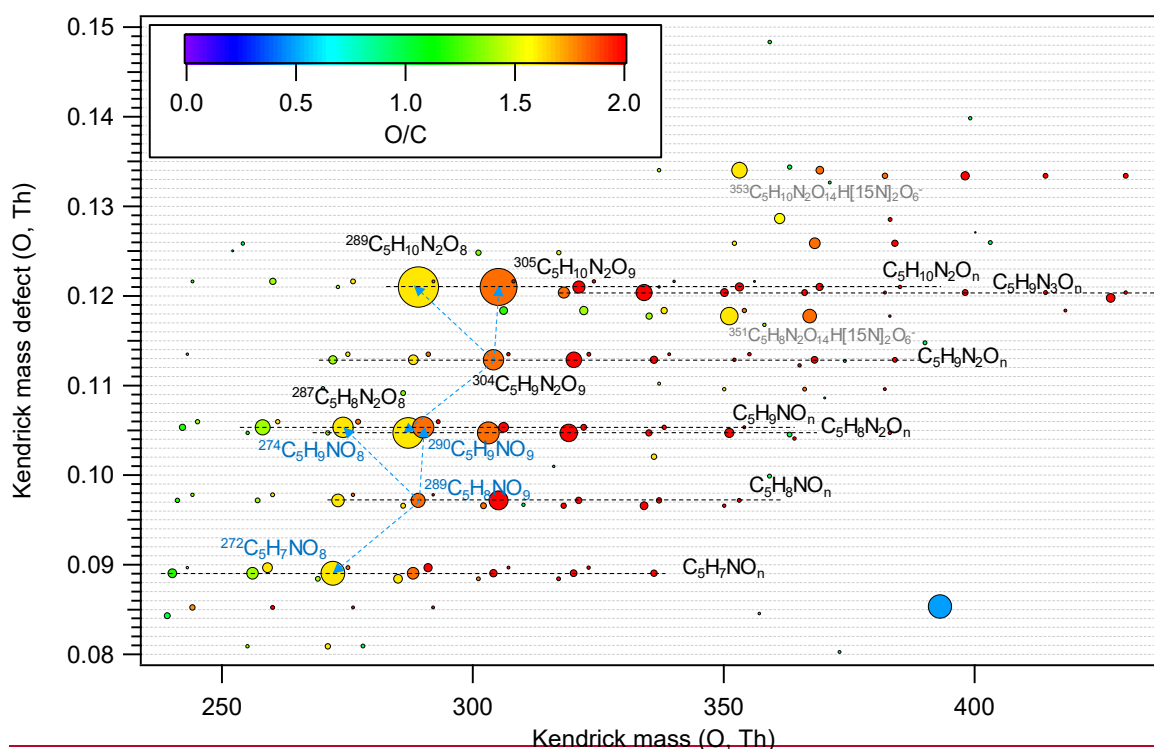
220

221

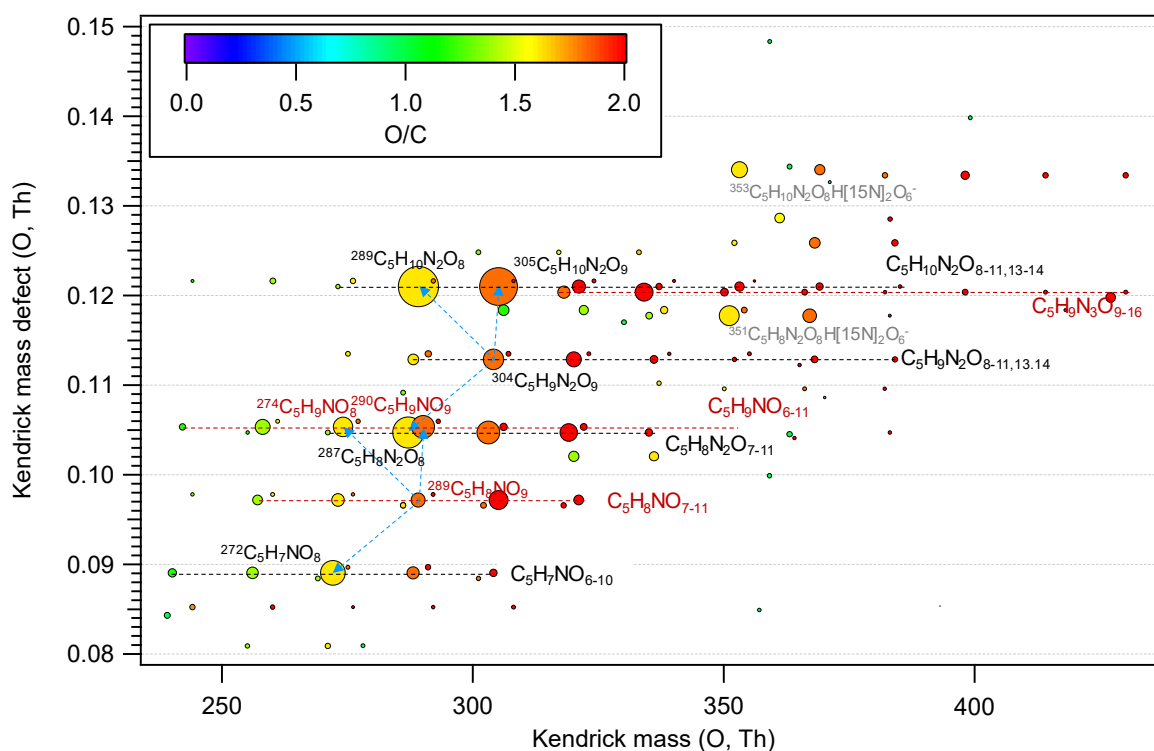
222 Figure 1. Mass spectrum of the HOM formed in the oxidation of isoprene by NO₃. HOM are detected as
 223 clusters with the reagent ion ¹⁵NO₃⁻, which is not shown in the molecular formula in the figure for simplicity. Panel

224 a and b show the average spectrum during the first isoprene addition period (P1) and for the whole period of six
225 isoprene additions (P1-6), respectively. The insets show the contributions of different classes of HOM. 1-3N-
226 monomer refers to the monomers containing 1-3 nitrogen atoms in the molecular formula.

227 HOM monomers were classified into 1N-, 2N-, and 3N-monomers according to the number of nitrogen
228 atoms that they contain. HOM without nitrogen atoms were barely observed except for very minor peaks (<~1% of
229 the maximum peak) possibly assigned to $C_5H_{10}O_8$ and $C_5H_8O_{11}$. The contribution of 2N-monomers such as
230 $C_5H_{10}N_2O_n$ and $C_5H_8N_2O_n$ was higher than that of the 1N-HOM monomers, and that of 3N-monomers was the least
231 (Fig. 1, inset). The most abundant monomers were $C_5H_{10}N_2O_8$, $C_5H_{10}N_2O_9$, and $C_5H_8N_2O_8$. The termination products
232 of $C_5H_9NO_8$, $C_5H_9NO_9$, and $C_5H_7NO_8$ also showed relatively high abundance. These limited number of compounds
233 dominated the HOM monomers. Since 2N-monomers were second-generation products as discussed below, the
234 higher abundance 2N- monomers indicate that the second-generation HOM play an important role in the reaction of
235 NO_3 with isoprene in the reaction conditions of our study, as also seen by Wu et al. (2020) . This is more evident for
236 the mass spectrum averaged over six isoprene addition periods (Fig. 1b), where the abundance of $C_5H_{10}N_2O_n$ and
237 $C_5H_8N_2O_n$ were more dominant. This observation is in contrast with the finding for the reaction of O_3 with BVOC
238 which contains only one double bond such as α -pinene (Ehn et al., 2014), where HOM are mainly first-generation
239 products formed via autoxidation. The higher abundance of HOM 2N-monomers than 1N-monomers is likely because
240 HOM production rate via the autoxidation of 1N-monomer RO_2 following the reaction of isoprene with NO_3 may be
241 slower than that of the reaction of 1N-monomers (including both HOM and non-HOM monomers) with NO_3 . We
242 would like to note that some less oxygenated 1N-monomers such as $C_5H_9NO_{4/5}$ and $C_5H_7NO_4$ may have high
243 abundance but are not detected by NO_3 -CIMS and are not HOM and thus not included in HOM 1N-monomers.



244



245

246 Figure 2. Kendrick mass defect plot for O of HOM monomers. The m/z in the molecular formula include the reagent ion
 247 $^{15}\text{NO}_3^-$, which is not shown for simplicity. The size (area) of circles is set to be proportional to the average peak intensity
 248 of each molecular formula during the first isoprene addition period (P1). The species at m/z 351 and 353 (labelled in grey)
 249 are the adducts of $\text{C}_5\text{H}_8\text{N}_2\text{O}_8$ and $\text{C}_5\text{H}_9\text{N}_2\text{O}_8$ with $\text{H}[^{15}\text{N}]_2\text{O}_6^-$, respectively. The blue dashed lines with arrows
 250 indicate the termination product hydroperoxide (M+H), alcohol (M-O+H), and ketone (M-O-H) with M the molecular
 251 formula of a HOM RO_2 .

252 3.2.2 1N-monomers

253 In our experiments we observed a $\text{C}_5\text{H}_8\text{NO}_n\cdot$ ($n=7-12$) series (series M1), as well as its corresponding
 254 termination products $\text{C}_5\text{H}_7\text{NO}_{n-1}$, $\text{C}_5\text{H}_9\text{NO}_{n-1}$, and $\text{C}_5\text{H}_9\text{NO}_n$ via the reactions with RO_2 and HO_2 , which contain
 255 carbonyl, hydroxyl, and hydroperoxy group, respectively. Overall, the peak intensities of $\text{C}_5\text{H}_9\text{NO}_n$ and
 256 $\text{C}_5\text{H}_7\text{NO}_n$ series first increased and then decreased as oxygen number increased (Fig. 2), with the peak intensity
 257 of $\text{C}_5\text{H}_9\text{NO}_8$ and $\text{C}_5\text{H}_7\text{NO}_8$ being the highest within their respective series when averaged over the whole
 258 experiment period.

259

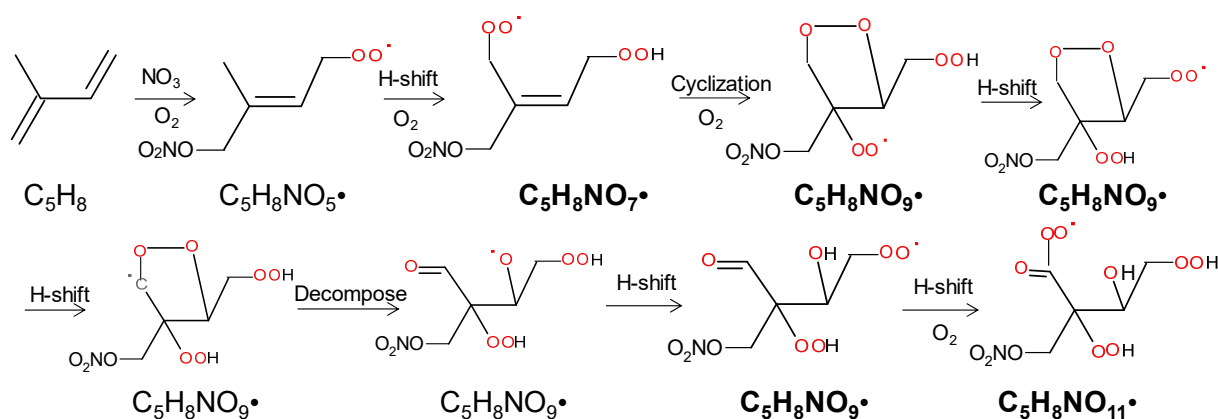
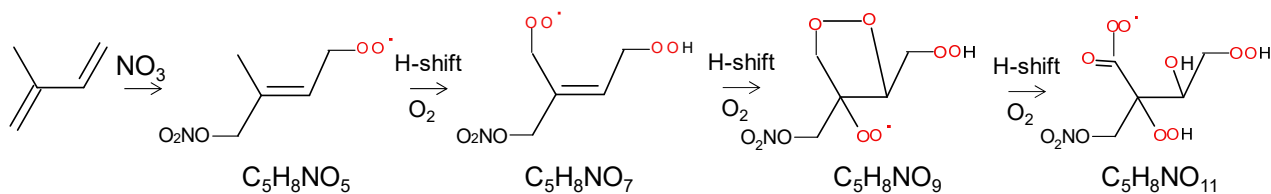
Table 1. HOM monomers formed in the oxidation of isoprene by NO_3 .

Series Number	Product	Type ^a	Pathway of RO_2
M1a/b	$\text{C}_5\text{H}_8\text{NO}_n$ ($n=7-12$)	RO_2	Isoprene+ NO_3
	$\text{C}_5\text{H}_9\text{NO}_n$ ($n=6-11$)	$\text{ROOH}/\underline{\text{ROH}}$	Isoprene+ NO_3 + NO_3
	$\text{C}_5\text{H}_7\text{NO}_{n-1}$ ($n=6-10$)	R=O	
M2a/b	$\text{C}_5\text{H}_9\text{N}_2\text{O}_n$ ($n=9-11,13,14$) ^b	RO_2	Isoprene + NO_3 + NO_3
	$\text{C}_5\text{H}_{10}\text{N}_2\text{O}_n$ ($n=8-11,13,14$) ^b	$\text{ROOH}/\underline{\text{ROH}}$	
	$\text{C}_5\text{H}_8\text{N}_2\text{O}_{n-1}$ ($n=7-11$)	R=O	

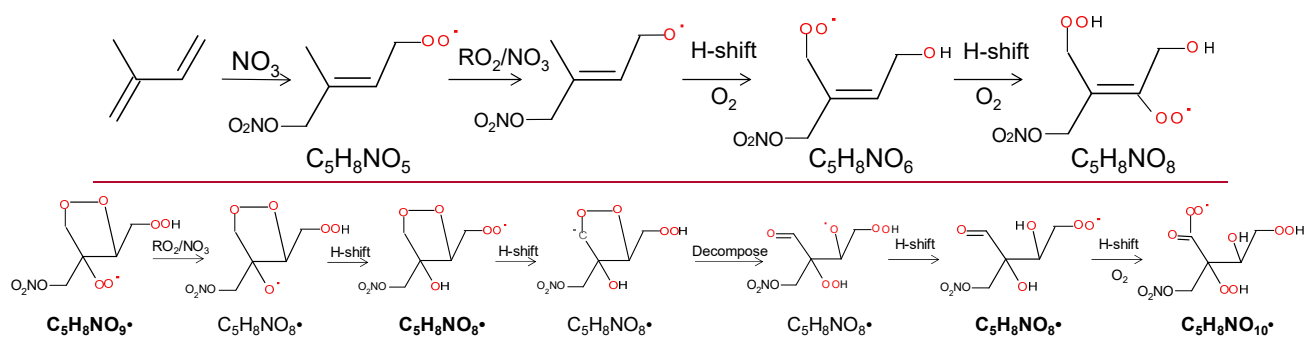
	$C_5H_9N_3O_{n+2}$ ($n=9-16$) ^b	<u>PNRO₂NO₂</u>	
M3	$C_5H_7N_2O_{n-(n=9)}$	RO ₂	
	$C_5H_8N_2O_{n-(n=8,9)}$	ROOH	Isoprene +NO ₃ +NO ₃
	$C_5H_6N_2O_{n+1}$ ($n=8$)	R=O	
M4	$C_5H_{10}NO_{n-(n=8-9)}$	RO ₂	
	$C_5H_{11}NO_{n-(n=7-9)}$	ROOH/ <u>ROH</u>	Isoprene +NO ₃ +OH
	$C_5H_9NO_{n+1}$ ($n=7-8$)	R=O	

^a: RO₂ denotes peroxy radical and ROOH, ROH, and R=O, and RO₂NO₂ denote denote the termination products containing hydroperoxy, hydroxyl, and carbonyl group, and peroxynitrate, respectively.

^b: Peak assignment of compounds with n=13,14 may be subject to uncertainties.



(a)



(b)

271 Scheme 1. The example pathways to form HOM RO₂ C₅H₈NO_n• (n=7, 9, 11) series (a) and C₅H₈NO_n•
272 (n=8, 10, ~~12~~) series (b) in the reaction of isoprene with NO₃. The detected products are in bold.

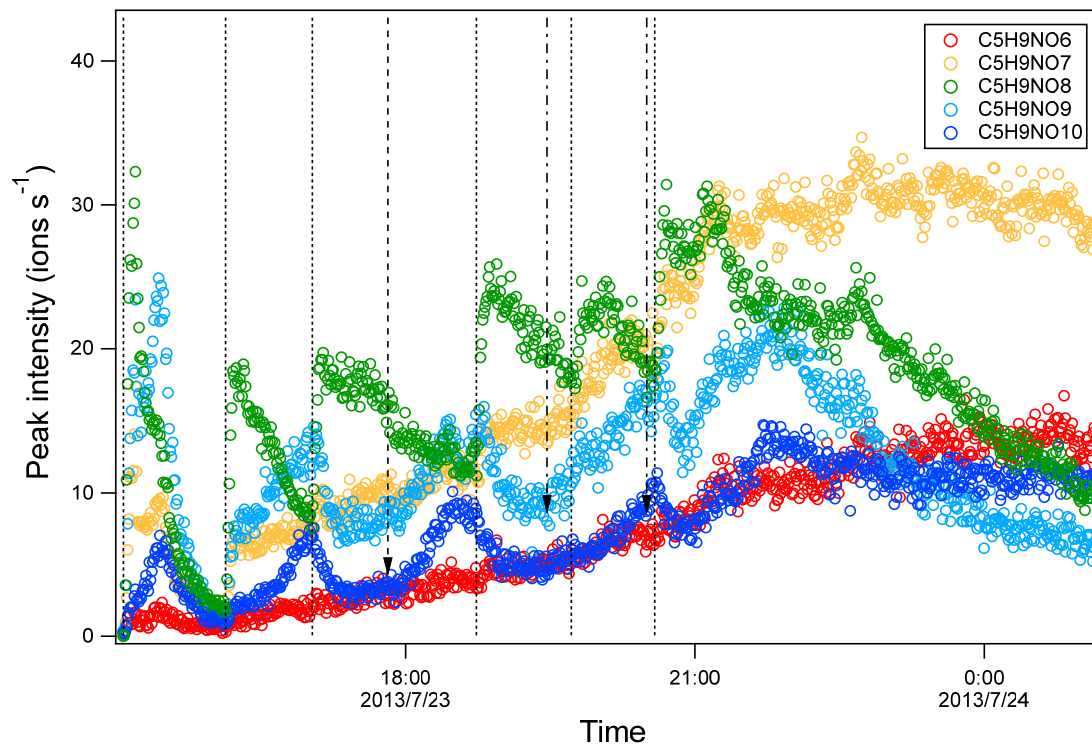
273 C₅H₈NO_n• with odd number oxygen atoms (n=7, 9, 11, series M1a) were possibly formed by the attack
274 of NO₃ to one double bond (preferentially to C1 according to previous studies (Skov et al., 1992; Berndt and
275 Böge, 1997; Schwantes et al., 2015) and followed by autoxidation (Scheme 1a). We would like to note that
276 NO₃-CIMS only observed HOM with oxygen numbers ≥ 6 in this study due to its selectivity of detection.
277 C₅H₈NO_n• with even number oxygen atoms (n=8, 10, ~~12~~) (series M1b in Table 1) were possibly formed after
278 H-shift of an alkoxy radical formed in reaction R5-R4 or R6-R5 and subsequent O₂ addition (“alkoxy-peroxy”
279 channel) (Scheme 1b), where the alkoxy radicals can be formed both from the RO₂+NO₃ and RO₂+RO₂ reactions.
280 The hydroxy-RO₂ formed can undergo further autoxidation adding two oxygen atoms after each H-shift. We
281 would like to note that the scheme and other schemes in this study only show example isomers and pathways to form
282 these molecules. It is likely that many of the reactions occurring are not the dominant channels as otherwise there
283 would be much higher HOM yield as discussed below.

284 Some HOM monomers may contain multiple isomers and be formed via different pathways. For
285 example, C₅H₉NO_n can contain alcohols (~~C₅H₉NO_n~~) ~~corresponding to~~ derived from RO₂ C₅H₈NO_{n+1}•,
286 hydroperoxides derived from (~~C₅H₉NO_n~~) ~~corresponding to~~ RO₂ C₅H₈NO_n• or the ketones from RO₂ C₅H₁₀NO_{n+1}•.
287 Some RO₂ C₅H₈NO_n• may be formed via the reaction of first-generation products with NO₃ in addition to direct
288 reaction of isoprene with NO₃. For example, C₅H₈NO₇• can be formed by the reaction of NO₃ with C₅H₈O₂,
289 which is a first-generation product observed previously ~~in~~ the reaction of isoprene with NO₃ or OH (Scheme
290 S1b) (Kwan et al., 2012). Moreover, RO₂ C₅H₈NO_n• can be formed from C5-carbonylnitrate, a first-generation
291 product, with OH (Scheme S1a). Trace amount of OH can be produced in the reaction of isoprene with NO₃
292 (Kwan et al., 2012; Wennberg et al., 2018). OH can also be formed via Criegee intermediates formed in the
293 isoprene+O₃ reaction (Nguyen et al., 2016), but this OH source was likely minor because the contribution of the
294 isoprene+O₃ reaction to total isoprene loss was negligible (<5%, Fig. S2). In addition, C₅H₈NO₈• may also be
295 formed by the reaction of NO₃ with C₅H₈O₃, which is a first-generation product observed in the reaction of
296 isoprene with OH (Kwan et al., 2012). The C₅H₈NO_n• formed via direct reaction of isoprene with NO₃ is a first-
297 generation RO₂ while that formed via other indirect pathways is a second-generation RO₂. The time profile of
298 the isomers from these two pathways, however, are expected to be different as will be discussed below.

299 Time series of HOM can shed light on their formation mechanisms. It is expected that first-generation
300 products increase fast with isoprene addition and reach a maximum earlier in the presence of wall loss of organic
301 vapour, while second-generation products reach a maximum in the later stage or increase continuously if the
302 production rate is higher than the loss rate. As a reference to analyze the time profiles of HOM, the times profile
303 of isoprene, NO₃, and N₂O₅ are also shown (Fig. S3S4). After isoprene was added in each period, NO₃ and N₂O₅
304 dropped dramatically and then gradually increased. We found that termination products within the same M1
305 series showed different time profiles. For example, in C₅H₉NO_n series, C₅H₉NO₈ clearly increased
306 instantaneously with isoprene addition, and decreased fast afterwards (Fig. 3a), indicating that it was a first-

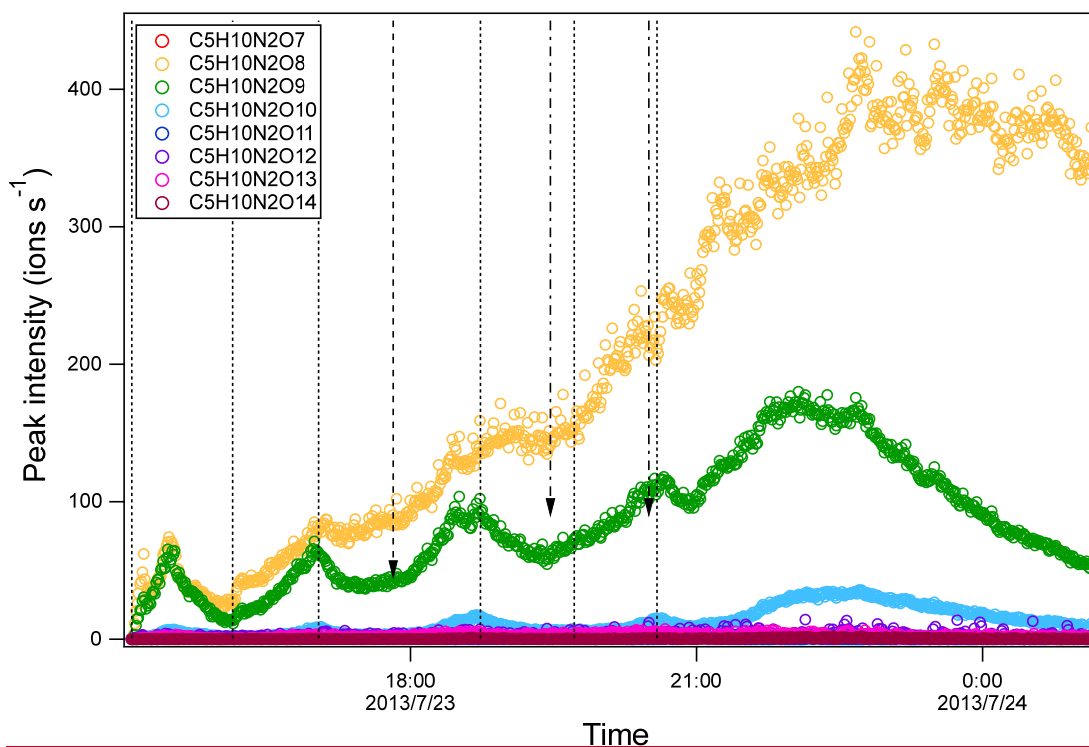
307 generation product, which was expected according to the mechanism Scheme 1. $C_5H_9NO_6$ and $C_5H_9NO_{10}$ had a
308 general increasing trend with time. While $C_5H_9NO_6$ increased continuously with time, $C_5H_9NO_{10}$ reached
309 maximum intensity in the late phase of each isoprene addition period and then decreased naturally or after
310 isoprene addition. The faster loss of $C_5H_9NO_{10}$ than $C_5H_9NO_6$ may result from the faster wall loss due to its
311 lower volatility. $C_5H_9NO_7$ and $C_5H_9NO_9$ showed a mixing time profile with features of the former two kinds of
312 time profiles, increasing almost instantaneously with isoprene additions, especially in the first two periods,
313 while increasing continuously or decreasing first with isoprene additions and then increasing later in each
314 periods. This kind of time series indicates that there were significant contributions from both first- and second-
315 generation products.

316 The second-generation products may be different isomers formed in pathways other than shown in
317 Scheme 1. Second-generation $C_5H_9NO_6$ can be formed via $C_5H_8NO_7\cdot$, which can also be formed by the reaction
318 of NO_3 and O_2 with $C_5H_8O_2$ as mentioned above (Scheme S2b), or by the reaction of OH with $C_5H_7NO_4$ (Scheme
319 S2a). The time profiles of $C_5H_8NO_7\cdot$ did showed more contribution of second-generation processes because it
320 continuously increased with time in general. If the pathways via the reaction of NO_3 and O_2 with $C_5H_8O_2$ and
321 the reaction of OH with $C_5H_7NO_4$ contribute most to $C_5H_9NO_6$, $C_5H_9NO_6$ would show mostly a time profile of
322 second-generation products. Similarly, second-generation $C_5H_9NO_7$ can be formed via $C_5H_8NO_7\cdot$ or $C_5H_8NO_8\cdot$.
323 The time series of ~~$C_5H_8NO_7$~~ ~~$C_5H_8NO_8$~~ did show the contribution of both the first- and second-generation
324 processes, which generally increased with time while also responding to isoprene addition (Fig. S4S5). ~~The time~~
325 ~~profiles of $C_5H_8NO_7\cdot$ showed more contribution of second-generation processes because it continuously~~
326 ~~increased with time in general. If the pathways via the reaction of NO_3 and O_2 with $C_5H_8O_2$ and the reaction of~~
327 ~~OH with $C_5H_7NO_4$ contribute most to $C_5H_9NO_6$, $C_5H_9NO_6$ would show mostly a time profile of second-~~
328 ~~generation products. Similar to $C_5H_9NO_6$, the second-generation pathway for $C_5H_9NO_7$, $C_5H_9NO_9$, and~~
329 ~~$C_5H_9NO_{10}$ are shown in Scheme S1, S3, S4. For the RO_2 in $C_5H_8NO_n\cdot$ series other than $C_5H_8NO_{7/8}\cdot$, the peak~~
330 of $C_5H_8NO_n\cdot$ overlaps with $C_5H_{10}N_2O_n$ in the mass spectra, which is a much larger peak, and thus cannot be
331 differentiated from $C_5H_{10}N_2O_n$. Therefore, it is not possible to obtain reliable separate time profiles in order to
332 differentiate their major sources. It is worth noting that nitrate CIMS may not be able to sensitively detect all
333 isomers of $C_5H_9NO_6$ due to the sensitivity limitation. Therefore, we cannot exclude the possibility that the
334 absence of some first-generation isomers of $C_5H_9NO_6$ was due to the low sensitivity of these isomers. ~~Similar~~
335 ~~to $C_5H_9NO_6$, the second-generation pathway for $C_5H_9NO_7$, $C_5H_9NO_9$, and $C_5H_9NO_{10}$ are shown in Scheme S1,~~
336 ~~S3, S4.~~

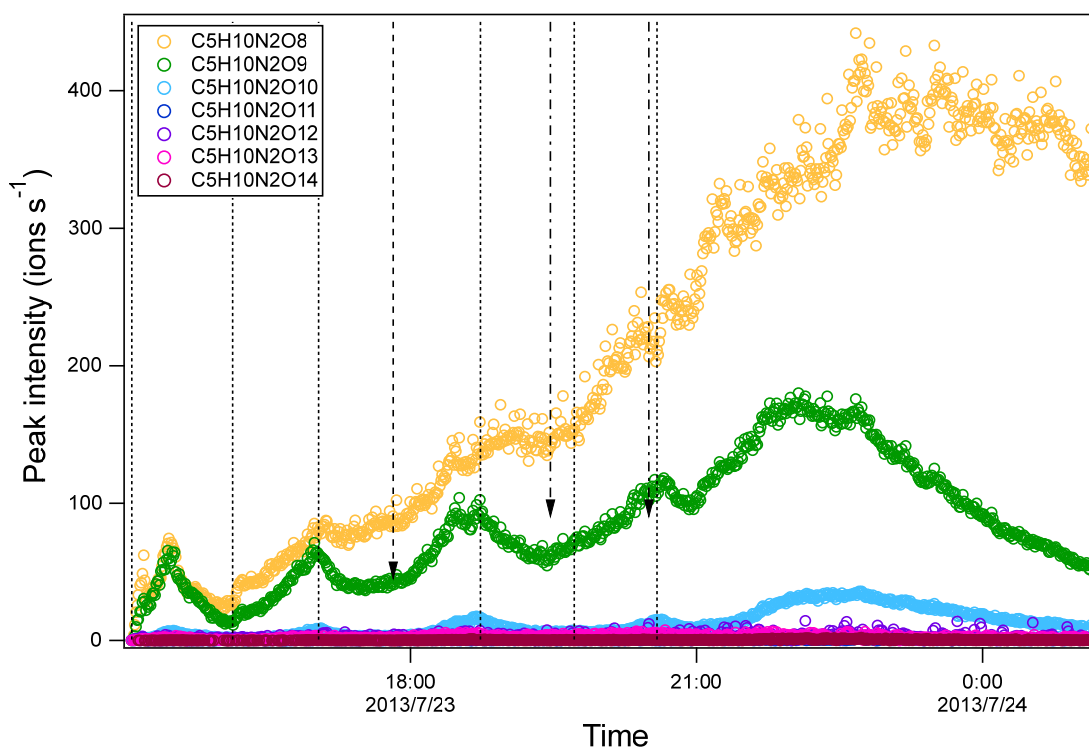


337
338

(a)



339



340

341

(b)

342

343

344

345

Figure 3. Time series of peak intensity of several HOM monomers of $C_5H_9NO_n$ series (a) and of $C_5H_{10}N_2O_n$ series (b). They are likely the termination products of RO_2 $C_5H_8NO_n\bullet$ and $C_5H_9N_2O_n\bullet$, respectively. The dashed lines indicate the time of isoprene additions. The long-dashed arrow indicates the time of NO_2 addition. The dash-dotted arrows indicate the time of O_3 additions.

346 Among the termination products of the 1N-monomer RO₂, carbonyl and hydroxyl/hydroperoxide
347 species had comparable abundance in general (Table S1), suggesting that disproportionation reactions between
348 RO₂ and RO₂ forming hydroxy and carbonyl species (R1-2) was likely an important RO₂ termination pathway.
349 However, dependence of the exact ratio of carbonyl species to hydroxyl/hydroperoxide species on the number
350 of oxygen atoms did not show a clear trend (Table S1), suggesting that the reactions of HOM RO₂ depended on
351 their specific structure. There was no clear difference in the abundance between the termination products from
352 C₅H₈NO_n• with odd and even number of oxygen atom in general, although the most abundant termination
353 product of C₅H₈NO_n•, i.e. C₅H₇NO₈, was likely formed from C₅H₈NO₉• in series M1a. This fact indicates that
354 both the peroxy pathway and alkoxy-peroxy pathway were important for the HOM formation in the
355 isoprene+NO₃ reaction under our conditions, in agreement with the significant formation of alkoxy radicals
356 from the reaction of RO₂ with NO₃ and RO₂.

357 In addition to the termination products of RO₂ M1, minor peaks of the RO₂ series C₅H₁₀NO_n• (n=8-9) (M4,
358 Table 1) and their corresponding termination products including hydroperoxide, alcohol and carbonyl species were
359 detected (Table S3). C₅H₁₀NO_n were likely formed by sequential addition of NO₃ and OH to two double bonds of
360 isoprene (Scheme S5). OH can react fast with isoprene or with the first-generation products of the reaction of isoprene
361 with NO₃, thus forming C₅H₁₀NO_n•. In addition, a few very minor but noticeable peaks of C₅H₉O_n• and their
362 corresponding termination products C₅H₁₀O_n and C₅H₈O_n were also observed. These HOM may be formed by the
363 reactions of isoprene with trace amount of OH and with O₃, although their contributions to reacted isoprene were
364 negligible. These HOM were also observed in the reaction of isoprene with O₃ with and without OH scavengers
365 (Jokinen et al., 2015).

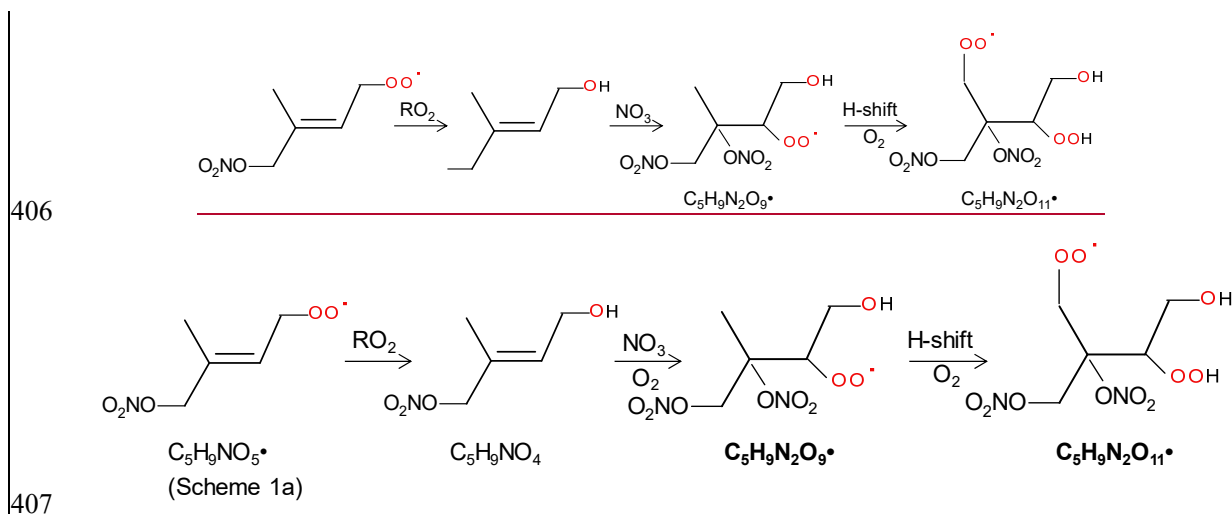
366 Among 1N-monomer HOM, C₅H₉NO₇ has been observed in the particle phase using ESI-TOFMS by
367 Ng et al. (2008) while others have not been observed in previous laboratory studies of the reaction of isoprene
368 with NO₃, to our knowledge. A number of C₅ organic nitrates have been observed in field studies. For example,
369 C₅H₇₋₁₁NO₄₋₉ have been observed in aerosol particles during the Southern Oxidant and Aerosol Study in rural
370 Alabama, US, where isoprene is abundant (Lee et al., 2016). Those compounds were also observed in chamber
371 experiments of the reaction of isoprene with OH in the presence of NO_x (Lee et al., 2016). C₅H_xNO₄₋₉ and
372 C₅H_xNO₄₋₁₀ have been observed in the gas phase and particle, respectively, in a rural area in southwest Germany
373 (Huang et al., 2019).

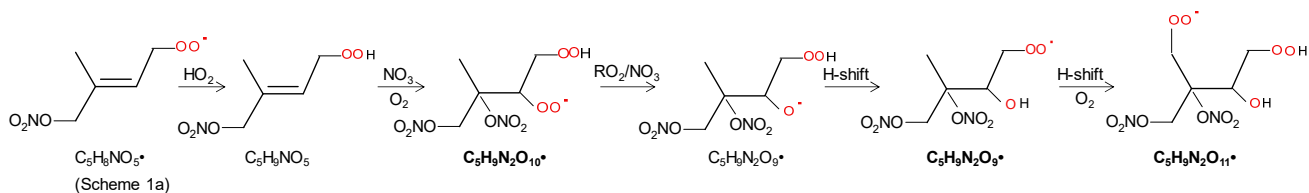
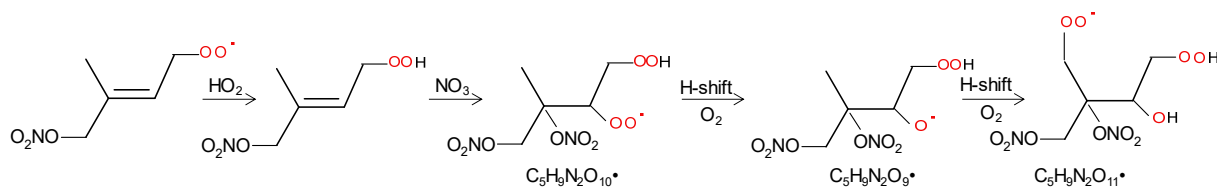
374 3.2.3 2N-monomers

375 The 2N-monomer RO₂ series C₅H₉N₂O_n•(n=9-14) series, were observed, as well as its likely
376 termination products, C₅H₈N₂O_n and C₅H₁₀N₂O_n, which contain a carbonyl and hydroxyl or hydroperoxide
377 functional group, respectively. The RO₂ series C₅H₉N₂O_n• with oddeven number of oxygen atoms (n=9, 11)
378 (M2a in Table 1) were likely formed from the first-generation product C₅H₉NO₄ (C5-hydroxynitrate) by adding
379 NO₃ to the remaining double bond, forming C₅H₉N₂O₉•, followed by autoxidation (Scheme 2a). This RO₂ series
380 can also be formed by the addition of NO₃ to the double bond of first-generation products (e.g. C₅H₉NO₅, C5-
381 nitrooxyhydroperoxide) and a subsequent alkoxy-peroxy step (Scheme 2b). C₅H₉N₂O_n• with even number of

382 oxygen atoms (n=8, 10, 12) (M2b in Table 1), can be formed by the addition of NO₃ to the double bond of
 383 C₅H₉NO₅ followed by autoxidation (Scheme. 3a), or of C₅H₉NO₄ followed by an alkoxy-peroxy step (Scheme.
 384 3b). The formation pathways of C₅H₉N₂O_{13/14}• and C₅H₉N₂O₈• cannot be well explained, as they contain too
 385 many or too few oxygen atoms to be formed via the pathways in Scheme 2 or 3. In Scheme 2 and 3, we show the
 386 reactions starting from 1-NO₃-isoprene-4-OO as an example. In the supplement, we have also shown the pathways
 387 starting from 1-NO₃-isoprene-2-OO peroxy radicals, which is indicated in a recent study by Vereecken et al. (2021)
 388 to be the dominant RO₂ in the reaction of isoprene with NO₃. The formation pathways of C₅H₉N₂O_{13/14}• cannot be
 389 well explained, as they contain too many oxygen atoms to be formed via the pathways in Scheme 2 or 3.

390 Formation through either Scheme 2 or 3 means that C₅H₈N₂O_n and C₅H₁₀N₂O_n were second-generation
 391 products. The time series of C₅H₁₀N₂O_n species clearly indicates that they were indeed second-generation
 392 products. C₅H₁₀N₂O_n species generally did not increase immediately with isoprene addition (Fig. 3b), but
 393 increased gradually with time and reached its maximum in the later stage of each period before decreasing with
 394 time (in the period 1 and 6), or decreasing after the next isoprene addition (periods 2-5). This time profile can
 395 be explained by the time series of the precursor of C₅H₁₀N₂O_n, C₅H₉N₂O_n• (RO₂) (Fig. S5S6). The changing rate
 396 (production rate minus destruction rate) of C₅H₁₀N₂O_n concentration was dictated by the concentration of
 397 C₅H₉N₂O_n• and the wall loss rate. During periods 2 to 5, C₅H₉N₂O_n• gradually increased but decreased sharply
 398 after the isoprene additions, resulted from chemical reactions of C₅H₉N₂O_n• and additionally from wall loss.
 399 When the rate of change of the C₅H₁₀N₂O_n concentration was positive, the concentration of C₅H₁₀N₂O_n increased
 400 with time. After isoprene additions, the rate of change of the C₅H₁₀N₂O_n concentration decreased dramatically
 401 to even negative, leading to decreasing concentrations. Similar to C₅H₁₀N₂O_n, the C₅H₈N₂O_n series did not
 402 respond immediately to isoprene additions (Fig. S6S7), which is expected for second-generation products
 403 according to the mechanism discussed above (Scheme 2-3). Particularly, the continuing increase of C₅H₈N₂O_n
 404 even after isoprene was completely depleted (—at ≈21:40, Fig. S76) clearly indicates that these compounds were
 405 second-generation products, although in the end they decreased due to wall loss.



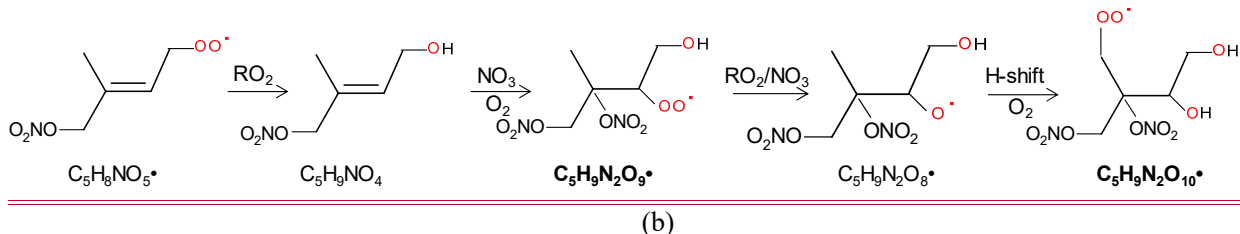
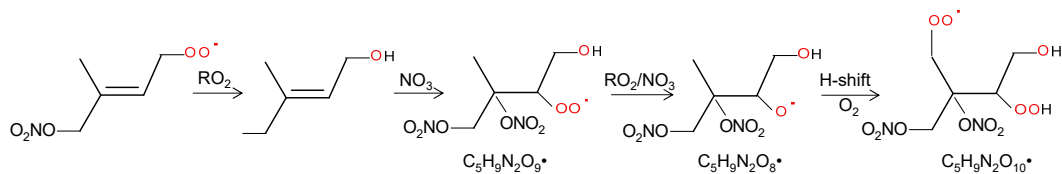
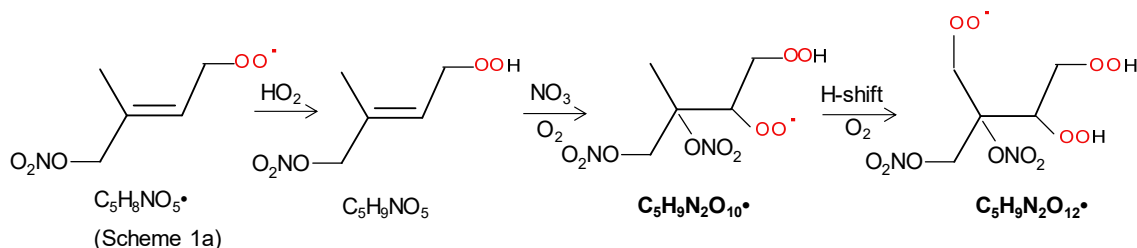
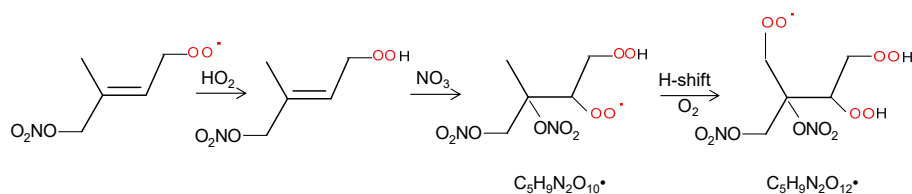


415

416

417

Scheme 2. The example pathways to form $C_5H_9N_2O_n$ ($n=9, 11$) HOM RO_2 series by RO_2 channel (a) and alkoxy-peroxy channel. The detected products are in bold.



423

424

425

Scheme 3. The example pathways to form $C_5H_9N_2O_n$ ($n=8, 10, 12$) HOM RO_2 series by RO_2 channel (a) and alkoxy-peroxy channel (b). The detected products are in bold.

According to the finding of Ng et al. (2008), C5-hydroxynitrate decays much faster than C5-nitrooxyhydroperoxides. Additionally, C5-hydroxynitrate concentration is expected to be higher than that of nitrooxyhydroperoxides because RO_2+RO_2 forming alcohol is likely more important than RO_2+HO_2 forming

426 hydroperoxide in this study. Therefore, it is likely that $C_5H_9N_2O_n\bullet$ M2a series was mainly formed from $C_5H_9NO_4$
427 instead of $C_5H_9NO_5$, while $C_5H_9N_2O_n\bullet$ M2b were formed from $C_5H_9NO_4$ followed by an alkoxy-peroxy step.
428 That is, Scheme 2a and 3b~~Scheme 2 was appear~~ more likely.

429 Similar to $C_5H_8NO_n\bullet$, the intensity of carbonyl species from $C_5H_9N_2O_n\bullet$ was also comparable with that
430 of hydroxyl/hydroperoxide species, suggesting that RO_2+RO_2 reaction forming ketone and alcohol was likely
431 an important pathway of HOM formation in the isoprene+NO₃ reaction. In general, the intensity of the
432 termination products from $C_5H_9N_2O_n\bullet$ with both even and odd oxygen numbers were comparable. This again
433 suggests that both peroxy and alkoxy-peroxy pathways were important for HOM formation in the isoprene+NO₃
434 reaction. The intensity of ~~$C_5H_{10}N_2O_n$~~ and $C_5H_8N_2O_n$ first increased and then decreased with oxygen number
435 while $C_5H_{10}N_2O_n$ decreased with oxygen number, with ~~the~~ $C_5H_{10}N_2O_8$ and $C_5H_8N_2O_8$ being the most abundant
436 within their respective series.

437 Some 2N-monomers have been detected in previous studies of the reaction of isoprene with NO_3 .
438 $C_5H_{10}N_2O_8$ has been detected in the particle phase by Ng et al. (2008) and $C_5H_8N_2O_7$ was detected in the gas
439 phase by Kwan et al. (2012). $C_5H_9N_2O_9\bullet$ has been proposed to be formed via the pathway as in Scheme 2a (Ng
440 et al., 2008), and it was directly detected in our study. $C_5H_8N_2O_7$ species has been proposed to be a dinitrooxy
441 epoxide formed by the oxidation of nitrooxyhydroperoxide (Kwan et al., 2012), instead of being a dinitrooxy
442 ketone proposed in our study, a termination product of $C_5H_9N_2O_8\bullet$. Admittedly, $C_5H_8N_2O_7$ may contain both
443 isomers. In addition, Ng et al. (2008) detected $C_5H_8N_2O_6$ in the gas phase, which was not detected in this study
444 likely due to the selectivity of NO_3^- -CIMS. (~~Xu et al., 2021~~)

445 One could suppose that $C_5H_7N_2O_n\bullet$ should also be formed since C5-nitrooxycarbonyl ($C_5H_7NO_4$) also
446 contains one double bond that can be attacked by NO_3 in a second oxidation step. However, concentrations of
447 $C_5H_7N_2O_n$ were too low to assign molecular formulas with confidence except for $C_5H_7N_2O_9\bullet$, clearly showing
448 that $C_5H_7N_2O_n\bullet$ was not important. This fact is consistent with the finding of Ng et al. (2008) that C5-
449 nitrooxycarbonyls react slowly with NO_3 . Additionally, the peroxy radical formed in the reaction of C5-
450 nitrooxycarbonyls with NO_3 likely leads to more fragmentation in H-shift as found in the OH oxidation of
451 methacrolein (Crouse et al., 2012), which may also contribute to the low abundance of $C_5H_7N_2O_n$. ~~In addition,~~
452 ~~the~~ presence of HOM containing two N atoms is in line with the finding by Faxon et al. (2018) who detected
453 products containing two N atoms in the reaction of NO_3 with limonene, which also contain two carbon double
454 bonds. It is anticipated that for VOCs with more than one double bond, NO_3 can add to all the double bonds as
455 for isoprene and limonene.

456 3.2.4 3N-monomers

457 HOM containing three nitrogen atoms, $C_5H_9N_3O_n$ ($n=9-16$), were observed. These compounds were
458 possibly peroxy nitrates formed by the reaction of RO_2 ($C_5H_9N_2O_n\bullet$) with NO_2 . The time series of $C_5H_9N_3O_n$
459 was examined to check whether they match such a mechanism. If $C_5H_9N_3O_n$ were formed by the reaction of
460 $C_5H_9N_2O_{n-2}\bullet$ with NO_2 , the concentration would be a function of the concentrations of $C_5H_9N_2O_{n-2}\bullet$ and NO_2 as
461 follows:

$$462 \quad \frac{d[C_5H_9N_3O_n]}{dt} = k[C_5H_9N_2O_{n-2}\bullet][NO_2] - k_{wall}[C_5H_9N_3O_n]$$

463 where $[C_5H_9N_3O_n]$, $[C_5H_9N_2O_{n-2}\bullet]$, and $[NO_2]$ are the concentration of these species, k is the rate
 464 constant and k_{wall} is the wall loss rate. Because the products of $C_5H_9N_2O_{n-2}\bullet$ and NO_2 were at their maximum at
 465 the end of each period and decreased rapidly after isoprene addition (Fig. S7S8), the concentration should have
 466 the-its maximum increasing rate at the end of each isoprene addition period. However, we found that only
 467 $C_5H_9N_3O_{12, 15, 16}$ showed such a time profile (Fig. S8S9), while $C_5H_9N_3O_{9, 10, 11, 13, 14}$ generally increased with
 468 time, different from what one would expect based on the proposed pathway. Therefore, it is likely that
 469 $C_5H_9N_3O_{12, 15, 16}$ were mainly formed via the reaction of $C_5H_9N_2O_n\bullet$ with NO_2 , whereas $C_5H_9N_3O_{9,10,11,13,14}$ were
 470 not. Moreover, $C_5H_9N_3O_9$ cannot be explained by the reaction $C_5H_9N_2O_n\bullet$ ($n \geq 9$) with NO_2 or NO_3 , because these
 471 reactions would add at least one more oxygen atom. One possible pathway to form $C_5H_9N_3O_9$ was the direct
 472 addition of N_2O_5 to the carbon double bond of C5-hydroxynitrate, forming a nitronitrate. Such an mechanism
 473 has been proposed previously in the heterogeneous reaction of N_2O_5 with 1-palmitoyl-2-oleoyl-sn-glycero-3-
 474 phosphocholine (POPC) because $-NO_2$ and $-NO_3$ groups were detected (Lai and Finlayson-Pitts, 1991). This
 475 pathway generally matched the time series of $C_5H_9N_3O_{9,10,11,13,14}$ typical of second-generation products since
 476 C5-hydroxynitrate was a first-generation product. It is possible that the main pathway of $C_5H_9N_3O_{9,10,11,13,14}$ was
 477 the reaction of $C_5H_9NO_{4,5,6}$ with N_2O_5 , although the reaction of N_2O_5 with $C=C$ double bonds in common alkenes
 478 and unsaturated alcohols are believed to be not important (Japar and Niki, 1975; Pfrang et al., 2006).

479 3N-monomers, $C_5H_9N_3O_{10}$, has been observed in the particles formed in the isoprene+ NO_3 reaction by
 480 Ng et al. (2008). Here a complete series of $C_5H_9N_3O_n$ were observed. $C_5H_9N_3O_{10}$ was previously proposed to
 481 be formed by another pathway, i.e. the reaction of RO_2 ($C_5H_9N_2O_9\bullet$) and NO_3 (Ng et al., 2008). We further
 482 examined the possibility of such a pathway in our study. Similar to NO_2 , if $C_5H_9N_3O_n$ were formed by the
 483 reaction of $C_5H_9N_2O_{n-2}\bullet$ with NO_3 , the concentration would have the-its maximum increasing rate at the end of
 484 each isoprene addition period. Among $C_5H_9N_2O_n\bullet$, the precursors of $C_5H_9N_3O_n$, $C_5H_9N_2O_{9, 10, 13, 14}\bullet$ showed a
 485 maximum increasing rate and a subsequent decrease after isoprene addition. The difference in oxygen number
 486 between $C_5H_9N_3O_{12, 15, 16}$, the termination products, and $C_5H_9N_2O_{9, 10, 13, 14}\bullet$, the corresponding RO_2 with the
 487 consistent time profile is mostly two. Since the reaction of $C_5H_9N_2O_n$ with NO_2 and NO_3 result an increased
 488 oxygen number by two and by one, respectively, we infer that it is more likely that $C_5H_9N_3O_{12, 15, 16}$ were formed
 489 by the reaction of $C_5H_9N_2O_{10, 13, 14}\bullet$ with NO_2 rather than NO_3 , and thus they were likely peroxy nitrates rather
 490 than nitrates formed by the reaction of RO_2 with NO_3 . Since alkyl peroxy nitrates decompose rapidly (Finlayson-
 491 Pitts and Pitts, 2000; Ziemann and Atkinson, 2012), it is possible that these compounds contained
 492 peroxyacylnitrates.

493 Little attention has been paid to the RO_2+NO_2 pathway in nighttime chemistry of isoprene in the
 494 literature (Wennberg et al., 2018), which is likely due to the instability of the products. According to this
 495 pathway, $C_5H_8N_2O_n$, which was proposed to be a ketone formed via $C_5H_9N_2O_9\bullet$ in the M2 series (Table 1) as
 496 discussed above, can also comprise peroxy nitrates formed by the reaction of $C_5H_8NO_n\bullet$ (M1a RO_2) with NO_2 .

3N dimer such as $C_5H_9N_3O_{10}$ as well as 2N-monomers such as $C_5H_8N_2O_8$ and $C_5H_8N_2O_{10}$ have been observed in a recent field study in polluted cities in east China (Xu et al., 2021).

3.3 HOM dimers and their formation

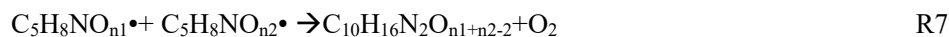
Table 2. HOM dimers and trimers formed in the oxidation of isoprene by NO_3 .

Series Number	Formula	Type	Pathway of RO_2
Dimer 1	$C_{10}H_{16}N_2O_n$ (n=10-17)	ROOR ^a	$M1^b + M1$
Dimer 2	$C_{10}H_{17}N_3O_n$ (n=11-19)	ROOR	$M1+M2/M3+M4$
Dimer 3	$C_{10}H_{18}N_4O_n$ (n=15-18)	ROOR	$M2+M2$
Dimer 4	$C_{10}H_{18}N_2O_n$ (n=10-16)	ROOR	$M1+M4$
Dimer 5	$C_{10}H_{15}N_3O_n$ (n=13-17)	ROOR	$M1+M3$
Dimer 6	$C_{10}H_{19}N_3O_n$ (n=14-15)	ROOR	$M2+M4$
Dimer 7	$C_{10}H_{14}N_2O_n$ (n= 10-12 16)	ROOR	Unknown
Dimer 8	$C_{10}H_{15}NO_n$ (n=9-12)	ROOR	$C_{10}H_{16}NO_n$
Dimer 9	$C_{10}H_{17}NO_n$ (n= 11-12 15)	ROOR	$C_{10}H_{16}NO_n$
Dimer R1	$C_{10}H_{16}N_3O_n$ (n=12-15)	RO_2	Dimer 1+ NO_3
Dimer R2	$C_{10}H_{17}N_2O_n$ (n=11-12)	RO_2	Dimer 1+OH
Dimer R3	$C_{10}H_{17}N_4O_n$ (n=16-18)	RO_2	Dimer 2+ NO_3
Dimer R4	$C_{10}H_{16}NO_n$ (n=10- 14)	RO_2	$M1+C_5H_8$
Trimer 1	$C_{15}H_{24}N_4O_n$ (n=17- 22)	ROOR	Dimer R1+M1
Trimer 2	$C_{15}H_{25}N_5O_n$ (n=20-22)	ROOR	Dimer R3+M1; Dimer R1+M2
Trimer 3	$C_{15}H_{25}N_3O_n$ (n= 13-14 20)	ROOR	Dimer R2+M1; Dimer R4+M2
Trimer 4	$C_{15}H_{26}N_4O_n$ (n=17-21)	ROOR	Dimer R2+M2

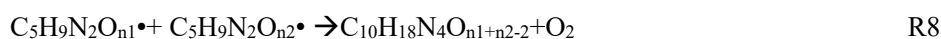
^a: ROOR denotes for organic peroxide.

^b: The numbering is referred to Table 1.

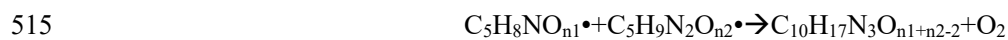
A number of HOM dimer series were observed, including $C_{10}H_{16}N_2O_n$ (n=10-17), $C_{10}H_{17}N_3O_n$ (n=11-19), and $C_{10}H_{18}N_4O_n$ (n=15-18), $C_{10}H_{18}N_2O_n$ (n=10-16), $C_{10}H_{15}N_3O_n$ (n=~~13-14~~), and $C_{10}H_{19}N_3O_n$ (n=14-15) series (Table 2, Table S3). $C_{10}H_{16}N_2O_n$ series (dimer 1, Table 2) was likely formed by the accretion reaction of two monomer RO_2 of M1a/b (Reaction R7).



Similarly, $C_{10}H_{18}N_4O_n$ series (dimer 2, Table 2) were likely formed by the accretion reaction of two monomer RO_2 of M2 (Reaction R8). As n1 and n2 are ≥ 9 , the number of oxygen in $C_{10}H_{18}N_4O_n$ is expected to be ≥ 16 . This is consistent with our observation that only $C_{10}H_{18}N_4O_n$ with $n \geq 16$ had significant concentrations.



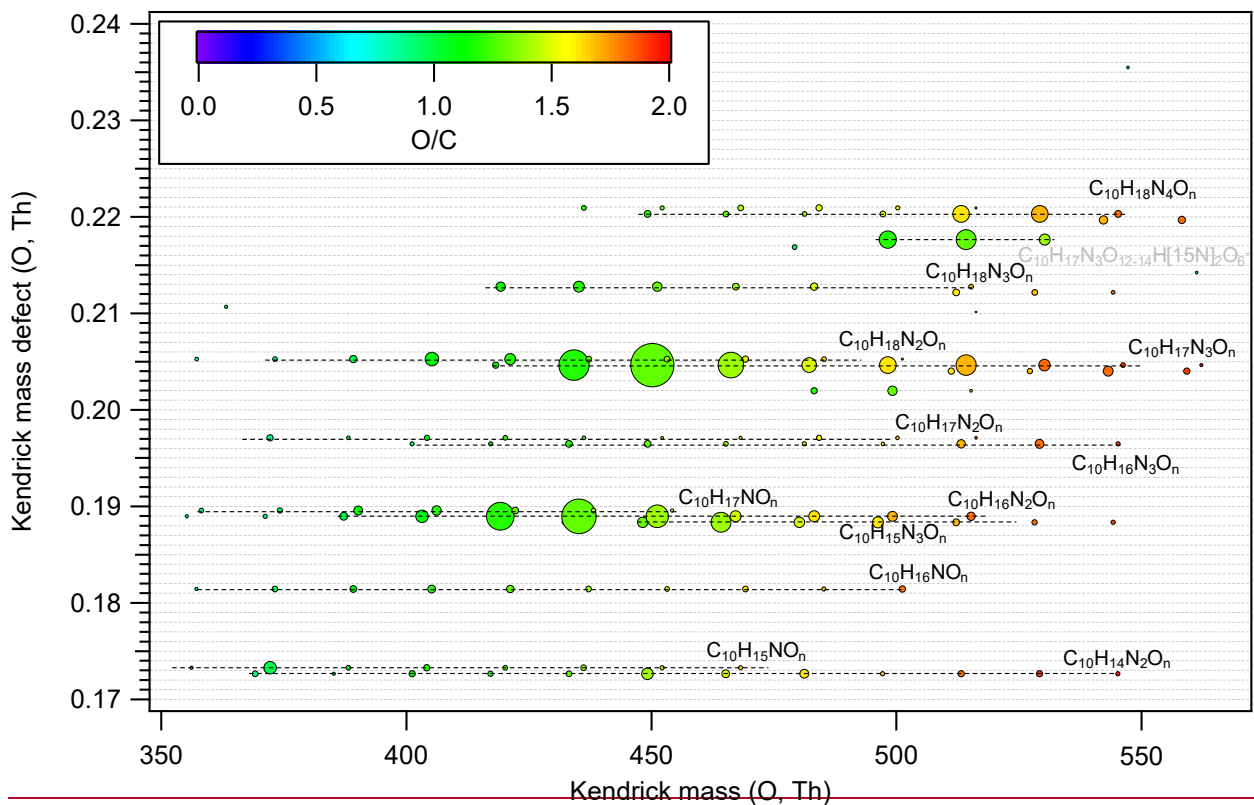
$C_{10}H_{17}N_3O_n$ series (dimer 3, Table 2) were likely formed by the cross accretion reaction of one M1 RO_2 and one M2 RO_2 (reaction R9). Since n1 is ≥ 5 and n2 is ≥ 9 , the number of oxygen atoms in $C_{10}H_{17}N_3O_n$ is expected to be ≥ 12 , which is also roughly consistent with our observation that only $C_{10}H_{17}N_3O_n$ with $n \geq 11$ were detected.



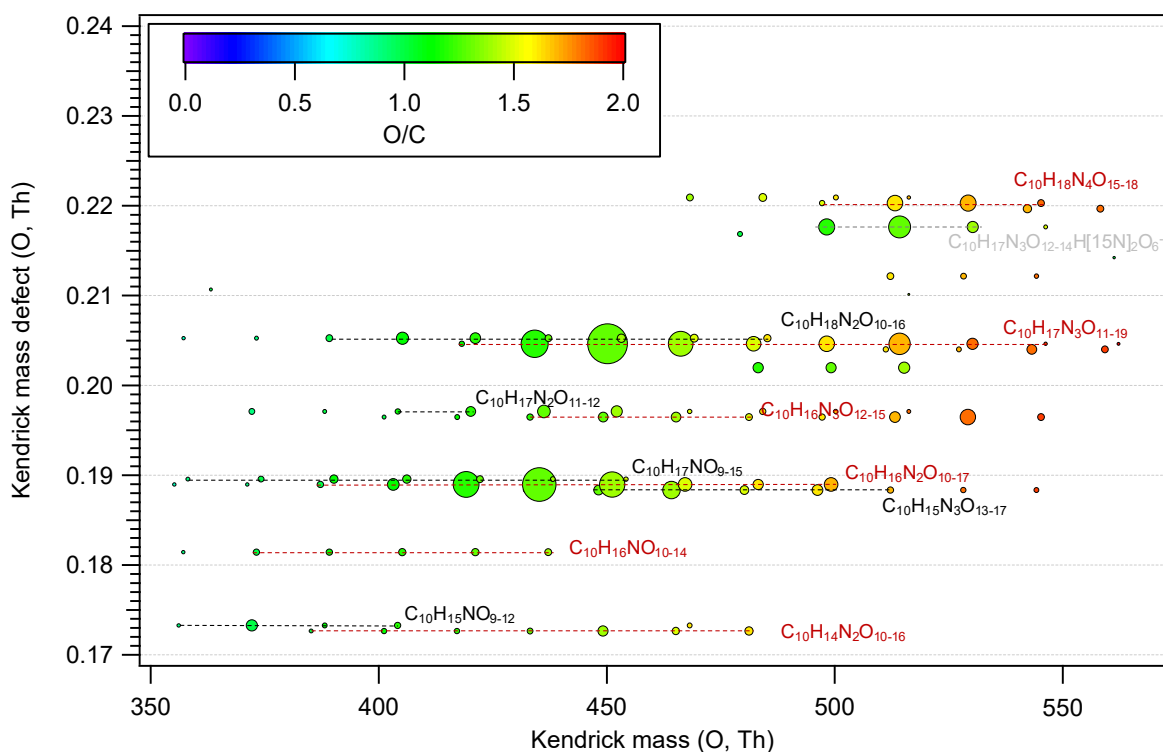
R9

516 Similarly, $\text{C}_{10}\text{H}_{18}\text{N}_2\text{O}_n$ ($n=10-16$) and $\text{C}_{10}\text{H}_{15}\text{N}_3\text{O}_n$ ($n=13-17$) series (dimer 4, dimer 5, Table 2) were likely formed
 517 from the accretion reaction ~~of~~between one M1 RO_2 and one M4 RO_2 , and ~~of~~between one M1 RO_2 and one M3 RO_2
 518 ($\text{C}_5\text{H}_7\text{N}_2\text{O}_9\bullet$). Other dimer series than dimer 1-5 were also present. However, they had quite low intensity (Fig. 4),
 519 which was consistent with the low abundance of their parent monomer RO_2 . They can be formed from various
 520 accretion reactions of monomer RO_2 . For example, $\text{C}_{10}\text{H}_{19}\text{N}_3\text{O}_n$ can be formed by the accretion reaction of
 521 $\text{C}_5\text{H}_9\text{N}_2\text{O}_n\bullet$ and $\text{C}_5\text{H}_{10}\text{NO}_n\bullet$ (Table 2).

522 Similar to monomers, a few species dominated in HOM dimers spectrum. The dominant dimer series were
 523 $\text{C}_{10}\text{H}_{17}\text{N}_3\text{O}_x$ and $\text{C}_{10}\text{H}_{16}\text{N}_2\text{O}_x$ series, with $\text{C}_{10}\text{H}_{17}\text{N}_3\text{O}_{12-14}$ and $\text{C}_{10}\text{H}_{16}\text{N}_2\text{O}_{12-14}$ showing highest intensity among each
 524 series (Fig. 4). In addition, the O/C ratio or oxidation state of HOM dimers were generally lower than that of
 525 monomers (Fig. 2, Fig. 4), which resulted from the loss of two oxygen atoms in the accretion reaction of two
 526 monomer RO_2 .



527



528

529

530

531

532

Figure 4. Kendrick mass defect plot for O of HOM dimers formed in isoprene+NO₃the isoprene+NO₃ reaction.

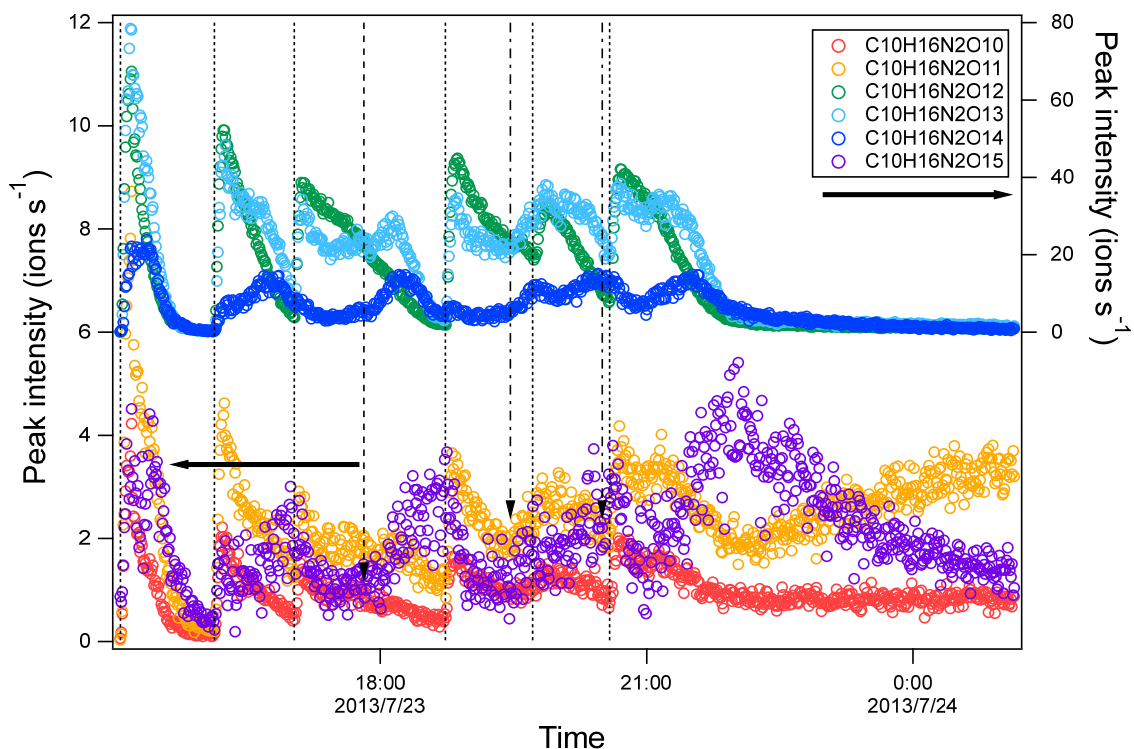
The size (area) of circles is set to be proportional to the average peak intensity of each molecular formula during the first

isoprene addition period (P1). The molecular formula include the reagent ion ¹⁵NO₃⁻, which is not shown for simplicity.

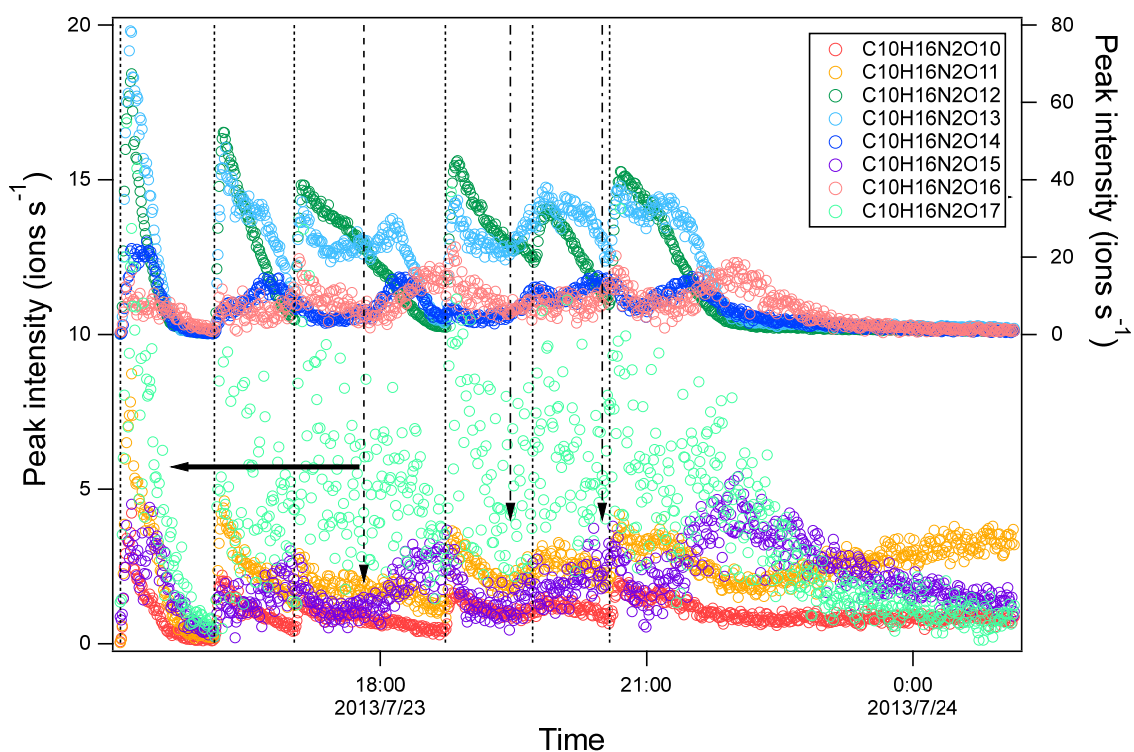
The species labelled in grey (C₁₀H₁₇N₃O₁₂₋₁₄, H[¹⁵N]₂O₆⁻) are the adducts of C₁₀H₁₇N₃O₁₂₋₁₄ with H[¹⁵N]₂O₆⁻.

533 According to the mechanism above (R7-9), we attempt to explain the relative intensities of the dimers using
534 the signal intensities of monomer RO₂. Assuming that the rate constant for each of HOM-RO₂+ HOM-RO₂ reaction
535 forming dimers is the same considering that all HOM-RO₂ are highly oxygenated with a number of functional groups,
536 it is expected that the dimer formed by the recombination between the most abundant RO₂ has the highest intensity.
537 The most abundant monomer RO₂ were C₅H₉N₂O₉• and C₅H₉N₂O₁₀• and thus the most abundant dimers are expected
538 to be C₁₀H₁₆N₄O₁₆, C₁₀H₁₆N₄O₁₇, and C₁₀H₁₆N₄O₁₈. This expected result is in contrast with our observation showing
539 that the most abundant dimers were C₁₀H₁₇N₃O₁₂₋₁₄ and C₁₀H₁₆N₂O₁₂₋₁₄ (Fig. 4). The discrepancy is possibly
540 attributed to the presence of less oxygenated RO₂ (with O₂≤5) that have a low detection sensitivity in the NO₃-CIMS
541 (Riva et al., 2019) due to their lower oxygenation compared with other HOM RO₂ shown above. These RO₂ may
542 react with C₅H₉N₂O₉• and C₅H₉N₂O₁₀•. For example, C₅H₈NO₅• (RO₂) is proposed to be an important first-
543 generation RO₂ in the oxidation of isoprene by NO₃ (Ng et al., 2008; Rollins et al., 2009; Kwan et al., 2012;
544 Schwantes et al., 2015). Although C₅H₈NO₅• showed very low signal in our mass spectra, it was likely to have high
545 abundance since it was the first RO₂ formed in the reaction of isoprene with NO₃. Indeed, we found that the
546 termination products of C₅H₈NO₅• such as C₅H₉NO₅, C₅H₇NO₄, and C₅H₉NO₄ had high abundance in another study
547 Wu et al. (2020), indicating the high abundance of C₅H₈NO₅•. The accretion reaction of C₅H₈NO₅• with C₅H₉N₂O₉₋₁₀•
548 and C₅H₈NO₉₋₁₀• can explain the high abundance of C₁₀H₁₇N₃O₁₂₋₁₄ and C₁₀H₁₆N₂O₁₂₋₁₄ among all dimers.

549 Provided that C₅H₈NO₅• is abundant, we still cannot explain the relative intensity of C₁₀H₁₇N₃O₁₂,
550 C₁₀H₁₇N₃O₁₃, and C₁₀H₁₇N₃O₁₄ that were all formed by the accretion reaction with C₅H₈NO₅•. C₁₀H₁₇N₃O₁₂ should
551 have the highest intensity among C₁₀H₁₇N₃O₁₂₋₁₄ as its precursor RO₂, C₅H₉N₂O₉•, is the most abundant. This
552 suggests that accretion reactions other than those of C₅H₈NO₅• with C₅H₉N₂O₉₋₁₀• also contributed to
553 C₁₀H₁₇N₃O₁₂₋₁₄. Admittedly, the assumption of different RO₂ having similar rate constants in accretion reactions
554 may not be valid. For example, self-reaction of tertiary RO₂ is slower than secondary and primary RO₂ (Jenkin et
555 al., 1998; Finlayson-Pitts and Pitts, 2000). Different rate constants may also lead to the observation that the most
556 abundant dimers could not be explained the most abundant RO₂.



557



558

559 Figure 5. Time series of peak intensity of several HOM dimers of $C_{10}H_{16}N_2O_n$ series. The dashed lines indicate the
 560 time of isoprene additions. The long-dashed arrow indicates the time of NO_2 addition. The dash-dotted arrows
 561 indicate the time of O_3 additions. The horizontal arrows indicate y-axis scales for different markers.

562 The time profiles of $C_{10}H_{16}N_2O_n$ indicate contributions of both the first- and second-generation products.
 563 The dominance of the first- or second-generation products depended on the specific compounds. Most $C_{10}H_{16}N_2O_n$
 564 compounds increased instantaneously after isoprene additions, indicating significant contributions of first-generation

565 products. Since the formation of $C_{10}H_{16}N_2O_n$ likely involved $C_5H_8NO_5^\bullet$ as discussed above, the instantaneous
 566 increase may result from the increase of $C_5H_8NO_5^\bullet$ as well as other first-generation RO_2 . After the initial increase,
 567 $C_{10}H_{16}N_2O_{10-12}$ then decayed with time (Fig. 5) while $C_{10}H_{16}N_2O_{13-15}$ increased again in the later phase of a period
 568 besides and when NO_2 and O_3 were added. The second increase indicated that $C_{10}H_{16}N_2O_{13-15}$ may contain more
 569 than one isomers, which had different production pathways. As discussed above, $C_5H_8NO_n^\bullet$ can be either a first-
 570 generation RO_2 formed directly via the reaction of isoprene with NO_3 and autoxidation, or a second-generation RO_2 ,
 571 e.g. formed via the reaction of with $C_5H_8O_2$ with NO_3 . Therefore the second increase of $C_{10}H_{16}N_2O_{13-15}$ may result
 572 from the reaction of two first-generation RO_2 and of two second-generation RO_2 or between one first-generation
 573 and one second-generation RO_2 . The increase of $C_{10}H_{16}N_2O_{14-15}$ after isoprene addition was not obviouslarge,
 574 indicating the larger contributions from second-generation products compared with other $C_{10}H_{16}N_2O_n$. Overall,
 575 as the number of oxygen increased, the contribution of second-generation products to $C_{10}H_{16}N_2O_n$ increased.

576 In contrast to $C_{10}H_{16}N_2O_n$ series, $C_{10}H_{18}N_4O_n$ increased gradually after each isoprene addition and then
 577 decreased afterward (Fig. 6), either naturally or after isoprene additions, which is typical for second-generation
 578 products. Since $C_{10}H_{18}N_4O_n$ was likely formed by the accretion reaction of $C_5H_9N_2O_n^\bullet$ (RO_2), the time profile
 579 of $C_{10}H_{18}N_4O_n$ was as expected since $C_5H_9N_2O_n^\bullet$ was formed via the reaction of NO_3 with first-generation
 580 products $C_5H_9NO_n$. The $C_{10}H_{18}N_4O_n$ concentration depended on the product of the concentrations of two
 581 $C_5H_9N_2O_n^\bullet$. Taking $C_{10}H_{18}N_4O_{16}$ as an example, its concentration can be expressed as follows:

$$582 \quad \frac{d[C_{10}H_{18}N_4O_{16}]}{dt} = k[C_5H_9N_2O_9][C_5H_9N_2O_9] - k_w[C_{10}H_{18}N_4O_{16}]$$

583 When the concentration of $C_5H_9N_2O_9^\bullet$ increased, the changing rate of $C_{10}H_{18}N_4O_{16}$ was positive and increased
 584 and thus the concentration of $C_{10}H_{18}N_4O_{16}$ increased. When the concentration $C_5H_9N_2O_9^\bullet$ decreased sharply
 585 after isoprene additions, the changing rate of $C_{10}H_{18}N_4O_{16}$ decreased and even became negative values, and thus
 586 the concentration of $C_{10}H_{18}N_4O_{16}$ decreased after isoprene addition.

587 Similar to the $C_{10}H_{16}N_2O_n$ series, while $C_{10}H_{17}N_3O_n$ first increased instantaneously with isoprene
 588 addition, it increased again during the later stage of each period (Fig. [S9S10](#)), showing a mixed behavior of the
 589 first-generation products and second-generation products. The time series of $C_{10}H_{17}N_3O_n$ was as expected in
 590 general because $C_{10}H_{17}N_3O_n$ was likely formed via the accretion reaction of $C_5H_8NO_n^\bullet$ (M1 RO_2) and
 591 $C_5H_9N_2O_n^\bullet$ (M2 RO_2), which were first- or second-generation, and second-generation RO_2 , respectively,

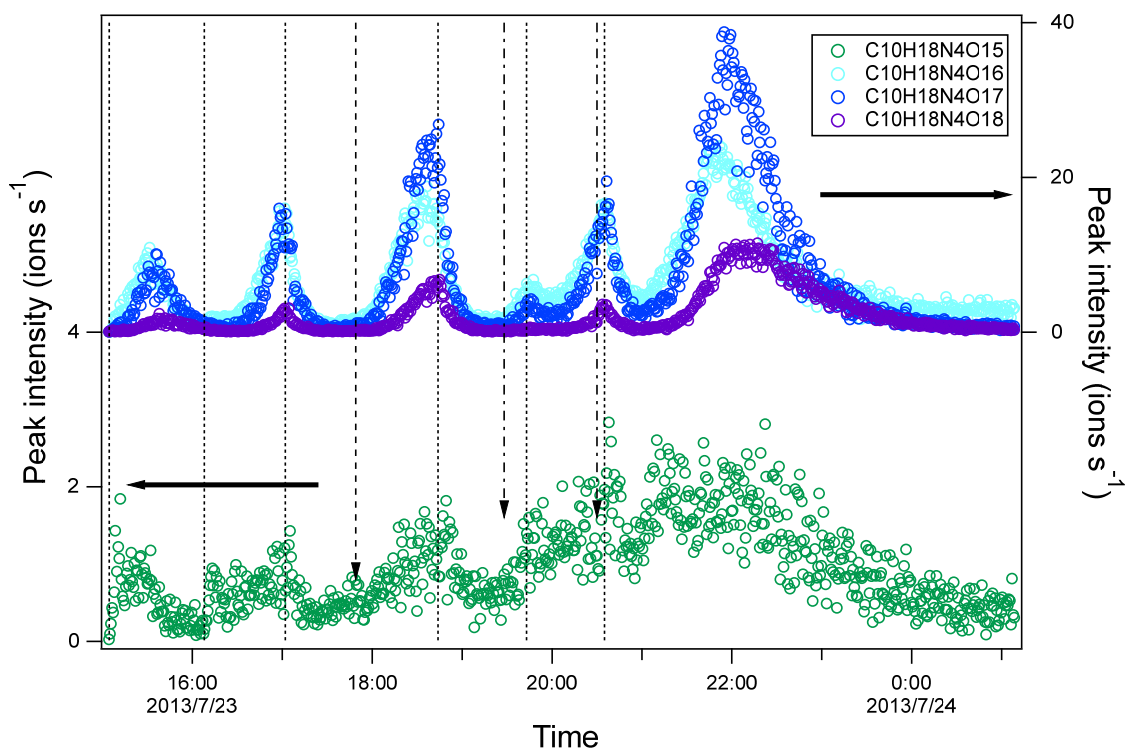
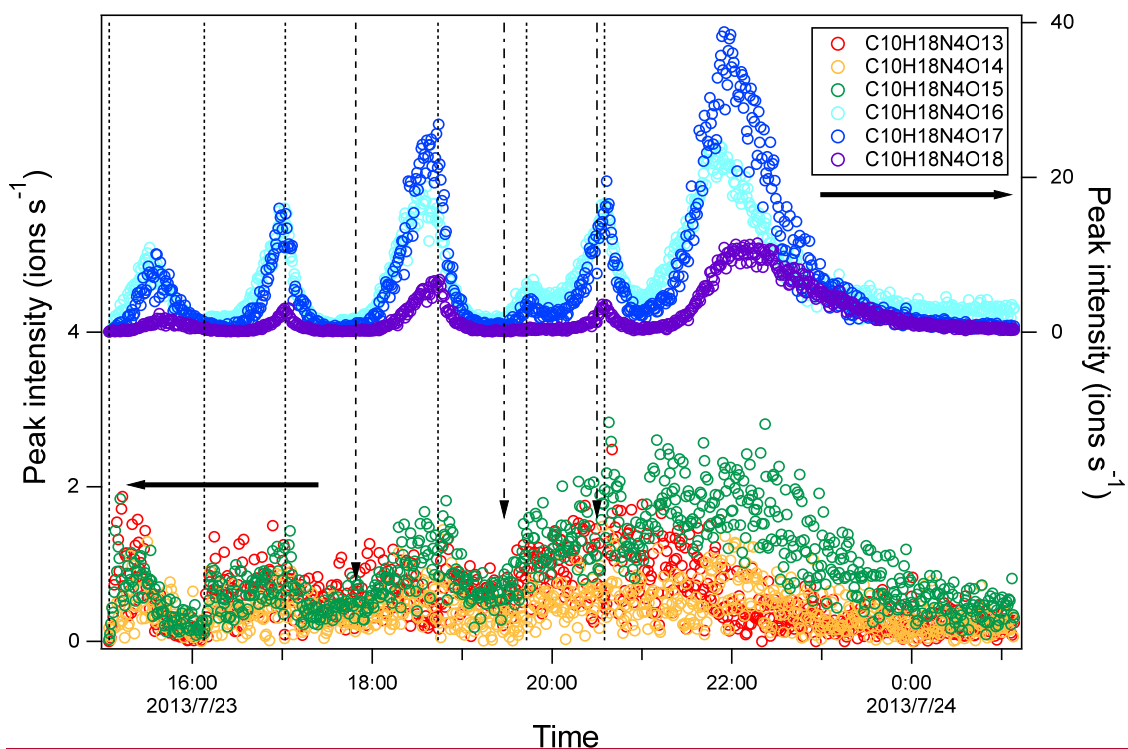


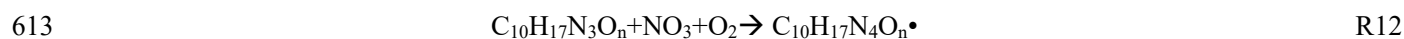
Figure 6. Time series of peak intensity of several HOM dimers of $C_{10}H_{18}N_4O_n$ series. The dashed lines indicate the time of isoprene additions. The long-dashed arrow indicates the time of NO_2 addition. The dash-dotted arrows indicate the time of O_3 additions. The horizontal arrows indicate y-axis scales for different markers.

Some dimers that cannot be explained by accretion reactions such as $C_{10}H_{16}N_3O_n$ ($n=12-15$), $C_{10}H_{17}N_2O_n$ ($n=11-12$), $C_{10}H_{16}NO_n$ ($n=10-16$), $C_{10}H_{15}NO_n$ ($n=9-12$), $C_{10}H_{17}NO_n$ ($n=11-15$) were also observed. These dimers had low abundance. We note that due to their low signals in the mass spectra, their assignment and thus range of n may be

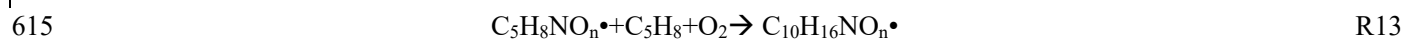
600 subject to uncertainties. Since $C_{10}H_{16}NO_n$ ($n=10-16$) \bullet , $C_{10}H_{16}N_3O_n$ ($n=12-15$) \bullet , and $C_{10}H_{17}N_2O_n$ \bullet contain unpaired
601 electrons, they cannot be formed via the direct accretion reaction of two RO_2 . Instead, $C_{10}H_{16}N_3O_n$ ($n=12-15$) \bullet (dimer
602 R1) and $C_{10}H_{17}N_2O_n$ \bullet (dimer R2) were likely RO_2 formed by the reaction of HOM dimers containing a double bond
603 (dimer 1) with NO_3 and with OH, respectively, followed by the reaction with O_2 .



606 The corresponding termination products of $C_{10}H_{16}N_3O_n$ \bullet RO_2 series such as $C_{10}H_{15}N_3O_n$ (ketone), $C_{10}H_{17}N_3O_n$
607 (hydroperoxide/alcohol) were also observed, although these compounds can also be formed via reactions between
608 two RO_2 radicals (R9 and R11). Among the termination products, $C_{10}H_{15}N_3O_n$ had low intensity. Reaction R13 and
609 the termination reaction of $C_{10}H_{17}N_2O_n$ \bullet with HO_2 provided an additional pathway to $C_{10}H_{17}N_3O_n$ besides the R9
610 pathway discussed above. Similarly, other dimers may also be formed by the termination reactions of dimer RO_2
611 with RO_2 or HO_2 . E.g., $C_{10}H_{18}N_4O_n$ can be formed via termination reaction of $C_{10}H_{17}N_4O_n$ \bullet with another RO_2 wherein
612 $C_{10}H_{17}N_4O_n$ \bullet can be formed as follows:



614 $C_{10}H_{16}NO_n$ ($n=10-14$) \bullet could be explained by the reaction of monomer RO_2 with isoprene.



616 Only $C_{10}H_{16}NO_n$ \bullet with $n \geq 10$ were detected, while according to the mechanism of self-reaction between $C_5H_8NO_n$ \bullet ,
617 the n range of $C_{10}H_{16}NO_n$ \bullet is expected to be 7-14. The absence of $C_{10}H_{16}NO_n$ ($n < 10$) \bullet is likely attributed to their low
618 abundance, which might result from low precursor concentrations, low reaction rates with isoprene, and/or faster
619 reactive losses with other radicals. It seems that only $C_5H_8NO_n$ \bullet with more than eight oxygen atoms reacted with
620 isoprene, because only $C_{10}H_{16}NO_n$ with $n > 8$ were detected. Such a reaction of RO_2 with isoprene has been proposed
621 by Ng et al. (2008) and Kwan et al. (2012). The corresponding termination products of $C_{10}H_{16}NO_n$ \bullet are $C_{10}H_{15}NO_n$
622 (ketone) and $C_{10}H_{17}NO_n$ species (hydroperoxide/alcohol). $C_{10}H_{17}NO_n$ species showed a time profile of typical first-
623 generation products (Fig. [S10S11](#)), i.e. increasing immediately with isoprene addition and then decaying with time.
624 This behaviour further supports the possibility of reaction R13. Yet, the reaction rate of alkene with RO_2 is likely low
625 due to the high activation energy (Stark, 1997, 2000). It is worth noting that to our knowledge no experimental kinetic
626 data on the addition of RO_2 to alkenes in the gas phase in atmospheric relevant conditions are available, though fast,
627 low-barrier ring closure reactions in unsaturated RO_2 radicals have been reported (Vereecken and Peeters, 2004, 2012;
628 Kaminski et al., 2017; Richters et al., 2017; Chen et al., 2021). We would like to note that there is unlikely interference
629 to C_{10} -HOM from monoterpenes, which has been reported previously (Bernhammer et al., 2018), as the concentration
630 of monoterpenes in the chamber during this study was below the limit of detection, which was ~ 50 ppt
631 (3 σ) (Bernhammer et al., 2018)

632 Some of the dimers discussed above have been observed in previous studies. Ng et al. (2008) found
633 $C_{10}H_{16}N_2O_8$ and $C_{10}H_{16}N_2O_9$ in the gas phase and $C_{10}H_{17}N_3O_{12}$, $C_{10}H_{17}N_3O_{13}$, $C_{10}H_{18}N_4O_{16}$, and $C_{10}H_{17}N_5O_{18}$ in the
634 particle phase. $C_{10}H_{16}N_2O_8$ and $C_{10}H_{16}N_2O_9$ were also observed in our study, but their intensity in the MS was too
635 low to assign molecular formulas with high confidence. The low intensity may be due to the low sensitivity of
636 $C_{10}H_{16}N_2O_{8,9}$ in NO_3^- -CIMS. According to modelling results of the products formed in cyclohexene ozonolysis by
637 Hyttinen et al. (2015), at least two hydrogen bond donor functional groups are needed for a compound to be detected

638 in a nitrate CIMS. As C₁₀H₁₆N₂O₈ and C₁₀H₁₆N₂O₉ have no and only one H-bond donor function groups, respectively,
 639 they are expected to have low sensitivity in NO₃⁻-CIMS. Moreover, the low intensity can be partly attributed to the
 640 much lower isoprene concentrations used in this study compared to previous studies, leading to the low concentration
 641 of C₁₀H₁₆N₂O₈ and C₁₀H₁₆N₂O₉ (Ng et al., 2008). C₁₀H₁₇N₃O₁₂, C₁₀H₁₇N₃O₁₃, C₁₀H₁₈N₄O₁₆, and C₁₀H₁₇N₅O₁₈ were
 642 all observed in the gas phase in this study, wherein the concentration of C₁₀H₁₇N₅O₁₈ was very low. The formation
 643 pathways of C₁₀H₁₇N₃O₁₂, C₁₀H₁₇N₃O₁₃, and C₁₀H₁₈N₄O₁₆ (R8) were generally similar to those proposed by Ng et al.
 644 (2008) except that the products from H-shift of RO₂ were involved in the formation of C₁₀H₁₇N₃O₁₃. Among the two
 645 pathways of C₁₀H₁₈N₄O₁₆ formation (R8 and via R12), our results indicate that R8 was the main pathway, based on
 646 the low concentrations of C₁₀H₁₇N₄O_{16/17}• and other termination product of them, C₁₀H₁₆N₄O_{15/16}. That the time
 647 profile of C₁₀H₁₈N₄O₁₆ was consistent with what is expected from R8 as discussed above offers additional evidence
 648 to that conclusion.

649 3.4 HOM trimers and their formation

650 A series of HOM trimers were observed, such as C₁₅H₂₄N₄O_n (n=17-23~~22~~), C₁₅H₂₅N₅O_n (n=20-22), C₁₅H₂₅N₃O_n
 651 (n=12~~13~~-20), C₁₅H₂₆N₄O_n (n=17-21), and C₁₅H₂₄N₂O_n (n=12-16). Among the trimers, C₁₅H₂₄N₄O_n (n=17-23~~22~~) was the most
 652 abundant series (Fig. ~~S4~~S12). The C₁₅H₂₄N₄O_n series can be explained by the accretion reaction of one
 653 monomer HOM RO₂ and one dimer HOM RO₂.



655 The formation pathways of dimer RO₂ C₁₀H₁₆N₃O_n (n=14~~12~~-20~~15~~) and C₁₀H₁₇N₂O_n are shown above (reaction
 656 ~~R14~~R10 and R11).

657 The other trimers were likely formed via similar pathways (Table 2 and Supplement S2). Since NO₃⁻-CIMS
 658 cannot provide the structural information of these HOM trimers, we cannot elucidate the major pathways. However,
 659 in all these pathways, dimer-RO₂ is necessary to form a trimer, and most of the dimer-RO₂ formation pathways
 660 require at least one double bond in the dimer molecule except for the reaction of RO₂ with isoprene. Since one
 661 double bond has already reacted in the monomer-RO₂ formation, we anticipate that in the reaction with NO₃ it is
 662 more favourable for precursors (VOC) containing more than one double bonds to form trimer molecules than
 663 precursors containing only one double bond, as it is easier to generate new RO₂ radicals from these dimers by
 664 attack on the remaining double bond(s).

665 The time profile of C₁₅H₂₄N₄O_n showed the mixed behavior of first- and second-generation products (Fig.
 666 S13), consistent with the mechanism discussed above since C₅H₈NO_n• and C₁₀H₁₆N₃O_n• were of first- or second-
 667 generation and second-generation, respectively. The contributions of the second-generation products became
 668 larger as the number of oxygen atoms increased. In contrast, C₁₅H₂₅N₃O_n showed instantaneous increase with
 669 isoprene addition (Fig. S14), which was typical for time profiles of first-generation products. Both proposed~~the~~
 670 formation pathways of C₁₅H₂₅N₃O_n (RS6 and RS7) contained a second-generation RO₂, which was not in line with
 671 the time profile observed. The observation cannot be well explained, unless we assume molecular adducts of a dimer
 672 with one monomer. It is also possible that some C₁₀H₁₇N₂O_n• were formed very fast or that there were other
 673 formation pathways of C₁₅H₂₅N₃O_n ~~that have not been~~ accounted for here.

674 3.5 Contributions of monomers, dimer, and trimers to HOM

675 The concentration (represented by peak intensity) of monomers was higher than that of dimers, but overall
676 their concentrations remained of the same order of magnitude (Fig 1a, inset). The concentration of trimers was much
677 lower than that of monomers and dimers. The relative contributions of monomers, dimers, and trimers evolved in
678 time due to the changing concentration of each HOM species. Comparing the contributions of various classes of
679 HOM in period 1 with those in periods 1-6 reveals that the relative contribution of monomers increased with time,
680 especially that of 2N-monomers, while the contribution of dimers decreased. This trend is attributed to the larger wall
681 loss of dimers compared to monomers because of their lower volatility and also to the continuous formation of
682 second-generation monomers, mostly 2N-monomers. Overall, the relative contribution of total HOM monomers
683 decreased immediately after isoprene addition while the contribution of HOM dimers increased rapidly (Fig. S14S15),
684 which was attributed to the faster increase of dimers intensity due to their rapid formation. Afterwards, the
685 contribution of monomers to total HOM gradually increased and that of dimers decreased, which was partly due to
686 the faster wall loss rate of dimers and to the continuous formation of second-generation monomers.

687 3.6 Yield of HOM

688 The HOM yield in the oxidation of isoprene by NO₃ was estimated using the sensitivity of H₂SO₄. It was
689 derived for the first isoprene addition period to minimize the contribution of multi-generation products and to better
690 compare with the data in literature, thus denoted as primary HOM yield (Pullinen et al., 2020) and was estimated to
691 be 1.2%^{+1.3%}_{-0.7%} ~~using the sensitivity of H₂SO₄ (Pullinen et al., 2020)~~. The uncertainty was estimated as shown in the
692 Supplement S1. Despite the uncertainty, the primary HOM yield here was much higher than the HOM yield from the
693 ozonolysis and photooxidation of isoprene (Jokinen et al., 2015). The difference may be attributed to the more
694 efficient oxygenation in the addition of NO₃ to carbon double bonds. Compared with the reaction with O₃ or OH, the
695 initial peroxy radicals contains 5 oxygen atoms when isoprene reacts with NO₃, while the initial peroxy radicals
696 contains only 3 oxygen atoms when reacting with OH, and the ozonide contains 3 oxygen atoms in the case of O₃.

697 4 Conclusion and implications

698 HOM formation in the reaction of isoprene with NO₃ was investigated in the SAPHIR chamber. A number
699 of HOM monomers, dimers, and trimers containing one to five nitrogen atoms were detected, and their time-
700 dependent concentration profiles were tracked throughout the experiment. ~~The~~ Some formation mechanisms ~~of~~ for
701 various HOM were proposed according to the molecular formula identified, and the available literature. HOM showed
702 a variety of time profiles with multiple isoprene additions during the reaction. First-generation HOM increased
703 instantaneously after isoprene addition and then decreased while second-generation HOM increased gradually and
704 then decreased with time, reaching a maximum concentration at the later stage of each period. The time profiles
705 provide additional constraints on their formation mechanism beside the molecular formula, suggesting whether they
706 were first-generation products or second-generation products or a combination of both. 1N-monomers (mostly C₅)
707 were likely formed by NO₃ addition to a double bond of isoprene, forming monomer RO₂, followed by autoxidation
708 and termination via the reaction with HO₂, RO₂, and NO₃. Time series suggest that some 1N-monomer could also be

709 formed by the reaction of first-generation products with NO_3 , and thus be of second-generation. 2N-monomers were
710 likely formed via the reaction of first-generation products such as C5-hydroxynitrate with NO_3 and thus second-
711 generation products. 3N-monomers likely comprised peroxy/peroxyacyl nitrates formed by the reaction of 2N-
712 monomer RO_2 with NO_2 , and possibly nitronitrates formed via the direct addition of N_2O_5 to the first-generation
713 products. HOM dimers were mostly formed by the accretion reactions between various HOM monomer RO_2 , either
714 first-generation or second-generation or with the contributions of both, and thus showed time profiles typical of either
715 first-generation products, or second-generation products, or a mixture-combination of both. Additionally, some
716 dimers peroxy radicals (dimer RO_2) were formed by the reaction of NO_3 dimer with NO_3 -dimers containing a C=C
717 double bond forming dimer RO_2 . HOM trimers were proposed to be formed by accretion reactions between the
718 monomer RO_2 and dimer $\text{RO}_{2,2}$, ~~the latter formed by the reaction of NO_3 with dimers containing a C=C double bond.~~

719 Overall, both HOM monomers and dimers contribute significantly to total HOM while trimers only
720 contributed a minor fraction. Within both the monomer and dimer compounds, a limited set of compounds dominated
721 the abundance, such as $\text{C}_5\text{H}_8\text{N}_2\text{O}_n$, $\text{C}_5\text{H}_{10}\text{N}_2\text{O}_n$, $\text{C}_{10}\text{H}_{17}\text{N}_3\text{O}_n$, and $\text{C}_{10}\text{H}_{16}\text{N}_2\text{O}_n$ series. 2N-monomers, which were
722 second-generation products, dominated in monomers and accounted for ~34% of all HOM, indicating the important
723 role of second-generation oxidation in HOM formation in the isoprene+ NO_3 reaction~~isoprene+ NO_3~~ . Both RO_2
724 autoxidation and “alkoxy-peroxy” pathways were found to be important for 1N- and 2N-HOM formation. In total,
725 the yield of HOM monomers, dimers, and trimers accounted for $1.3\%_{-0.7\%}^{+1.3\%}$ of the isoprene reacted, which was much
726 higher than the HOM yield in the oxidation of isoprene by OH and O_3 reported in the literature (Jokinen et al., 2015).
727 This means that the reaction of isoprene with NO_3 is a competitive pathway of HOM formation from isoprene.

728 The HOM in the reaction of isoprene with NO_3 may account for a significant fraction of SOA. If all the
729 HOM condense on particles, using the molecular weight of the HOM with the least molecular weight observed in
730 this study ($\text{C}_5\text{H}_9\text{NO}_6$), the HOM yield corresponds to a SOA yield of 3.6%. Although SOA concentrations were not
731 measured in this study, Ng et al. (2008) reported a SOA yield of the isoprene+ NO_3 reaction~~isoprene+ NO_3~~ of 4.3%-
732 23.8%. Rollins et al. (2009) reported a SOA yield of 2% at low organic aerosol loading ($\sim 0.52 \mu\text{g m}^{-3}$) and 14% if
733 the further oxidation of the first-generation products are considered in the isoprene+ NO_3 reaction~~isoprene+ NO_3~~ .
734 Comparing the potential SOA yield produced by HOM with SOA yields in the literature suggests that HOM may
735 play an important role in the SOA formation in the isoprene+ NO_3 reaction~~isoprene+ NO_3~~ .

736 The RO_2 lifetime is approximately 20-50 s in our experiments, which is generally comparable or shorter than
737 the lifetime of RO_2 in the ambient atmosphere at night, varying from several 10 s to several 100 s (Fry et al., 2018),
738 depending on the NO_3 , HO_2 , and RO_2 concentrations. Assuming a HO_2 , RO_2 , and NO_3 concentration of 5 ppt, 5 ppt
739 (Tan et al., 2019), and 300 ppt (Brown and Stutz, 2012) respectively, the RO_2 lifetime in our study is comparable to
740 the nighttime RO_2 lifetime (50 s) found in urban locations and areas influenced by urban plume. In areas with longer
741 RO_2 lifetime such as remote areas, the autoxidation is expected to be more important relative to bimolecular reactions.
742 This may enhance HOM yield and thus enhance SOA yield. However, on the other hand, at lower RO_2 concentration
743 and thus longer RO_2 lifetime, reduced rates of RO_2+RO_2 reactions producing low-volatility dimers can reduce the
744 SOA yield via reducing dimer yield (McFiggans et al., 2019; Pullinen et al., 2020). The RO_2 fate in our experiments
745 is dominated the reaction RO_2+NO_3 with significant contribution of RO_2+RO_2 , which can also represent the RO_2 fate

746 in the urban areas and areas influenced by urban plume. Our experiment condition cannot represent the chemistry in
747 HO₂-dominated regions such as clean forest environment (Schwantes et al., 2015).

748 We observed the second-generation products formed by the reaction of first-generation products. The
749 lifetime of first-generation nitrates in the ambient atmosphere, according their rate constants with OH and NO₃
750 (Wennberg et al., 2018), are ~5 h and ~1.3-4 h, respectively, with respect to the reaction with OH and NO₃ assuming
751 a typical OH concentration of 2×10⁶ molecules cm⁻³ (Lu et al., 2014; Tan et al., 2019) and NO₃ concentration of 100-
752 300 ppt in urban areas (Brown and Stutz, 2012). Therefore, they have the chance to react further with OH and NO₃
753 at dawn. In our experiments, the lifetimes of these first-generation nitrates with respect to OH and NO₃ are
754 comparable to the aforementioned lifetime due to comparable OH and NO₃ concentrations with these ambient
755 conditions. Therefore, our findings on the second-generation products are relevant to the ambient urban atmosphere
756 and areas influenced by urban plumes. Some of these products such as C₅H₈₁₀N₂O₈ and multi-generation
757 nitrooxyorganosulfates have been observed in recent field studies in polluted megacities in east China (Hamilton et
758 al., 2021; Xu et al., 2021).

759 **Data availability**

760 All the data in the figures of this study are available upon request to the corresponding author (t.mentel@fz-juelich.
761 de).

762 **Competing interests**

763 The authors declare that they have no conflict of interest.

764 **Author contribution**

765 TFM, HF, SS, DZ, IP, AW, and AKS designed the experiments. Instrument deployment and operation were carried
766 out by IP, HF, SS, IA, RT, FR, DZ, and RW. Data analysis was done by DZ, HF, SS, RW, IA, RT, FR, YG, SK. DZ,
767 TFM, RW, JW, SK, and LV interpreted the compiled data set. DZ and TFM wrote the paper. All co-authors discussed
768 the results and commented on the paper.

769 **Acknowledgements**

770 We thank the SAPHIR team for supporting our measurements and providing helpful data. D. Zhao and Y. Guo would
771 like to thank the support of National Natural Science Foundation of China (41875145). We would like to thank three
772 anonymous reviewers and Kristian Møller for their helpful comments.

References

- [Atkinson, R., Baulch, D. L., Cox, R. A., Crowley, J. N., Hampson, R. F., Hynes, R. G., Jenkin, M. E., Rossi, M. J., and Troe, J.: Evaluated kinetic and photochemical data for atmospheric chemistry: Volume II - gas phase reactions of organic species, *Atmos. Chem. Phys.*, 6, 3625-4055, 2006.](#)
- [Ayres, B. R., Allen, H. M., Draper, D. C., Brown, S. S., Wild, R. J., Jimenez, J. L., Day, D. A., Campuzano-Jost, P., Hu, W., de Gouw, J., Koss, A., Cohen, R. C., Duffey, K. C., Romer, P., Baumann, K., Edgerton, E., Takahama, S., Thornton, J. A., Lee, B. H., Lopez-Hilfiker, F. D., Mohr, C., Wennberg, P. O., Nguyen, T. B., Teng, A., Goldstein, A. H., Olson, K., and Fry, J. L.: Organic nitrate aerosol formation via \$\text{NO}_3\$ + biogenic volatile organic compounds in the southeastern United States, *Atmos. Chem. Phys.*, 15, 13377-13392, 10.5194/acp-15-13377-2015, 2015.](#)
- [Berndt, T., and Böge, O.: Gas-phase reaction of \$\text{NO}_3\$ radicals with isoprene: a kinetic and mechanistic study, *Int. J. Chem. Kinet.*, 29, 755-765, 10.1002/\(sici\)1097-4601\(1997\)29:10<755::Aid-kin4>3.0.Co;2-I, 1997.](#)
- [Berndt, T., Mender, B., Scholz, W., Fischer, L., Herrmann, H., Kulmala, M., and Hansel, A.: Accretion Product Formation from Ozonolysis and OH Radical Reaction of alpha-Pinene: Mechanistic Insight and the Influence of Isoprene and Ethylene, *Environ. Sci. Technol.*, 52, 11069-11077, 10.1021/acs.est.8b02210, 2018a.](#)
- [Berndt, T., Scholz, W., Mentler, B., Fischer, L., Herrmann, H., Kulmala, M., and Hansel, A.: Accretion Product Formation from Self- and Cross-Reactions of \$\text{RO}_2\$ Radicals in the Atmosphere, *Angew. Chem.-Int. Edit.*, 57, 3820-3824, 10.1002/anie.201710989, 2018b.](#)
- [Bernhammer, A. K., Fischer, L., Mentler, B., Heinritzi, M., Simon, M., and Hansel, A.: Production of highly oxygenated organic molecules \(HOMs\) from trace contaminants during isoprene oxidation, *Atmos. Meas. Tech.*, 11, 4763-4773, 10.5194/amt-11-4763-2018, 2018.](#)
- [Bianchi, F., Kurten, T., Riva, M., Mohr, C., Rissanen, M. P., Roldin, P., Berndt, T., Crouse, J. D., Wennberg, P. O., Mentel, T. F., Wildt, J., Junninen, H., Jokinen, T., Kulmala, M., Worsnop, D. R., Thornton, J. A., Donahue, N., Kjaergaard, H. G., and Ehn, M.: Highly Oxygenated Organic Molecules \(HOM\) from Gas-Phase Autoxidation Involving Peroxy Radicals: A Key Contributor to Atmospheric Aerosol, *Chem. Rev.*, 119, 3472-3509, 10.1021/acs.chemrev.8b00395, 2019.](#)
- [Boyd, C. M., Sanchez, J., Xu, L., Eugene, A. J., Nah, T., Tuet, W. Y., Guzman, M. I., and Ng, N. L.: Secondary organic aerosol formation from the beta-pinene+ \$\text{NO}_3\$ system: effect of humidity and peroxy radical fate, *Atmos. Chem. Phys.*, 15, 7497-7522, 10.5194/acp-15-7497-2015, 2015.](#)
- [Boyd, C. M., Nah, T., Xu, L., Berkemeier, T., and Ng, N. L.: Secondary Organic Aerosol \(SOA\) from Nitrate Radical Oxidation of Monoterpenes: Effects of Temperature, Dilution, and Humidity on Aerosol Formation, Mixing, and Evaporation, *Environ. Sci. Technol.*, 51, 7831-7841, 10.1021/acs.est.7b01460, 2017.](#)
- [Brown, S. S., deGouw, J. A., Warneke, C., Ryerson, T. B., Dube, W. P., Atlas, E., Weber, R. J., Peltier, R. E., Neuman, J. A., Roberts, J. M., Swanson, A., Flocke, F., McKeen, S. A., Brioude, J., Sommariva, R., Trainer, M., Fehsenfeld, F. C., and Ravishankara, A. R.: Nocturnal isoprene oxidation over the Northeast United States in summer and its impact on reactive nitrogen partitioning and secondary organic aerosol, *Atmos. Chem. Phys.*, 9, 3027-3042, 10.5194/acp-9-3027-2009, 2009.](#)
- [Brown, S. S., Dube, W. P., Peischl, J., Ryerson, T. B., Atlas, E., Warneke, C., de Gouw, J. A., Hekkert, S. t. L., Brock, C. A., Flocke, F., Trainer, M., Parrish, D. D., Fehsenfeld, F. C., and Ravishankara, A. R.: Budgets for nocturnal VOC oxidation by nitrate radicals aloft during the 2006 Texas Air Quality Study, *J. Geophys. Res.-Atmos.*, 116, 10.1029/2011jd016544, 2011.](#)

[Brown, S. S., and Stutz, J.: Nighttime radical observations and chemistry, Chem. Soc. Rev., 41, 6405-6447, 10.1039/c2cs35181a, 2012.](#)

[Chen, J., Møller, K. H., Wennberg, P. O., and Kjaergaard, H. G.: Unimolecular Reactions Following Indoor and Outdoor Limonene Ozonolysis, J. Phys. Chem. A 125, 669-680, 10.1021/acs.jpca.0c09882, 2021.](#)

[Claflin, M. S., and Ziemann, P. J.: Identification and Quantitation of Aerosol Products of the Reaction of \$\beta\$ -Pinene with \$\text{NO}_3\$ Radicals and Implications for Gas- and Particle-Phase Reaction Mechanisms, The Journal of Physical Chemistry A, 122, 3640-3652, 10.1021/acs.jpca.8b00692, 2018.](#)

[Crouse, J. D., Knap, H. C., Ørnso, K. B., Jørgensen, S., Paulot, F., Kjaergaard, H. G., and Wennberg, P. O.: Atmospheric Fate of Methacrolein. 1. Peroxy Radical Isomerization Following Addition of OH and \$\text{O}_2\$, The Journal of Physical Chemistry A, 116, 5756-5762, 10.1021/jp211560u, 2012.](#)

[Crouse, J. D., Nielsen, L. B., Jørgensen, S., Kjaergaard, H. G., and Wennberg, P. O.: Autoxidation of Organic Compounds in the Atmosphere, J. Phys. Chem. Lett., 4, 3513-3520, 10.1021/jz4019207, 2013.](#)

[Draper, D. C., Myllys, N., Hyttinen, N., Møller, K. H., Kjaergaard, H. G., Fry, J. L., Smith, J. N., and Kurten, T.: Formation of Highly Oxidized Molecules from \$\text{NO}_3\$ Radical Initiated Oxidation of Delta-3-Carene: A Mechanistic Study, Acs Earth and Space Chemistry, 3, 1460-1470, 10.1021/acsearthspacechem.9b00143, 2019.](#)

[Ehn, M., Thornton, J. A., Kleist, E., Sipila, M., Junninen, H., Pullinen, I., Springer, M., Rubach, F., Tillmann, R., Lee, B., Lopez-Hilfiker, F., Andres, S., Acir, I. H., Rissanen, M., Jokinen, T., Schobesberger, S., Kangasluoma, J., Kontkanen, J., Nieminen, T., Kurten, T., Nielsen, L. B., Jørgensen, S., Kjaergaard, H. G., Canagaratna, M., Dal Maso, M., Berndt, T., Petaja, T., Wahner, A., Kerminen, V. M., Kulmala, M., Worsnop, D. R., Wildt, J., and Mentel, T. F.: A large source of low-volatility secondary organic aerosol, Nature, 506, 476-479, 10.1038/nature13032, 2014.](#)

[Ehn, M., Berndt, T., Wildt, J., and Mentel, T.: Highly Oxygenated Molecules from Atmospheric Autoxidation of Hydrocarbons: A Prominent Challenge for Chemical Kinetics Studies, Int. J. Chem. Kinet., 49, 821-831, 10.1002/kin.21130, 2017.](#)

[Eisele, F. L., and Tanner, D. J.: Measurement of the gas phase concentration of \$\text{H}_2\text{SO}_4\$ and methane sulfonic acid and estimates of \$\text{H}_2\text{SO}_4\$ production and loss in the atmosphere, 98, 9001-9010, 10.1029/93jd00031, 1993.](#)

[Faxon, C., Hammes, J., Le Breton, M., Pathak, R. K., and Hallquist, M.: Characterization of organic nitrate constituents of secondary organic aerosol \(SOA\) from nitrate-radical-initiated oxidation of limonene using high-resolution chemical ionization mass spectrometry, Atmos. Chem. Phys., 18, 5467-5481, 10.5194/acp-18-5467-2018, 2018.](#)

[Finlayson-Pitts, B., and Pitts, J.: Chemistry of the upper and lower atmosphere, Academic Press, San Diego, 2000.](#)

[Fry, J. L., Kiendler-Scharr, A., Rollins, A. W., Wooldridge, P. J., Brown, S. S., Fuchs, H., Dube, W., Mensah, A., dal Maso, M., Tillmann, R., Dorn, H. P., Brauers, T., and Cohen, R. C.: Organic nitrate and secondary organic aerosol yield from \$\text{NO}_3\$ oxidation of beta-pinene evaluated using a gas-phase kinetics/aerosol partitioning model, Atmos. Chem. Phys., 9, 1431-1449, 2009.](#)

[Fry, J. L., Kiendler-Scharr, A., Rollins, A. W., Brauers, T., Brown, S. S., Dorn, H. P., Dube, W. P., Fuchs, H., Mensah, A., Rohrer, F., Tillmann, R., Wahner, A., Wooldridge, P. J., and Cohen, R. C.: SOA from limonene: role of \$\text{NO}_3\$ in its generation and degradation, Atmos. Chem. Phys., 11, 3879-3894, 10.5194/acp-11-3879-2011, 2011.](#)

[Fry, J. L., Draper, D. C., Barsanti, K. C., Smith, J. N., Ortega, J., Winkle, P. M., Lawler, M. J., Brown, S. S., Edwards, P. M., Cohen, R. C., and Lee, L.: Secondary Organic Aerosol Formation and Organic Nitrate Yield from \$\text{NO}_3\$ Oxidation of Biogenic Hydrocarbons, Environ. Sci. Technol., 48, 11944-11953, 10.1021/es502204x, 2014.](#)

[Fry, J. L., Brown, S. S., Middlebrook, A. M., Edwards, P. M., Campuzano-Jost, P., Day, D. A., Jimenez, J. L., Allen, H. M., Ryerson, T. B., Pollack, I., Graus, M., Warneke, C., de Gouw, J. A., Brock, C. A., Gilman, J., Lerner, B. M., Dube, W. P., Liao, J., and Welti, A.: Secondary organic aerosol \(SOA\) yields from NO₃ radical + isoprene based on nighttime aircraft power plant plume transects, *Atmos. Chem. Phys.*, 18, 11663-11682, 10.5194/acp-18-11663-2018, 2018.](#)

[Fuchs, H., Dorn, H. P., Bachner, M., Bohn, B., Brauers, T., Gomm, S., Hofzumahaus, A., Holland, F., Nehr, S., Rohrer, F., Tillmann, R., and Wahner, A.: Comparison of OH concentration measurements by DOAS and LIF during SAPHIR chamber experiments at high OH reactivity and low NO concentration, *Atmos. Meas. Tech.*, 5, 1611-1626, 10.5194/amt-5-1611-2012, 2012.](#)

[Garmash, O., Rissanen, M. P., Pullinen, I., Schmitt, S., Kausiala, O., Tillmann, R., Percival, C., Bannan, T. J., Priestley, M., Hallquist, Å. M., Kleist, E., Kiendler-Scharr, A., Hallquist, M., Berndt, T., McFiggans, G., Wildt, J., Mentel, T., and Ehn, M.: Multi-generation OH oxidation as a source for highly oxygenated organic molecules from aromatics, *Atmos. Chem. Phys. Discuss.*, 2019, 1-33, 10.5194/acp-2019-582, 2019.](#)

[Geyer, A., Alicke, B., Konrad, S., Schmitz, T., Stutz, J., and Platt, U.: Chemistry and oxidation capacity of the nitrate radical in the continental boundary layer near Berlin, *J. Geophys. Res.-Atmos.*, 106, 8013-8025, 10.1029/2000jd900681, 2001.](#)

[Hamilton, J. F., Bryant, D. J., Edwards, P. M., Ouyang, B., Bannan, T. J., Mehra, A., Mayhew, A. W., Hopkins, J. R., Dunmore, R. E., Squires, F. A., Lee, J. D., Newland, M. J., Worrall, S. D., Bacak, A., Coe, H., Percival, C., Whalley, L. K., Heard, D. E., Slater, E. J., Jones, R. L., Cui, T., Surratt, J. D., Reeves, C. E., Mills, G. P., Grimmond, S., Sun, Y., Xu, W., Shi, Z., and Rickard, A. R.: Key Role of NO₃ Radicals in the Production of Isoprene Nitrates and Nitrooxyorganosulfates in Beijing, *Environ. Sci. Technol.*, 55, 842-853, 10.1021/acs.est.0c05689, 2021.](#)

[Huang, W., Saathoff, H., Shen, X. L., Ramisetty, R., Leisner, T., and Mohr, C.: Chemical Characterization of Highly Functionalized Organonitrates Contributing to Night-Time Organic Aerosol Mass Loadings and Particle Growth, *Environ. Sci. Technol.*, 53, 1165-1174, 10.1021/acs.est.8b05826, 2019.](#)

[Hyttinen, N., Kupiainen-Määttä, O., Rissanen, M. P., Muuronen, M., Ehn, M., and Kurtén, T.: Modeling the Charging of Highly Oxidized Cyclohexene Ozonolysis Products Using Nitrate-Based Chemical Ionization, *The Journal of Physical Chemistry A*, 119, 6339-6345, 10.1021/acs.jpca.5b01818, 2015.](#)

[Japar, S. M., and Niki, H.: Gas-phase reactions of the nitrate radical with olefins, *The Journal of Physical Chemistry*, 79, 1629-1632, 10.1021/j100583a002, 1975.](#)

[Jenkin, M. E., Saunders, S. M., and Pilling, M. J.: The tropospheric degradation of volatile organic compounds: A protocol for mechanism development, *Atmos. Environ.*, 31, 81-104, 10.1016/s1352-2310\(96\)00105-7, 1997.](#)

[Jenkin, M. E., Boyd, A. A., and Lesclaux, R.: Peroxy Radical Kinetics Resulting from the OH-Initiated Oxidation of 1,3-Butadiene, 2,3-Dimethyl-1,3-Butadiene and Isoprene, *J. Atmos. Chem.*, 29, 267-298, 10.1023/A:1005940332441, 1998.](#)

[Jenkin, M. E., Saunders, S. M., Wagner, V., and Pilling, M. J.: Protocol for the development of the Master Chemical Mechanism, MCM v3 \(Part B\): tropospheric degradation of aromatic volatile organic compounds, *Atmos. Chem. Phys.*, 3, 181-193, 2003.](#)

[Jenkin, M. E., Young, J. C., and Rickard, A. R.: The MCM v3.3.1 degradation scheme for isoprene, *Atmos. Chem. Phys.*, 15, 11433-11459, 10.5194/acp-15-11433-2015, 2015.](#)

[Jokinen, T., Sipila, M., Junninen, H., Ehn, M., Lonn, G., Hakala, J., Petaja, T., Mauldin, R. L., III, Kulmala, M., and Worsnop, D. R.: Atmospheric sulphuric acid and neutral cluster measurements using CI-API-TOF, *Atmos. Chem. Phys.*, 12, 4117-4125, 10.5194/acp-12-4117-2012, 2012.](#)

[Jokinen, T., Sipila, M., Richters, S., Kerminen, V. M., Paasonen, P., Stratmann, F., Worsnop, D., Kulmala, M., Ehn, M., Herrmann, H., and Berndt, T.: Rapid Autoxidation Forms Highly Oxidized RO₂ Radicals in the Atmosphere, *Angew. Chem.-Int. Edit.*, 53, 14596-14600, 10.1002/anie.201408566, 2014.](#)

[Jokinen, T., Berndt, T., Makkonen, R., Kerminen, V. M., Junninen, H., Paasonen, P., Stratmann, F., Herrmann, H., Guenther, A. B., Worsnop, D. R., Kulmala, M., Ehn, M., and Sipila, M.: Production of extremely low volatile organic compounds from biogenic emissions: Measured yields and atmospheric implications, *Proc. Nat. Acad. Sci. U.S.A.*, 112, 7123-7128, 10.1073/pnas.1423977112, 2015.](#)

[Kaminski, M., Fuchs, H., Acir, I.-H., Bohn, B., Brauers, T., Dorn, H.-P., Haeseler, R., Hofzumahaus, A., Li, X., Lutz, A., Nehr, S., Rohrer, F., Tillmann, R., Vereecken, L., Wegener, R., and Wahner, A.: Investigation of the beta-pinene photooxidation by OH in the atmosphere simulation chamber SAPHIR, *Atmos. Chem. Phys.*, 17, 6631-6650, 10.5194/acp-17-6631-2017, 2017.](#)

[Kenseth, C. M., Huang, Y. L., Zhao, R., Dalleska, N. F., Hethcox, C., Stoltz, B. M., and Seinfeld, J. H.: Synergistic O₃ + OH oxidation pathway to extremely low-volatility dimers revealed in beta-pinene secondary organic aerosol, *Proc. Nat. Acad. Sci. U.S.A.*, 115, 8301-8306, 10.1073/pnas.1804671115, 2018.](#)

[Kirkby, J., Duplissy, J., Sengupta, K., Frege, C., Gordon, H., Williamson, C., Heinritzi, M., Simon, M., Yan, C., Almeida, J., Tröstl, J., Nieminen, T., Ortega, I. K., Wagner, R., Adamov, A., Amorim, A., Bernhammer, A.-K., Bianchi, F., Breitenlechner, M., Brilke, S., Chen, X., Craven, J., Dias, A., Ehrhart, S., Flagan, R. C., Franchin, A., Fuchs, C., Guida, R., Hakala, J., Hoyle, C. R., Jokinen, T., Junninen, H., Kangasluoma, J., Kim, J., Krapf, M., Kürten, A., Laaksonen, A., Lehtipalo, K., Makhmutov, V., Mathot, S., Molteni, U., Onnela, A., Peräkylä, O., Piel, F., Petäjä, T., Praplan, A. P., Pringle, K., Rap, A., Richards, N. A. D., Riipinen, I., Rissanen, M. P., Rondo, L., Sarnela, N., Schobesberger, S., Scott, C. E., Seinfeld, J. H., Sipilä, M., Steiner, G., Stozhkov, Y., Stratmann, F., Tomé, A., Virtanen, A., Vogel, A. L., Wagner, A. C., Wagner, P. E., Weingartner, E., Wimmer, D., Winkler, P. M., Ye, P., Zhang, X., Hansel, A., Dommen, J., Donahue, N. M., Worsnop, D. R., Baltensperger, U., Kulmala, M., Carslaw, K. S., and Curtius, J.: Ion-induced nucleation of pure biogenic particles, *Nature*, 533, 521-526, 10.1038/nature17953, 2016.](#)

[Krechmer, J. E., Coggon, M. M., Massoli, P., Nguyen, T. B., Crounse, J. D., Hu, W. W., Day, D. A., Tyndall, G. S., Henze, D. K., Rivera-Rios, J. C., Nowak, J. B., Kimmel, J. R., Mauldin, R. L., Stark, H., Jayne, J. T., Sipila, M., Junninen, H., St Clair, J. M., Zhang, X., Feiner, P. A., Zhang, L., Miller, D. O., Brune, W. H., Keutsch, F. N., Wennberg, P. O., Seinfeld, J. H., Worsnop, D. R., Jimenez, J. L., and Canagaratna, M. R.: Formation of Low Volatility Organic Compounds and Secondary Organic Aerosol from Isoprene Hydroxyhydroperoxide Low-NO Oxidation, *Environ. Sci. Technol.*, 49, 10330-10339, 10.1021/acs.est.5b02031, 2015.](#)

[Kwan, A. J., Chan, A. W. H., Ng, N. L., Kjaergaard, H. G., Seinfeld, J. H., and Wennberg, P. O.: Peroxy radical chemistry and OH radical production during the NO₃-initiated oxidation of isoprene, *Atmos. Chem. Phys.*, 12, 7499-7515, 10.5194/acp-12-7499-2012, 2012.](#)

[Lai, C. C., and Finlayson-Pitts, B. J.: Reactions of dinitrogen pentoxide and nitrogen-dioxide with 1-palmitoyl-2-oleoyl-sn-glycero-3-phosphocholine, *Lipids*, 26, 306-314, 10.1007/bf02537142, 1991.](#)

[Lee, B. H., Mohr, C., Lopez-Hilfiker, F. D., Lutz, A., Hallquist, M., Lee, L., Romer, P., Cohen, R. C., Iyer, S., Kurten, T., Hu, W., Day, D. A., Campuzano-Jost, P., Jimenez, J. L., Xu, L., Ng, N. L., Guo, H., Weber, R. J., Wild, R. J., Brown, S. S., Koss, A., de Gouw, J., Olson, K., Goldstein, A. H., Seco, R., Kim, S., McAvey, K., Shepson, P. B.,](#)

[Starn, T., Baumann, K., Edgerton, E. S., Liu, J., Shilling, J. E., Miller, D. O., Brune, W., Schobesberger, S., D'Ambro, E. L., and Thornton, J. A.: Highly functionalized organic nitrates in the southeast United States: Contribution to secondary organic aerosol and reactive nitrogen budgets, Proc. Nat. Acad. Sci. U.S.A., 113, 1516-1521, 10.1073/pnas.1508108113, 2016.](#)

[Lu, K. D., Rohrer, F., Holland, F., Fuchs, H., Brauers, T., Oebel, A., Dlugi, R., Hu, M., Li, X., Lou, S. R., Shao, M., Zhu, T., Wahner, A., Zhang, Y. H., and Hofzumahaus, A.: Nighttime observation and chemistry of HO_x in the Pearl River Delta and Beijing in summer 2006, Atmos. Chem. Phys., 14, 4979-4999, 10.5194/acp-14-4979-2014, 2014.](#)

[Malkin, T. L., Goddard, A., Heard, D. E., and Seakins, P. W.: Measurements of OH and HO₂ yields from the gas phase ozonolysis of isoprene, Atmos. Chem. Phys., 10, 1441-1459, 10.5194/acp-10-1441-2010, 2010.](#)

[McFiggans, G., Mentel, T. F., Wildt, J., Pullinen, I., Kang, S., Kleist, E., Schmitt, S., Springer, M., Tillmann, R., Wu, C., Zhao, D., Hallquist, M., Faxon, C., Le Breton, M., Hallquist, Å. M., Simpson, D., Bergström, R., Jenkin, M. E., Ehn, M., Thornton, J. A., Alfarra, M. R., Bannan, T. J., Percival, C. J., Priestley, M., Topping, D., and Kiendler-Scharr, A.: Secondary organic aerosol reduced by mixture of atmospheric vapours, Nature, 565, 587-593, 10.1038/s41586-018-0871-y, 2019.](#)

[Mentel, T. F., Springer, M., Ehn, M., Kleist, E., Pullinen, I., Kurten, T., Rissanen, M., Wahner, A., and Wildt, J.: Formation of highly oxidized multifunctional compounds: autoxidation of peroxy radicals formed in the ozonolysis of alkenes - deduced from structure-product relationships, Atmos. Chem. Phys., 15, 6745-6765, 10.5194/acp-15-6745-2015, 2015.](#)

[Møller, K. H., Bates, K. H., and Kjaergaard, H. G.: The Importance of Peroxy Radical Hydrogen-Shift Reactions in Atmospheric Isoprene Oxidation, J. Phys. Chem. A 123, 920-932, 10.1021/acs.jpca.8b10432, 2019.](#)

[Molteni, U., Bianchi, F., Klein, F., El Haddad, I., Frege, C., Rossi, M. J., Dommen, J., and Baltensperger, U.: Formation of highly oxygenated organic molecules from aromatic compounds, Atmos. Chem. Phys., 18, 1909-1921, 10.5194/acp-18-1909-2018, 2018.](#)

[Molteni, U., Simon, M., Heinritzi, M., Hoyle, C. R., Bernhammer, A. K., Bianchi, F., Breitenlechner, M., Brilke, S., Dias, A., Duplissy, J., Frege, C., Gordon, H., Heyn, C., Jokinen, T., Kurten, A., Lehtipalo, K., Makhmutov, V., Petaja, T., Pieber, S. M., Praplan, A. P., Schobesberger, S., Steiner, G., Stozhkov, Y., Tome, A., Trostl, J., Wagner, A. C., Wagner, R., Williamson, C., Yan, C., Baltensperger, U., Curtius, J., Donahue, N. M., Hansel, A., Kirkby, J., Kulmala, M., Worsnop, D. R., and Dommen, J.: Formation of Highly Oxygenated Organic Molecules from alpha-Pinene Ozonolysis: Chemical Characteristics, Mechanism, and Kinetic Model Development, ACS Earth and Space Chemistry, 3, 873-883, 10.1021/acsearthspacechem.9b00035, 2019.](#)

[Nah, T., Sanchez, J., Boyd, C. M., and Ng, N. L.: Photochemical Aging of alpha-pinene and beta-pinene Secondary Organic Aerosol formed from Nitrate Radical Oxidation, Environ. Sci. Technol., 50, 222-231, 10.1021/acs.est.5b04594, 2016.](#)

[Ng, N. L., Kwan, A. J., Surratt, J. D., Chan, A. W. H., Chhabra, P. S., Sorooshian, A., Pye, H. O. T., Crounse, J. D., Wennberg, P. O., Flagan, R. C., and Seinfeld, J. H.: Secondary organic aerosol \(SOA\) formation from reaction of isoprene with nitrate radicals \(NO₃\), Atmos. Chem. Phys., 8, 4117-4140, 10.5194/acp-8-4117-2008, 2008.](#)

[Nguyen, T. B., Tyndall, G. S., Crounse, J. D., Teng, A. P., Bates, K. H., Schwantes, R. H., Coggon, M. M., Zhang, L., Feiner, P., Miller, D. O., Skog, K. M., Rivera-Rios, J. C., Dorris, M., Olson, K. F., Koss, A., Wild, R. J., Brown, S. S., Goldstein, A. H., de Gouw, J. A., Brune, W. H., Keutsch, F. N., Seinfeld, J. H., and Wennberg, P. O.: Atmospheric fates of Criegee intermediates in the ozonolysis of isoprene, Phys. Chem. Chem. Phys., 18, 10241-10254, 10.1039/c6cp00053c, 2016.](#)

[Novelli, A., Cho, C., Fuchs, H., Hofzumahaus, A., Rohrer, F., Tillmann, R., Kiendler-Scharr, A., Wahner, A., and Vereecken, L.: Experimental and theoretical study on the impact of a nitrate group on the chemistry of alkoxy radicals, *Phys. Chem. Chem. Phys.*, 23, 5474-5495, 10.1039/D0CP05555G, 2021.](#)

[Nozière, B., and Vereecken, L.: Direct Observation of Aliphatic Peroxy Radical Autoxidation and Water Effects: An Experimental and Theoretical Study, *Angew. Chem.-Int. Edit.*, 58, 13976-13982, 10.1002/anie.201907981, 2019.](#)

[Perring, A. E., Wisthaler, A., Graus, M., Wooldridge, P. J., Lockwood, A. L., Mielke, L. H., Shepson, P. B., Hansel, A., and Cohen, R. C.: A product study of the isoprene+NO₃ reaction, *Atmos. Chem. Phys.*, 9, 4945-4956, 10.5194/acp-9-4945-2009, 2009.](#)

[Pfrang, C., Martin, R. S., Canosa-Mas, C. E., and Wayne, R. P.: Gas-phase reactions of NO₃ and N₂O₅ with \(Z\)-hex-4-en-1-ol, \(Z\)-hex-3-en-1-ol \('leaf alcohol'\), \(E\)-hex-3-en-1-ol, \(Z\)-hex-2-en-1-ol and \(E\)-hex-2-en-1-ol, *Phys. Chem. Chem. Phys.*, 8, 354-363, 10.1039/b510835g, 2006.](#)

[Pullinen, I., Schmitt, S., Kang, S., Sarrafzadeh, M., Schlag, P., Andres, S., Kleist, E., Mentel, T. F., Rohrer, F., Springer, M., Tillmann, R., Wildt, J., Wu, C., Zhao, D., Wahner, A., and Kiendler-Scharr, A.: Impact of NO_x on secondary organic aerosol \(SOA\) formation from \$\alpha\$ -pinene and \$\beta\$ -pinene photooxidation: the role of highly oxygenated organic nitrates, *Atmos. Chem. Phys.*, 20, 10125-10147, 10.5194/acp-20-10125-2020, 2020.](#)

[Quelever, L. L. J., Kristensen, K., Jensen, L. N., Rosati, B., Teiwes, R., Daellenbach, K. R., Perakyla, O., Roldin, P., Bossi, R., Pedersen, H. B., Glasius, M., Bilde, M., and Ehn, M.: Effect of temperature on the formation of highly oxygenated organic molecules \(HOMs\) from alpha-pinene ozonolysis, *Atmos. Chem. Phys.*, 19, 7609-7625, 10.5194/acp-19-7609-2019, 2019.](#)

[Richters, S., Pfeifle, M., Olzmann, M., and Berndt, T.: endo-Cyclization of unsaturated RO₂ radicals from the gas-phase ozonolysis of cyclohexadienes, *Chem. Commun.*, 53, 4132-4135, 10.1039/c7cc01350g, 2017.](#)

[Rissanen, M. P., Kurten, T., Sipila, M., Thornton, J. A., Kangasluoma, J., Sarnela, N., Junninen, H., Jørgensen, S., Schallhart, S., Kajos, M. K., Taipale, R., Springer, M., Mentel, T. F., Ruuskanen, T., Petaja, T., Worsnop, D. R., Kjaergaard, H. G., and Ehn, M.: The Formation of Highly Oxidized Multifunctional Products in the Ozonolysis of Cyclohexene, *J. Am. Chem. Soc.*, 136, 15596-15606, 10.1021/ja507146s, 2014.](#)

[Rissanen, M. P., Kurten, T., Sipila, M., Thornton, J. A., Kausiala, O., Garmash, O., Kjaergaard, H. G., Petaja, T., Worsnop, D. R., Ehn, M., and Kulmala, M.: Effects of Chemical Complexity on the Autoxidation Mechanisms of Endocyclic Alkene Ozonolysis Products: From Methylcyclohexenes toward Understanding alpha-Pinene, *J. Phys. Chem. A* 119, 4633-4650, 10.1021/jp510966g, 2015.](#)

[Riva, M., Rantala, P., Krechmer, J. E., Perakyla, O., Zhang, Y. J., Heikkinen, L., Garmash, O., Yan, C., Kulmala, M., Worsnop, D., and Ehn, M.: Evaluating the performance of five different chemical ionization techniques for detecting gaseous oxygenated organic species, *Atmos. Meas. Tech.*, 12, 2403-2421, 10.5194/amt-12-2403-2019, 2019.](#)

[Rohrer, F., Bohn, B., Brauers, T., Bruning, D., Johnen, F. J., Wahner, A., and Kleffmann, J.: Characterisation of the photolytic HONO-source in the atmosphere simulation chamber SAPHIR, *Atmos. Chem. Phys.*, 5, 2189-2201, 2005.](#)

[Rollins, A. W., Kiendler-Scharr, A., Fry, J. L., Brauers, T., Brown, S. S., Dorn, H. P., Dube, W. P., Fuchs, H., Mensah, A., Mentel, T. F., Rohrer, F., Tillmann, R., Wegener, R., Wooldridge, P. J., and Cohen, R. C.: Isoprene oxidation by nitrate radical: alkyl nitrate and secondary organic aerosol yields, *Atmos. Chem. Phys.*, 9, 6685-6703, 2009.](#)

[Saunders, S. M., Jenkin, M. E., Derwent, R. G., and Pilling, M. J.: Protocol for the development of the Master Chemical Mechanism, MCM v3 \(Part A\): tropospheric degradation of non-aromatic volatile organic compounds, *Atmos. Chem. Phys.*, 3, 161-180, 2003.](#)

[Schwantes, R. H., Teng, A. P., Nguyen, T. B., Coggon, M. M., Crouse, J. D., St Clair, J. M., Zhang, X., Schilling, K. A., Seinfeld, J. H., and Wennberg, P. O.: Isoprene NO₃ Oxidation Products from the RO₂ + HO₂ Pathway, J. Phys. Chem. A 119, 10158-10171, 10.1021/acs.jpca.5b06355, 2015.](#)

[Skov, H., Hjorth, J., Lohse, C., Jensen, N. R., and Restelli, G.: Products and mechanisms of the reactions of the nitrate radical \(NO₃\) with isoprene, 1,3-butadiene and 2,3-dimethyl-1,3-butadiene in air, Atmospheric Environment. Part A. General Topics, 26, 2771-2783, \[https://doi.org/10.1016/0960-1686\\(92\\)90015-D\]\(https://doi.org/10.1016/0960-1686\(92\)90015-D\), 1992.](#)

[Stark, M. S.: Epoxidation of Alkenes by Peroxyl Radicals in the Gas Phase: Structure–Activity Relationships, The Journal of Physical Chemistry A, 101, 8296-8301, 10.1021/jp972054+, 1997.](#)

[Stark, M. S.: Addition of Peroxyl Radicals to Alkenes and the Reaction of Oxygen with Alkyl Radicals, J. Am. Chem. Soc., 122, 4162-4170, 10.1021/ja993760m, 2000.](#)

[Starn, T. K., Shepson, P. B., Bertman, S. B., Riemer, D. D., Zika, R. G., and Olszyna, K.: Nighttime isoprene chemistry at an urban-impacted forest site, 103, 22437-22447, <https://doi.org/10.1029/98JD01201>, 1998.](#)

[Stroud, C. A., Roberts, J. M., Williams, E. J., Hereid, D., Angevine, W. M., Fehsenfeld, F. C., Wisthaler, A., Hansel, A., Martinez-Harder, M., Harder, H., Brune, W. H., Hoenninger, G., Stutz, J., and White, A. B.: Nighttime isoprene trends at an urban forested site during the 1999 Southern Oxidant Study, 107, ACH 7-1-ACH 7-14, <https://doi.org/10.1029/2001JD000959>, 2002.](#)

[Takeuchi, M., and Ng, N. L.: Chemical composition and hydrolysis of organic nitrate aerosol formed from hydroxyl and nitrate radical oxidation of alpha-pinene and beta-pinene, Atmos. Chem. Phys., 19, 12749-12766, 10.5194/acp-19-12749-2019, 2019.](#)

[Tan, Z. F., Lu, K. D., Hofzumahaus, A., Fuchs, H., Bohn, B., Holland, F., Liu, Y. H., Rohrer, F., Shao, M., Sun, K., Wu, Y. S., Zeng, L. M., Zhang, Y. S., Zou, Q., Kiendler-Scharr, A., Wahner, A., and Zhang, Y. H.: Experimental budgets of OH, HO₂, and RO₂ radicals and implications for ozone formation in the Pearl River Delta in China 2014, Atmos. Chem. Phys., 19, 7129-7150, 10.5194/acp-19-7129-2019, 2019.](#)

[Tröstl, J., Chuang, W. K., Gordon, H., Heinritzi, M., Yan, C., Molteni, U., Ahlm, L., Frege, C., Bianchi, F., Wagner, R., Simon, M., Lehtipalo, K., Williamson, C., Craven, J. S., Duplissy, J., Adamov, A., Almeida, J., Bernhammer, A.-K., Breitenlechner, M., Brilke, S., Dias, A., Ehrhart, S., Flagan, R. C., Franchin, A., Fuchs, C., Guida, R., Gysel, M., Hansel, A., Hoyle, C. R., Jokinen, T., Junninen, H., Kangasluoma, J., Keskinen, H., Kim, J., Krapf, M., Kürten, A., Laaksonen, A., Lawler, M., Leiminger, M., Mathot, S., Möhler, O., Nieminen, T., Onnela, A., Petäjä, T., Piel, F. M., Miettinen, P., Rissanen, M. P., Rondo, L., Sarnela, N., Schobesberger, S., Sengupta, K., Sipilä, M., Smith, J. N., Steiner, G., Tomè, A., Virtanen, A., Wagner, A. C., Weingartner, E., Wimmer, D., Winkler, P. M., Ye, P., Carslaw, K. S., Curtius, J., Dommen, J., Kirkby, J., Kulmala, M., Riipinen, I., Worsnop, D. R., Donahue, N. M., and Baltensperger, U.: The role of low-volatility organic compounds in initial particle growth in the atmosphere, Nature, 533, 527-531, 10.1038/nature18271, 2016.](#)

[Valiev, R. R., Hasan, G., Salo, V.-T., Kubecka, J., and Kurten, T.: Intersystem Crossings Drive Atmospheric Gas-Phase Dimer Formation, The journal of physical chemistry. A, 123, 6596-6604, 10.1021/acs.jpca.9b02559, 2019.](#)

[Vereecken, L., and Peeters, J.: Nontraditional \(per\)oxy ring-closure paths in the atmospheric oxidation of isoprene and monoterpenes, J. Phys. Chem. A 108, 5197-5204, 10.1021/jp049219g, 2004.](#)

[Vereecken, L., Mueller, J. F., and Peeters, J.: Low-volatility poly-oxygenates in the OH-initiated atmospheric oxidation of alpha-pinene: impact of non-traditional peroxy radical chemistry, Phys. Chem. Chem. Phys., 9, 5241-5248, 10.1039/b708023a, 2007.](#)

[Vereecken, L., and Peeters, J.: A structure-activity relationship for the rate coefficient of H-migration in substituted alkoxy radicals, *Phys. Chem. Chem. Phys.*, 12, 12608-12620, 10.1039/c0cp00387e, 2010.](#)

[Vereecken, L., and Francisco, J. S.: Theoretical studies of atmospheric reaction mechanisms in the troposphere, *Chem. Soc. Rev.*, 41, 6259-6293, 10.1039/c2cs35070j, 2012.](#)

[Vereecken, L., and Peeters, J.: A theoretical study of the OH-initiated gas-phase oxidation mechanism of beta-pinene \(C₁₀H₁₆\): first generation products, *Phys. Chem. Chem. Phys.*, 14, 3802-3815, 10.1039/c2cp23711c, 2012.](#)

[Vereecken, L., and Nozière, B.: H migration in peroxy radicals under atmospheric conditions, *Atmos. Chem. Phys.*, 20, 7429-7458, 10.5194/acp-20-7429-2020, 2020.](#)

[Vereecken, L., Carlsson, P. T. M., Novelli, A., Bernard, F., Brown, S. S., Cho, C., Crowley, J. N., Fuchs, H., Mellouki, W., Reimer, D., Shenolikar, J., Tillmann, R., Zhou, L., Kiendler-Scharr, A., and Wahner, A.: Theoretical and experimental study of peroxy and alkoxy radicals in the NO₃-initiated oxidation of isoprene, *Phys. Chem. Chem. Phys.*, 23, 5496-5515, 10.1039/d0cp06267g, 2021.](#)

[Viggiano, A. A., Seeley, J. V., Mundis, P. L., Williamson, J. S., and Morris, R. A.: Rate Constants for the Reactions of XO₂-\(H₂O\)_n \(X = C, HC, and N\) and NO₃-\(HNO₃\)_n with H₂SO₄: Implications for Atmospheric Detection of H₂SO₄, *The Journal of Physical Chemistry A*, 101, 8275-8278, 10.1021/jp971768h, 1997.](#)

[Wagner, N. L., Dubé, W. P., Washenfelder, R. A., Young, C. J., Pollack, I. B., Ryerson, T. B., and Brown, S. S.: Diode laser-based cavity ring-down instrument for NO₃, N₂O₅, NO₂ and O₃ from aircraft, *Atmos. Meas. Tech.*, 4, 1227-1240, 10.5194/amt-4-1227-2011, 2011.](#)

[Wang, Y., Mehra, A., Krechmer, J. E., Yang, G., Hu, X., Lu, Y., Lambe, A., Canagaratna, M., Chen, J., Worsnop, D., Coe, H., and Wang, L.: Oxygenated products formed from OH-initiated reactions of trimethylbenzene: autoxidation and accretion, *Atmos. Chem. Phys.*, 20, 9563-9579, 10.5194/acp-20-9563-2020, 2020.](#)

[Wennberg, P. O., Bates, K. H., Crouse, J. D., Dodson, L. G., McVay, R. C., Mertens, L. A., Nguyen, T. B., Praske, E., Schwantes, R. H., Smarte, M. D., St Clair, J. M., Teng, A. P., Zhang, X., and Seinfeld, J. H.: Gas-Phase Reactions of Isoprene and Its Major Oxidation Products, *Chem. Rev.*, 118, 3337-3390, 10.1021/acs.chemrev.7b00439, 2018.](#)

[Wu, R., Vereecken, L., Tsiligiannis, E., Kang, S., Albrecht, S. R., Hantschke, L., Zhao, D., Novelli, A., Fuchs, H., Tillmann, R., Hohaus, T., Carlsson, P. T. M., Shenolikar, J., Bernard, F., Crowley, J. N., Fry, J. L., Brownwood, B., Thornton, J. A., Brown, S. S., Kiendler-Scharr, A., Wahner, A., Hallquist, M., and Mentel, T. F.: Molecular composition and volatility of multi-generation products formed from isoprene oxidation by nitrate radical, *Atmos. Chem. Phys. Discuss.*, 2020, 1-37, 10.5194/acp-2020-1180, 2020.](#)

[Xu, L., Guo, H. Y., Boyd, C. M., Klein, M., Bougiatioti, A., Cerully, K. M., Hite, J. R., Isaacman-VanWertz, G., Kreisberg, N. M., Knote, C., Olson, K., Koss, A., Goldstein, A. H., Hering, S. V., de Gouw, J., Baumann, K., Lee, S. H., Nenes, A., Weber, R. J., and Ng, N. L.: Effects of anthropogenic emissions on aerosol formation from isoprene and monoterpenes in the southeastern United States, *Proc. Nat. Acad. Sci. U.S.A.*, 112, 37-42, 10.1073/pnas.1417609112, 2015.](#)

[Xu, Z. N., Nie, W., Liu, Y. L., Sun, P., Huang, D. D., Yan, C., Krechmer, J., Ye, P. L., Xu, Z., Qi, X. M., Zhu, C. J., Li, Y. Y., Wang, T. Y., Wang, L., Huang, X., Tang, R. Z., Guo, S., Xiu, G. L., Fu, Q. Y., Worsnop, D., Chi, X. G., and Ding, A. J.: Multifunctional Products of Isoprene Oxidation in Polluted Atmosphere and Their Contribution to SOA, 48, e2020GL089276, <https://doi.org/10.1029/2020GL089276>, 2021.](#)

[Yan, C., Nie, W., Aijala, M., Rissanen, M. P., Canagaratna, M. R., Massoli, P., Junninen, H., Jokinen, T., Sarnela, N., Hame, S. A. K., Schobesberger, S., Canonaco, F., Yao, L., Prevot, A. S. H., Petaja, T., Kulmala, M., Sipila, M.,](#)

Worsnop, D. R., and Ehn, M.: Source characterization of highly oxidized multifunctional compounds in a boreal forest environment using positive matrix factorization, *Atmos. Chem. Phys.*, 16, 12715-12731, 10.5194/acp-16-12715-2016, 2016.

Yan, C., Nie, W., Vogel, A. L., Dada, L., Lehtipalo, K., Stolzenburg, D., Wagner, R., Rissanen, M. P., Xiao, M., Ahonen, L., Fischer, L., Rose, C., Bianchi, F., Gordon, H., Simon, M., Heinritzi, M., Garmash, O., Roldin, P., Dias, A., Ye, P., Hofbauer, V., Amorim, A., Bauer, P. S., Bergen, A., Bernhammer, A. K., Breitenlechner, M., Brilke, S., Buchholz, A., Mazon, S. B., Canagaratna, M. R., Chen, X., Ding, A., Dommen, J., Draper, D. C., Duplissy, J., Frege, C., Heyn, C., Guida, R., Hakala, J., Heikkinen, L., Hoyle, C. R., Jokinen, T., Kangasluoma, J., Kirkby, J., Kontkanen, J., Kurten, A., Lawler, M. J., Mai, H., Mathot, S., Mauldin, R. L., Molteni, U., Nichman, L., Nieminen, T., Nowak, J., Ojdanic, A., Onnela, A., Pajunoja, A., Petaja, T., Piel, F., Quelever, L. L. J., Sarnela, N., Schallhart, S., Sengupta, K., Sipila, M., Tome, A., Trostl, J., Vaisanen, O., Wagner, A. C., Ylisirnio, A., Zha, Q., Baltensperger, U., Carslaw, K. S., Curtius, J., Flagan, R. C., Hansel, A., Riipinen, I., Smith, J. N., Virtanen, A., Winkler, P. M., Donahue, N. M., Kerminen, V. M., Kulmala, M., Ehn, M., and Worsnop, D. R.: Size-dependent influence of NO_x on the growth rates of organic aerosol particles, *Science Advances*, 6, 9, 10.1126/sciadv.aay4945, 2020.

Zhao, D. F., Buchholz, A., Kortner, B., Schlag, P., Rubach, F., Kiendler-Scharr, A., Tillmann, R., Wahner, A., Flores, J. M., Rudich, Y., Watne, Å. K., Hallquist, M., Wildt, J., and Mentel, T. F.: Size-dependent hygroscopicity parameter (κ) and chemical composition of secondary organic cloud condensation nuclei, *Geophys. Res. Lett.*, 42, 10920-10928, 10.1002/2015gl066497, 2015a.

Zhao, D. F., Kaminski, M., Schlag, P., Fuchs, H., Acir, I. H., Bohn, B., Häsel, R., Kiendler-Scharr, A., Rohrer, F., Tillmann, R., Wang, M. J., Wegener, R., Wildt, J., Wahner, A., and Mentel, T. F.: Secondary organic aerosol formation from hydroxyl radical oxidation and ozonolysis of monoterpenes, *Atmos. Chem. Phys.*, 15, 991-1012, 10.5194/acp-15-991-2015, 2015b.

Zhao, D. F., Schmitt, S. H., Wang, M. J., Acir, I. H., Tillmann, R., Tan, Z. F., Novelli, A., Fuchs, H., Pullinen, I., Wegener, R., Rohrer, F., Wildt, J., Kiendler-Scharr, A., Wahner, A., and Mentel, T. F.: Effects of NO_x and SO₂ on the secondary organic aerosol formation from photooxidation of alpha-pinene and limonene, *Atmos. Chem. Phys.*, 18, 1611-1628, 10.5194/acp-18-1611-2018, 2018.

Ziemann, P. J., and Atkinson, R.: Kinetics, products, and mechanisms of secondary organic aerosol formation, *Chem. Soc. Rev.*, 41, 6582-6605, 10.1039/c2cs35122f, 2012.

Atkinson, R., Bauleh, D. L., Cox, R. A., Crowley, J. N., Hampson, R. F., Hynes, R. G., Jenkin, M. E., Rossi, M. J., and Troe, J.: Evaluated kinetic and photochemical data for atmospheric chemistry: Volume II – gas phase reactions of organic species, *Atmos. Chem. Phys.*, 6, 3625-4055, 2006.

Ayres, B. R., Allen, H. M., Draper, D. C., Brown, S. S., Wild, R. J., Jimenez, J. L., Day, D. A., Campuzano Jost, P., Hu, W., de Gouw, J., Koss, A., Cohen, R. C., Duffey, K. C., Romer, P., Baumann, K., Edgerton, E., Takahama, S., Thornton, J. A., Lee, B. H., Lopez-Hilfiker, F. D., Mohr, C., Wennberg, P. O., Nguyen, T. B., Teng, A., Goldstein, A. H., Olson, K., and Fry, J. L.: Organic nitrate aerosol formation via NO₃ + biogenic volatile organic compounds in the southeastern United States, *Atmos. Chem. Phys.*, 15, 13377-13392, 10.5194/acp-15-13377-2015, 2015.

Berndt, T., and Böge, O.: Gas phase reaction of NO₃ radicals with isoprene: a kinetic and mechanistic study, *Int. J. Chem. Kinet.*, 29, 755-765, 10.1002/(sici)1097-4601(1997)29:10<755::Aid-kin4>3.0.Co;2-I, 1997.

Berndt, T., Mender, B., Scholz, W., Fischer, L., Herrmann, H., Kulmala, M., and Hansel, A.: Accretion Product Formation from Ozonolysis and OH Radical Reaction of alpha-Pinene: Mechanistic Insight and the Influence of Isoprene and Ethylene, *Environ. Sci. Technol.*, 52, 11069-11077, 10.1021/acs.est.8b02210, 2018a.

Berndt, T., Scholz, W., Mentler, B., Fischer, L., Herrmann, H., Kulmala, M., and Hansel, A.: Accretion Product Formation from Self and Cross Reactions of RO₂ Radicals in the Atmosphere, *Angew. Chem. Int. Edit.*, 57, 3820-3824, 10.1002/anie.201710989, 2018b.

- Bernhammer, A. K., Fischer, L., Mentler, B., Heinritzi, M., Simon, M., and Hansel, A.: Production of highly oxygenated organic molecules (HOMs) from trace contaminants during isoprene oxidation, *Atmos. Meas. Tech.*, **11**, 4763–4773, 10.5194/amt-11-4763-2018, 2018.
- Bianchi, F., Kurten, T., Riva, M., Mohr, C., Rissanen, M. P., Roldin, P., Berndt, T., Crouse, J. D., Wennberg, P. O., Mentel, T. F., Wildt, J., Junninen, H., Jokinen, T., Kulmala, M., Worsnop, D. R., Thornton, J. A., Donahue, N., Kjaergaard, H. G., and Ehn, M.: Highly Oxygenated Organic Molecules (HOM) from Gas Phase Autoxidation Involving Peroxy Radicals: A Key Contributor to Atmospheric Aerosol, *Chem. Rev.*, **119**, 3472–3509, 10.1021/acs.chemrev.8b00395, 2019.
- Boyd, C. M., Sanchez, J., Xu, L., Eugene, A. J., Nah, T., Tuet, W. Y., Guzman, M. I., and Ng, N. L.: Secondary organic aerosol formation from the beta pinene+NO₃ system: effect of humidity and peroxy radical fate, *Atmos. Chem. Phys.*, **15**, 7497–7522, 10.5194/acp-15-7497-2015, 2015.
- Boyd, C. M., Nah, T., Xu, L., Berkemeier, T., and Ng, N. L.: Secondary Organic Aerosol (SOA) from Nitrate Radical Oxidation of Monoterpenes: Effects of Temperature, Dilution, and Humidity on Aerosol Formation, Mixing, and Evaporation, *Environ. Sci. Technol.*, **51**, 7831–7841, 10.1021/acs.est.7b01460, 2017.
- Brown, S. S., deGouw, J. A., Warneke, C., Ryerson, T. B., Dube, W. P., Atlas, E., Weber, R. J., Peltier, R. E., Neuman, J. A., Roberts, J. M., Swanson, A., Flocke, F., McKeen, S. A., Brioude, J., Sommariva, R., Trainer, M., Fehsenfeld, F. C., and Ravishankara, A. R.: Nocturnal isoprene oxidation over the Northeast United States in summer and its impact on reactive nitrogen partitioning and secondary organic aerosol, *Atmos. Chem. Phys.*, **9**, 3027–3042, 10.5194/acp-9-3027-2009, 2009.
- Brown, S. S., Dube, W. P., Peischl, J., Ryerson, T. B., Atlas, E., Warneke, C., de Gouw, J. A., Heldkert, S. t. L., Brock, C. A., Flocke, F., Trainer, M., Parrish, D. D., Fehsenfeld, F. C., and Ravishankara, A. R.: Budgets for nocturnal VOC oxidation by nitrate radicals aloft during the 2006 Texas Air Quality Study, *J. Geophys. Res. Atmos.*, **116**, 10.1029/2011jd016544, 2011.
- Brown, S. S., and Stutz, J.: Nighttime radical observations and chemistry, *Chem. Soc. Rev.*, **41**, 6405–6447, 10.1039/c2es35181a, 2012.
- Chen, J., Møller, K. H., Wennberg, P. O., and Kjaergaard, H. G.: Unimolecular Reactions Following Indoor and Outdoor Limonene Ozonolysis, *J. Phys. Chem. A* **125**, 669–680, 10.1021/acs.jpca.0c09882, 2021.
- Clafin, M. S., and Ziemann, P. J.: Identification and Quantitation of Aerosol Products of the Reaction of β Pinene with NO₃ Radicals and Implications for Gas and Particle Phase Reaction Mechanisms, *The Journal of Physical Chemistry A*, **122**, 3640–3652, 10.1021/acs.jpca.8b00692, 2018.
- Crouse, J. D., Knap, H. C., Ormso, K. B., Jørgensen, S., Paulot, F., Kjaergaard, H. G., and Wennberg, P. O.: Atmospheric Fate of Methacrolein. 1. Peroxy Radical Isomerization Following Addition of OH and O₂, *The Journal of Physical Chemistry A*, **116**, 5756–5762, 10.1021/jp211560u, 2012.
- Crouse, J. D., Nielsen, L. B., Jørgensen, S., Kjaergaard, H. G., and Wennberg, P. O.: Autoxidation of Organic Compounds in the Atmosphere, *J. Phys. Chem. Lett.*, **4**, 3513–3520, 10.1021/jz4019207, 2013.
- Draper, D. C., Myllys, N., Hyttinen, N., Møller, K. H., Kjaergaard, H. G., Fry, J. L., Smith, J. N., and Kurten, T.: Formation of Highly Oxidized Molecules from NO₃ Radical Initiated Oxidation of Delta-3-Carene: A Mechanistic Study, *Acc. Chem. Res.*, **52**, 1460–1470, 10.1021/acscentsci.7b00143, 2019.
- Ehn, M., Thornton, J. A., Kleist, E., Sipila, M., Junninen, H., Pullinen, I., Springer, M., Rubach, F., Tillmann, R., Lee, B., Lopez-Hilfiker, F., Andres, S., Acir, I. H., Rissanen, M., Jokinen, T., Schobesberger, S., Kangasluoma, J., Kontkanen, J., Nieminen, T., Kurten, T., Nielsen, L. B., Jørgensen, S., Kjaergaard, H. G., Canagaratna, M., Dal Maso, M., Berndt, T., Petaja, T., Wahner, A., Kerminen, V. M., Kulmala, M., Worsnop, D. R., Wildt, J., and Mentel, T. F.: A large source of low volatility secondary organic aerosol, *Nature*, **506**, 476–479, 10.1038/nature13032, 2014.
- Ehn, M., Berndt, T., Wildt, J., and Mentel, T.: Highly Oxygenated Molecules from Atmospheric Autoxidation of Hydrocarbons: A Prominent Challenge for Chemical Kinetics Studies, *Int. J. Chem. Kinet.*, **49**, 821–831, 10.1002/kin.21130, 2017.
- Eisele, F. L., and Tanner, D. J.: Measurement of the gas-phase concentration of H₂SO₄ and methane sulfonic acid and estimates of H₂SO₄ production and loss in the atmosphere, *J. Geophys. Res.*, **98**, 9001–9010, 10.1029/93jd00031, 1993.
- Faxon, C., Hammes, J., Le Breton, M., Pathak, R. K., and Hallquist, M.: Characterization of organic nitrate constituents of secondary organic aerosol (SOA) from nitrate radical initiated oxidation of limonene using high resolution chemical ionization mass spectrometry, *Atmos. Chem. Phys.*, **18**, 5467–5481, 10.5194/acp-18-5467-2018, 2018.
- Finlayson-Pitts, B., and Pitts, J.: *Chemistry of the upper and lower atmosphere*, Academic Press, San Diego, 2000.

- Fry, J. L., Kiendler-Scharr, A., Rollins, A. W., Wooldridge, P. J., Brown, S. S., Fuchs, H., Dube, W., Mensah, A., dal Maso, M., Tillmann, R., Dorn, H. P., Brauers, T., and Cohen, R. C.: Organic nitrate and secondary organic aerosol yield from NO₃ oxidation of beta-pinene evaluated using a gas-phase kinetics/aerosol partitioning model, *Atmos. Chem. Phys.*, **9**, 1431–1449, 2009.
- Fry, J. L., Kiendler-Scharr, A., Rollins, A. W., Brauers, T., Brown, S. S., Dorn, H. P., Dube, W. P., Fuchs, H., Mensah, A., Rohrer, F., Tillmann, R., Wahner, A., Wooldridge, P. J., and Cohen, R. C.: SOA from limonene: role of NO₃ in its generation and degradation, *Atmos. Chem. Phys.*, **11**, 3879–3894, [10.5194/acp-11-3879-2011](https://doi.org/10.5194/acp-11-3879-2011), 2011.
- Fry, J. L., Draper, D. C., Barsanti, K. C., Smith, J. N., Ortega, J., Winkle, P. M., Lawler, M. J., Brown, S. S., Edwards, P. M., Cohen, R. C., and Lee, L.: Secondary Organic Aerosol Formation and Organic Nitrate Yield from NO₃ Oxidation of Biogenic Hydrocarbons, *Environ. Sci. Technol.*, **48**, 11944–11953, [10.1021/es502204x](https://doi.org/10.1021/es502204x), 2014.
- Fry, J. L., Brown, S. S., Middlebrook, A. M., Edwards, P. M., Campuzano-Jost, P., Day, D. A., Jimenez, J. L., Allen, H. M., Ryerson, T. B., Pollack, I., Graus, M., Warneke, C., de Gouw, J. A., Brock, C. A., Gilman, J., Lerner, B. M., Dube, W. P., Liao, J., and Welti, A.: Secondary organic aerosol (SOA) yields from NO₃ radical + isoprene based on nighttime aircraft power plant plume transects, *Atmos. Chem. Phys.*, **18**, 11663–11682, [10.5194/acp-18-11663-2018](https://doi.org/10.5194/acp-18-11663-2018), 2018.
- Fuchs, H., Dorn, H. P., Bachner, M., Bohn, B., Brauers, T., Gomm, S., Hofzumahaus, A., Holland, F., Nehr, S., Rohrer, F., Tillmann, R., and Wahner, A.: Comparison of OH concentration measurements by DOAS and LIF during SAPHIR chamber experiments at high OH reactivity and low NO concentration, *Atmos. Meas. Tech.*, **5**, 1611–1626, [10.5194/amt-5-1611-2012](https://doi.org/10.5194/amt-5-1611-2012), 2012.
- Garmash, O., Rissanen, M. P., Pullinen, I., Schmitt, S., Kausiala, O., Tillmann, R., Pereival, C., Bannan, T. J., Priestley, M., Hallquist, Å. M., Kleist, E., Kiendler-Scharr, A., Hallquist, M., Berndt, T., McFiggans, G., Wildt, J., Mentel, T., and Ehn, M.: Multi-generation OH oxidation as a source for highly oxygenated organic molecules from aromatics, *Atmos. Chem. Phys. Discuss.*, **2019**, 1–33, [10.5194/acp-2019-582](https://doi.org/10.5194/acp-2019-582), 2019.
- Geyer, A., Alicke, B., Konrad, S., Schmitz, T., Stutz, J., and Platt, U.: Chemistry and oxidation capacity of the nitrate radical in the continental boundary layer near Berlin, *J. Geophys. Res. Atmos.*, **106**, 8013–8025, [10.1029/2000jd900681](https://doi.org/10.1029/2000jd900681), 2001.
- Hamilton, J. F., Bryant, D. J., Edwards, P. M., Ouyang, B., Bannan, T. J., Mehra, A., Mayhew, A. W., Hopkins, J. R., Dunmore, R. E., Squires, F. A., Lee, J. D., Newland, M. J., Worrall, S. D., Bacak, A., Coe, H., Pereival, C., Whalley, L. K., Heard, D. E., Slater, E. J., Jones, R. L., Cui, T., Surratt, J. D., Reeves, C. E., Mills, G. P., Grimmond, S., Sun, Y., Xu, W., Shi, Z., and Rieckard, A. R.: Key Role of NO₃ Radicals in the Production of Isoprene Nitrates and Nitrooxyorganosulfates in Beijing, *Environ. Sci. Technol.*, **55**, 842–853, [10.1021/acs.est.0e05689](https://doi.org/10.1021/acs.est.0e05689), 2021.
- Huang, W., Saathoff, H., Shen, X. L., Ramisetty, R., Leisner, T., and Mohr, C.: Chemical Characterization of Highly Functionalized Organonitrates Contributing to Night-Time Organic Aerosol Mass Loadings and Particle Growth, *Environ. Sci. Technol.*, **53**, 1165–1174, [10.1021/acs.est.8b05826](https://doi.org/10.1021/acs.est.8b05826), 2019.
- Hyttinen, N., Kupiainen-Määttä, O., Rissanen, M. P., Muuronen, M., Ehn, M., and Kurtén, T.: Modeling the Charging of Highly Oxidized Cyclohexene Ozonolysis Products Using Nitrate-Based Chemical Ionization, *The Journal of Physical Chemistry A*, **119**, 6339–6345, [10.1021/acs.jpca.5b01818](https://doi.org/10.1021/acs.jpca.5b01818), 2015.
- Japar, S. M., and Niki, H.: Gas phase reactions of the nitrate radical with olefins, *The Journal of Physical Chemistry*, **79**, 1629–1632, [10.1021/j100583a002](https://doi.org/10.1021/j100583a002), 1975.
- Jenkin, M. E., Saunders, S. M., and Pilling, M. J.: The tropospheric degradation of volatile organic compounds: A protocol for mechanism development, *Atmos. Environ.*, **31**, 81–104, [10.1016/s1352-2310\(96\)00105-7](https://doi.org/10.1016/s1352-2310(96)00105-7), 1997.
- Jenkin, M. E., Boyd, A. A., and Lesclaux, R.: Peroxy Radical Kinetics Resulting from the OH-Initiated Oxidation of 1,3-Butadiene, 2,3-Dimethyl-1,3-Butadiene and Isoprene, *J. Atmos. Chem.*, **29**, 267–298, [10.1023/A:1005940332441](https://doi.org/10.1023/A:1005940332441), 1998.
- Jenkin, M. E., Saunders, S. M., Wagner, V., and Pilling, M. J.: Protocol for the development of the Master Chemical Mechanism, MCM v3 (Part B): tropospheric degradation of aromatic volatile organic compounds, *Atmos. Chem. Phys.*, **3**, 181–193, 2003.
- Jenkin, M. E., Young, J. C., and Rieckard, A. R.: The MCM v3.3.1 degradation scheme for isoprene, *Atmos. Chem. Phys.*, **15**, 11433–11459, [10.5194/acp-15-11433-2015](https://doi.org/10.5194/acp-15-11433-2015), 2015.
- Jokinen, T., Sipila, M., Junninen, H., Ehn, M., Lonn, G., Hakala, J., Petaja, T., Mauldin, R. L., III, Kulmala, M., and Worsnop, D. R.: Atmospheric sulphuric acid and neutral cluster measurements using CI-API TOF, *Atmos. Chem. Phys.*, **12**, 4117–4125, [10.5194/acp-12-4117-2012](https://doi.org/10.5194/acp-12-4117-2012), 2012.

- Jokinen, T., Sipila, M., Richters, S., Kerminen, V. M., Paasonen, P., Stratmann, F., Worsnop, D., Kulmala, M., Ehn, M., Herrmann, H., and Berndt, T.: Rapid Autoxidation Forms Highly Oxidized RO₂ Radicals in the Atmosphere, *Angew. Chem. Int. Edit.*, **53**, 14596–14600, 10.1002/anie.201408566, 2014.
- Jokinen, T., Berndt, T., Makkonen, R., Kerminen, V. M., Junninen, H., Paasonen, P., Stratmann, F., Herrmann, H., Guenther, A. B., Worsnop, D. R., Kulmala, M., Ehn, M., and Sipila, M.: Production of extremely low volatile organic compounds from biogenic emissions: Measured yields and atmospheric implications, *Proc. Nat. Acad. Sci. U.S.A.*, **112**, 7123–7128, 10.1073/pnas.1423977112, 2015.
- Kaminski, M., Fuchs, H., Acir, I. H., Bohn, B., Brauers, T., Dorn, H. P., Haeseler, R., Hofzumahaus, A., Li, X., Lutz, A., Nehr, S., Rohrer, F., Tillmann, R., Vereecken, L., Wegener, R., and Wahner, A.: Investigation of the beta-pinene photooxidation by OH in the atmosphere simulation chamber SAPHIR, *Atmos. Chem. Phys.*, **17**, 6631–6650, 10.5194/acp-17-6631-2017, 2017.
- Kenseth, C. M., Huang, Y. L., Zhao, R., Dalleska, N. F., Hethcox, C., Stoltz, B. M., and Seinfeld, J. H.: Synergistic O₃ + OH oxidation pathway to extremely low volatility dimers revealed in beta-pinene secondary organic aerosol, *Proc. Nat. Acad. Sci. U.S.A.*, **115**, 8301–8306, 10.1073/pnas.1804671115, 2018.
- Kirkby, J., Duplissy, J., Sengupta, K., Frege, C., Gordon, H., Williamson, C., Heinritzi, M., Simon, M., Yan, C., Almeida, J., Tröstl, J., Nieminen, T., Ortega, I. K., Wagner, R., Adamov, A., Amorim, A., Bernhammer, A. K., Bianchi, F., Breitenlechner, M., Brilke, S., Chen, X., Craven, J., Dias, A., Ehrhart, S., Flagan, R. C., Franchin, A., Fuchs, C., Guida, R., Hakala, J., Hoyle, C. R., Jokinen, T., Junninen, H., Kangasluoma, J., Kim, J., Krapf, M., Kürten, A., Laaksonen, A., Lehtipalo, K., Makhmutov, V., Mathot, S., Molteni, U., Onnela, A., Peräkylä, O., Piel, F., Petäjä, T., Praplan, A. P., Pringle, K., Rap, A., Richards, N. A. D., Riipinen, I., Rissanen, M. P., Rondo, L., Sarnela, N., Schobesberger, S., Scott, C. E., Seinfeld, J. H., Sipilä, M., Steiner, G., Stozhkov, Y., Stratmann, F., Tomé, A., Virtanen, A., Vogel, A. L., Wagner, A. C., Wagner, P. E., Weingartner, E., Wimmer, D., Winkler, P. M., Ye, P., Zhang, X., Hansel, A., Dommen, J., Donahue, N. M., Worsnop, D. R., Baltensperger, U., Kulmala, M., Carslaw, K. S., and Curtius, J.: Ion-induced nucleation of pure biogenic particles, *Nature*, **533**, 521–526, 10.1038/nature17953, 2016.
- Krechermer, J. E., Coggon, M. M., Massoli, P., Nguyen, T. B., Crounse, J. D., Hu, W. W., Day, D. A., Tyndall, G. S., Henze, D. K., Rivera Rios, J. C., Nowak, J. B., Kimmel, J. R., Mauldin, R. L., Stark, H., Jayne, J. T., Sipila, M., Junninen, H., St Clair, J. M., Zhang, X., Feiner, P. A., Zhang, L., Miller, D. O., Brune, W. H., Keutsch, F. N., Wennberg, P. O., Seinfeld, J. H., Worsnop, D. R., Jimenez, J. L., and Canagaratna, M. R.: Formation of Low Volatility Organic Compounds and Secondary Organic Aerosol from Isoprene Hydroxyhydroperoxide Low-NO Oxidation, *Environ. Sci. Technol.*, **49**, 10330–10339, 10.1021/aes.est.5b02031, 2015.
- Kwan, A. J., Chan, A. W. H., Ng, N. L., Kjaergaard, H. G., Seinfeld, J. H., and Wennberg, P. O.: Peroxy radical chemistry and OH radical production during the NO₃-initiated oxidation of isoprene, *Atmos. Chem. Phys.*, **12**, 7499–7515, 10.5194/acp-12-7499-2012, 2012.
- Lai, C. C., and Finlayson-Pitts, B. J.: Reactions of dinitrogen pentoxide and nitrogen dioxide with 1-palmitoyl-2-oleoyl-sn-glycero-3-phosphocholine, *Lipids*, **26**, 306–314, 10.1007/bf02537142, 1991.
- Lee, B. H., Mohr, C., Lopez-Hilfiker, F. D., Lutz, A., Hallquist, M., Lee, L., Romer, P., Cohen, R. C., Iyer, S., Kurten, T., Hu, W., Day, D. A., Campuzano-Jost, P., Jimenez, J. L., Xu, L., Ng, N. L., Guo, H., Weber, R. J., Wild, R. J., Brown, S. S., Koss, A., de Gouw, J., Olson, K., Goldstein, A. H., Seo, R., Kim, S., McAvey, K., Shepson, P. B., Starn, T., Baumann, K., Edgerton, E. S., Liu, J., Shilling, J. E., Miller, D. O., Brune, W., Schobesberger, S., D'Ambro, E. L., and Thornton, J. A.: Highly functionalized organic nitrates in the southeast United States: Contribution to secondary organic aerosol and reactive nitrogen budgets, *Proc. Nat. Acad. Sci. U.S.A.*, **113**, 1516–1521, 10.1073/pnas.1508108113, 2016.
- Lu, K. D., Rohrer, F., Holland, F., Fuchs, H., Brauers, T., Oebel, A., Dlugi, R., Hu, M., Li, X., Lou, S. R., Shao, M., Zhu, T., Wahner, A., Zhang, Y. H., and Hofzumahaus, A.: Nighttime observation and chemistry of HO_x in the Pearl River Delta and Beijing in summer 2006, *Atmos. Chem. Phys.*, **14**, 4979–4999, 10.5194/acp-14-4979-2014, 2014.
- Malkin, T. L., Goddard, A., Heard, D. E., and Seakins, P. W.: Measurements of OH and HO₂ yields from the gas phase ozonolysis of isoprene, *Atmos. Chem. Phys.*, **10**, 1441–1459, 10.5194/acp-10-1441-2010, 2010.
- McFiggans, G., Mentel, T. F., Wildt, J., Pullinen, I., Kang, S., Kleist, E., Schmitt, S., Springer, M., Tillmann, R., Wu, C., Zhao, D., Hallquist, M., Faxon, C., Le Breton, M., Hallquist, A. M., Simpson, D., Bergström, R., Jenkin, M. E., Ehn, M., Thornton, J. A., Alfarra, M. R., Bannan, T. J., Percival, C. J., Priestley, M., Topping, D., and Kiendler-Sehr, A.: Secondary organic aerosol reduced by mixture of atmospheric vapours, *Nature*, **565**, 587–593, 10.1038/s41586-018-0871-y, 2019.
- Mentel, T. F., Springer, M., Ehn, M., Kleist, E., Pullinen, I., Kurten, T., Rissanen, M., Wahner, A., and Wildt, J.: Formation of highly oxidized multifunctional compounds: autoxidation of peroxy radicals formed in the ozonolysis of alkenes—deduced from structure-product relationships, *Atmos. Chem. Phys.*, **15**, 6745–6765, 10.5194/acp-15-6745-2015, 2015.
- Møller, K. H., Bates, K. H., and Kjaergaard, H. G.: The Importance of Peroxy Radical Hydrogen Shift Reactions in Atmospheric Isoprene Oxidation, *J. Phys. Chem. A* **123**, 920–932, 10.1021/aes.jpca.8b10432, 2019.

Molteni, U., Bianchi, F., Klein, F., El Haddad, I., Frege, C., Rossi, M. J., Dommen, J., and Baltensperger, U.: Formation of highly oxygenated organic molecules from aromatic compounds, *Atmos. Chem. Phys.*, **18**, 1909–1921, 10.5194/acp-18-1909-2018, 2018.

Molteni, U., Simon, M., Heinritzi, M., Hoyle, C. R., Bernhammer, A. K., Bianchi, F., Breitenlechner, M., Brilke, S., Dias, A., Duplissy, J., Frege, C., Gordon, H., Heyn, C., Jokinen, T., Kurten, A., Lehtipalo, K., Makhmutov, V., Petaja, T., Pieber, S. M., Praplan, A. P., Schobesberger, S., Steiner, G., Stozhkov, Y., Tome, A., Trostl, J., Wagner, A. C., Wagner, R., Williamson, C., Yan, C., Baltensperger, U., Curtius, J., Donahue, N. M., Hansel, A., Kirkby, J., Kulmala, M., Worsnop, D. R., and Dommen, J.: Formation of Highly Oxygenated Organic Molecules from α -Pinene Ozonolysis: Chemical Characteristics, Mechanism, and Kinetic Model Development, *Acs Earth and Space Chemistry*, **3**, 873–883, 10.1021/acsearthspacechem.9b00035, 2019.

Nah, T., Sanchez, J., Boyd, C. M., and Ng, N. L.: Photochemical Aging of α -pinene and β -pinene Secondary Organic Aerosol formed from Nitrate Radical Oxidation, *Environ. Sci. Technol.*, **50**, 222–231, 10.1021/acs.est.5b04594, 2016.

Ng, N. L., Kwan, A. J., Surratt, J. D., Chan, A. W. H., Chhabra, P. S., Sorooshian, A., Pye, H. O. T., Crounse, J. D., Wennberg, P. O., Flagan, R. C., and Seinfeld, J. H.: Secondary organic aerosol (SOA) formation from reaction of isoprene with nitrate radicals (NO_3), *Atmos. Chem. Phys.*, **8**, 4117–4140, 10.5194/acp-8-4117-2008, 2008.

Nguyen, T. B., Tyndall, G. S., Crounse, J. D., Teng, A. P., Bates, K. H., Schwantes, R. H., Coggon, M. M., Zhang, L., Feiner, P., Miller, D. O., Skog, K. M., Rivera-Rios, J. C., Dorris, M., Olson, K. F., Koss, A., Wild, R. J., Brown, S. S., Goldstein, A. H., de Gouw, J. A., Brune, W. H., Keutsch, F. N., Seinfeld, J. H., and Wennberg, P. O.: Atmospheric fates of Criegee intermediates in the ozonolysis of isoprene, *Phys. Chem. Chem. Phys.*, **18**, 10241–10254, 10.1039/c6cp00053e, 2016.

Novelli, A., Cho, C., Fuchs, H., Hofzumahaus, A., Rohrer, F., Tillmann, R., Kiendler-Scharr, A., Wahner, A., and Vereecken, L.: Experimental and theoretical study on the impact of a nitrate group on the chemistry of alkoxy radicals, *Phys. Chem. Chem. Phys.*, **23**, 5474–5495, 10.1039/D0CP05555G, 2021.

Nozière, B., and Vereecken, L.: Direct Observation of Aliphatic Peroxy Radical Autoxidation and Water Effects: An Experimental and Theoretical Study, *Angew. Chem. Int. Edit.*, **58**, 13976–13982, 10.1002/anie.201907981, 2019.

Perring, A. E., Wisthaler, A., Graus, M., Wooldridge, P. J., Lockwood, A. L., Mielke, L. H., Shepson, P. B., Hansel, A., and Cohen, R. C.: A product study of the isoprene+ NO_3 reaction, *Atmos. Chem. Phys.*, **9**, 4945–4956, 10.5194/acp-9-4945-2009, 2009.

Pfrang, C., Martin, R. S., Canosa-Mas, C. E., and Wayne, R. P.: Gas-phase reactions of NO_3 and N_2O_5 with (Z)-hex-4-en-1-ol, (Z)-hex-3-en-1-ol ('leaf alcohol'), (E)-hex-3-en-1-ol, (Z)-hex-2-en-1-ol and (E)-hex-2-en-1-ol, *Phys. Chem. Chem. Phys.*, **8**, 354–363, 10.1039/b510835g, 2006.

Pullinen, I., Schmitt, S., Kang, S., Sarrafzadeh, M., Schlag, P., Andres, S., Kleist, E., Mentel, T. F., Rohrer, F., Springer, M., Tillmann, R., Wildt, J., Wu, C., Zhao, D., Wahner, A., and Kiendler-Scharr, A.: Impact of NO_x on secondary organic aerosol (SOA) formation from α -pinene and β -pinene photooxidation: the role of highly oxygenated organic nitrates, *Atmos. Chem. Phys.*, **20**, 10125–10147, 10.5194/acp-20-10125-2020, 2020.

Quelever, L. L. J., Kristensen, K., Jensen, L. N., Rosati, B., Teiwes, R., Daellenbach, K. R., Perakyla, O., Roldin, P., Bossi, R., Pedersen, H. B., Glasius, M., Bilde, M., and Ehn, M.: Effect of temperature on the formation of highly oxygenated organic molecules (HOMs) from α -pinene ozonolysis, *Atmos. Chem. Phys.*, **19**, 7609–7625, 10.5194/acp-19-7609-2019, 2019.

Richters, S., Pfeifle, M., Olzmann, M., and Berndt, T.: endo-Cyclization of unsaturated RO_2 radicals from the gas-phase ozonolysis of cyclohexadienes, *Chem. Commun.*, **53**, 4132–4135, 10.1039/c7cc01350g, 2017.

Rissanen, M. P., Kurten, T., Sipila, M., Thornton, J. A., Kangasluoma, J., Sarnela, N., Junninen, H., Jørgensen, S., Schallhart, S., Kajos, M. K., Taipale, R., Springer, M., Mentel, T. F., Ruuskanen, T., Petaja, T., Worsnop, D. R., Kjaergaard, H. G., and Ehn, M.: The Formation of Highly Oxidized Multifunctional Products in the Ozonolysis of Cyclohexene, *J. Am. Chem. Soc.*, **136**, 15596–15606, 10.1021/ja507146s, 2014.

Rissanen, M. P., Kurten, T., Sipila, M., Thornton, J. A., Kausiala, O., Garmash, O., Kjaergaard, H. G., Petaja, T., Worsnop, D. R., Ehn, M., and Kulmala, M.: Effects of Chemical Complexity on the Autoxidation Mechanisms of Endocyclic Alkene Ozonolysis Products: From Methylcyclohexenes toward Understanding α -Pinene, *J. Phys. Chem. A* **119**, 4633–4650, 10.1021/jp510966g, 2015.

Riva, M., Rantala, P., Kreechmer, J. E., Perakyla, O., Zhang, Y. J., Heikkinen, L., Garmash, O., Yan, C., Kulmala, M., Worsnop, D., and Ehn, M.: Evaluating the performance of five different chemical ionization techniques for detecting gaseous oxygenated organic species, *Atmos. Meas. Tech.*, **12**, 2403–2421, 10.5194/amt-12-2403-2019, 2019.

Rohrer, F., Bohn, B., Brauers, T., Bruning, D., Johnen, F. J., Wahner, A., and Kleffmann, J.: Characterisation of the photolytic HONO -source in the atmosphere simulation chamber SAPHIR, *Atmos. Chem. Phys.*, **5**, 2189–2201, 2005.

Rollins, A. W., Kiendler-Scharr, A., Fry, J. L., Brauers, T., Brown, S. S., Dorn, H. P., Dube, W. P., Fuchs, H., Mensah, A., Mentel, T. F., Rohrer, F., Tillmann, R., Wegener, R., Wooldridge, P. J., and Cohen, R. C.: Isoprene oxidation by nitrate radical: alkyl nitrate and secondary organic aerosol yields, *Atmos. Chem. Phys.*, 9, 6685–6703, 2009.

Saunders, S. M., Jenkin, M. E., Derwent, R. G., and Pilling, M. J.: Protocol for the development of the Master Chemical Mechanism, MCM v3 (Part A): tropospheric degradation of non-aromatic volatile organic compounds, *Atmos. Chem. Phys.*, 3, 161–180, 2003.

Schwantes, R. H., Teng, A. P., Nguyen, T. B., Coggon, M. M., Crouse, J. D., St. Clair, J. M., Zhang, X., Schilling, K. A., Seinfeld, J. H., and Wennberg, P. O.: Isoprene NO₃ Oxidation Products from the RO₂ + HO₂ Pathway, *J. Phys. Chem. A* 119, 10158–10171, [10.1021/acs.jpca.5b06355](https://doi.org/10.1021/acs.jpca.5b06355), 2015.

Skov, H., Hjorth, J., Lohse, C., Jensen, N. R., and Restelli, G.: Products and mechanisms of the reactions of the nitrate radical (NO₃) with isoprene, 1,3-butadiene and 2,3-dimethyl-1,3-butadiene in air, *Atmospheric Environment. Part A. General Topics*, 26, 2771–2783, [https://doi.org/10.1016/0960-1686\(92\)90015-D](https://doi.org/10.1016/0960-1686(92)90015-D), 1992.

Stark, M. S.: Epoxidation of Alkenes by Peroxyl Radicals in the Gas Phase: Structure–Activity Relationships, *The Journal of Physical Chemistry A*, 101, 8296–8301, [10.1021/jp972054+](https://doi.org/10.1021/jp972054+), 1997.

Stark, M. S.: Addition of Peroxyl Radicals to Alkenes and the Reaction of Oxygen with Alkyl Radicals, *J. Am. Chem. Soc.*, 122, 4162–4170, [10.1021/ja993760m](https://doi.org/10.1021/ja993760m), 2000.

Starn, T. K., Shepson, P. B., Bertman, S. B., Riemer, D. D., Zika, R. G., and Olszyna, K.: Nighttime isoprene chemistry at an urban-impacted forest site, 103, 22437–22447, <https://doi.org/10.1029/98JD01201>, 1998.

Stroud, C. A., Roberts, J. M., Williams, E. J., Hereid, D., Angevine, W. M., Fehsenfeld, F. C., Wisthaler, A., Hansel, A., Martinez-Harder, M., Harder, H., Brune, W. H., Hoenninger, G., Stutz, J., and White, A. B.: Nighttime isoprene trends at an urban forested site during the 1999 Southern Oxidant Study, 107, ACH 7-1–ACH 7-14, <https://doi.org/10.1029/2001JD000959>, 2002.

Takeuchi, M., and Ng, N. L.: Chemical composition and hydrolysis of organic nitrate aerosol formed from hydroxyl and nitrate radical oxidation of alpha-pinene and beta-pinene, *Atmos. Chem. Phys.*, 19, 12749–12766, [10.5194/aep-19-12749-2019](https://doi.org/10.5194/aep-19-12749-2019), 2019.

Tan, Z. F., Lu, K. D., Hofzumahaus, A., Fuchs, H., Bohn, B., Holland, F., Liu, Y. H., Rohrer, F., Shao, M., Sun, K., Wu, Y. S., Zeng, L. M., Zhang, Y. S., Zou, Q., Kiendler-Scharr, A., Wahner, A., and Zhang, Y. H.: Experimental budgets of OH, HO₂, and RO₂ radicals and implications for ozone formation in the Pearl River Delta in China 2014, *Atmos. Chem. Phys.*, 19, 7129–7150, [10.5194/aep-19-7129-2019](https://doi.org/10.5194/aep-19-7129-2019), 2019.

Tröstl, J., Chuang, W. K., Gordon, H., Heinritzi, M., Yan, C., Molteni, U., Ahlm, L., Frege, C., Bianchi, F., Wagner, R., Simon, M., Lehtipalo, K., Williamson, C., Craven, J. S., Duplissy, J., Adamov, A., Almeida, J., Bernhammer, A. K., Breitenlechner, M., Brilke, S., Dias, A., Ehrhart, S., Flagan, R. C., Franchin, A., Fuchs, C., Guida, R., Gysel, M., Hansel, A., Hoyle, C. R., Jokinen, T., Junninen, H., Kangasluoma, J., Keskinen, H., Kim, J., Krapf, M., Kürten, A., Laaksonen, A., Lawler, M., Leiminger, M., Mathot, S., Möhler, O., Nieminen, T., Onnela, A., Petäjä, T., Piel, F. M., Miettinen, P., Rissanen, M. P., Rondo, L., Sarnela, N., Schobesberger, S., Sengupta, K., Sipilä, M., Smith, J. N., Steiner, G., Tomé, A., Virtanen, A., Wagner, A. C., Weingartner, E., Wimmer, D., Winkler, P. M., Ye, P., Carslaw, K. S., Curtius, J., Dommen, J., Kirkby, J., Kulmala, M., Riipinen, I., Worsnop, D. R., Donahue, N. M., and Baltensperger, U.: The role of low volatility organic compounds in initial particle growth in the atmosphere, *Nature*, 533, 527–531, [10.1038/nature18271](https://doi.org/10.1038/nature18271), 2016.

Valiev, R. R., Hasan, G., Salo, V. T., Kubecka, J., and Kurten, T.: Intersystem Crossings Drive Atmospheric Gas-Phase Dimer Formation, *The Journal of Physical Chemistry. A*, 123, 6596–6604, [10.1021/acs.jpca.9b02559](https://doi.org/10.1021/acs.jpca.9b02559), 2019.

Vereecken, L., and Peeters, J.: Nontraditional (per)oxy ring-closure paths in the atmospheric oxidation of isoprene and monoterpenes, *J. Phys. Chem. A* 108, 5197–5204, [10.1021/jp049219g](https://doi.org/10.1021/jp049219g), 2004.

Vereecken, L., Mueller, J. F., and Peeters, J.: Low volatility poly-oxygenates in the OH-initiated atmospheric oxidation of alpha-pinene: impact of non-traditional peroxy radical chemistry, *Phys. Chem. Chem. Phys.*, 9, 5241–5248, [10.1039/b708023a](https://doi.org/10.1039/b708023a), 2007.

Vereecken, L., and Peeters, J.: A structure-activity relationship for the rate coefficient of H-migration in substituted alkoxy radicals, *Phys. Chem. Chem. Phys.*, 12, 12608–12620, [10.1039/e0cp00387e](https://doi.org/10.1039/e0cp00387e), 2010.

Vereecken, L., and Francisco, J. S.: Theoretical studies of atmospheric reaction mechanisms in the troposphere, *Chem. Soc. Rev.*, 41, 6259–6293, [10.1039/e2cs35070j](https://doi.org/10.1039/e2cs35070j), 2012.

Vereecken, L., and Peeters, J.: A theoretical study of the OH-initiated gas-phase oxidation mechanism of beta-pinene (C₁₀H₁₆): first generation products, *Phys. Chem. Chem. Phys.*, 14, 3802–3815, [10.1039/c2ep23711e](https://doi.org/10.1039/c2ep23711e), 2012.

- Vereecken, L., and Nozière, B.: H migration in peroxy radicals under atmospheric conditions, *Atmos. Chem. Phys.*, 20, 7429–7458, 10.5194/acp-20-7429-2020, 2020.
- Vereecken, L., Carlsson, P. T. M., Novelli, A., Bernard, F., Brown, S. S., Cho, C., Crowley, J. N., Fuchs, H., Mellouki, W., Reimer, D., Shenolikar, J., Tillmann, R., Zhou, L., Kiendler-Scharr, A., and Wahner, A.: Theoretical and experimental study of peroxy and alkoxy radicals in the NO₃-initiated oxidation of isoprene, *Phys. Chem. Chem. Phys.*, 23, 5496–5515, 10.1039/d0cp06267g, 2021.
- Viggiano, A. A., Seeley, J. V., Mundis, P. L., Williamson, J. S., and Morris, R. A.: Rate Constants for the Reactions of XO₃ (H₂O)_n (X = C, HC, and N) and NO₃ (HNO₃)_n with H₂SO₄: Implications for Atmospheric Detection of H₂SO₄, *The Journal of Physical Chemistry A*, 101, 8275–8278, 10.1021/jp971768h, 1997.
- Wagner, N. L., Dubé, W. P., Washenfelder, R. A., Young, C. J., Pollack, I. B., Ryerson, T. B., and Brown, S. S.: Diode laser-based cavity ring-down instrument for NO₃, N₂O₅, NO, NO₂ and O₃ from aircraft, *Atmos. Meas. Tech.*, 4, 1227–1240, 10.5194/amt-4-1227-2011, 2011.
- Wang, Y., Mehra, A., Krechmer, J. E., Yang, G., Hu, X., Lu, Y., Lambe, A., Canagaratna, M., Chen, J., Worsnop, D., Coe, H., and Wang, L.: Oxygenated products formed from OH-initiated reactions of trimethylbenzene: autoxidation and accretion, *Atmos. Chem. Phys.*, 20, 9563–9579, 10.5194/acp-20-9563-2020, 2020.
- Wennberg, P. O., Bates, K. H., Crounse, J. D., Dodson, L. G., McVay, R. C., Mertens, L. A., Nguyen, T. B., Praske, E., Schwantes, R. H., Smarte, M. D., St. Clair, J. M., Teng, A. P., Zhang, X., and Seinfeld, J. H.: Gas-Phase Reactions of Isoprene and Its Major Oxidation Products, *Chem. Rev.*, 118, 3337–3390, 10.1021/acs.chemrev.7b00439, 2018.
- Wu, R., Vereecken, L., Tsiligiannis, E., Kang, S., Albrecht, S. R., Hantschke, L., Zhao, D., Novelli, A., Fuchs, H., Tillmann, R., Hohaus, T., Carlsson, P. T. M., Shenolikar, J., Bernard, F., Crowley, J. N., Fry, J. L., Brownwood, B., Thornton, J. A., Brown, S. S., Kiendler-Scharr, A., Wahner, A., Hallquist, M., and Mentel, T. F.: Molecular composition and volatility of multi-generation products formed from isoprene oxidation by nitrate radical, *Atmos. Chem. Phys. Discuss.*, 2020, 1–37, 10.5194/acp-2020-1180, 2020.
- Xu, L., Guo, H. Y., Boyd, C. M., Klein, M., Bougiatioti, A., Cerully, K. M., Hite, J. R., Isaacman-VanWertz, G., Kreisberg, N. M., Knote, C., Olson, K., Koss, A., Goldstein, A. H., Hering, S. V., de Gouw, J., Baumann, K., Lee, S. H., Nenes, A., Weber, R. J., and Ng, N. L.: Effects of anthropogenic emissions on aerosol formation from isoprene and monoterpenes in the southeastern United States, *Proc. Nat. Acad. Sci. U.S.A.*, 112, 37–42, 10.1073/pnas.1417609112, 2015.
- Xu, Z. N., Nie, W., Liu, Y. L., Sun, P., Huang, D. D., Yan, C., Krechmer, J., Ye, P. L., Xu, Z., Qi, X. M., Zhu, C. J., Li, Y. Y., Wang, T. Y., Wang, L., Huang, X., Tang, R. Z., Guo, S., Xiu, G. L., Fu, Q. Y., Worsnop, D., Chi, X. G., and Ding, A. J.: Multifunctional Products of Isoprene Oxidation in Polluted Atmosphere and Their Contribution to SOA, 48, e2020GL089276, <https://doi.org/10.1029/2020GL089276>, 2021.
- Yan, C., Nie, W., Aijala, M., Rissanen, M. P., Canagaratna, M. R., Massoli, P., Junninen, H., Jokinen, T., Sarnela, N., Hame, S. A. K., Schobesberger, S., Canonaco, F., Yao, L., Prevot, A. S. H., Petaja, T., Kulmala, M., Sipila, M., Worsnop, D. R., and Ehn, M.: Source characterization of highly oxidized multifunctional compounds in a boreal forest environment using positive matrix factorization, *Atmos. Chem. Phys.*, 16, 12715–12731, 10.5194/acp-16-12715-2016, 2016.
- Yan, C., Nie, W., Vogel, A. L., Dada, L., Lehtipalo, K., Stolzenburg, D., Wagner, R., Rissanen, M. P., Xiao, M., Ahonen, L., Fischer, L., Rose, C., Bianchi, F., Gordon, H., Simon, M., Heinritzi, M., Garmash, O., Roldin, P., Dias, A., Ye, P., Hofbauer, V., Amorim, A., Bauer, P. S., Bergen, A., Bernhammer, A. K., Breitenlechner, M., Brilke, S., Buchholz, A., Mazon, S. B., Canagaratna, M. R., Chen, X., Ding, A., Dommen, J., Draper, D. C., Duplissy, J., Frege, C., Heyn, C., Guida, R., Hakala, J., Heikkinen, L., Hoyle, C. R., Jokinen, T., Kangasluoma, J., Kirkby, J., Kontkanen, J., Kurten, A., Lawler, M. J., Mai, H., Mathot, S., Mauldin, R. L., Molteni, U., Niehman, L., Nieminen, T., Nowak, J., Ojdanic, A., Onnela, A., Pajunoja, A., Petaja, T., Piel, F., Quelever, L. L. J., Sarnela, N., Schallhart, S., Sengupta, K., Sipila, M., Tome, A., Trostl, J., Vaisanen, O., Wagner, A. C., Ylisirnio, A., Zha, Q., Baltensperger, U., Carslaw, K. S., Curtius, J., Flagan, R. C., Hansel, A., Riipinen, I., Smith, J. N., Virtanen, A., Winkler, P. M., Donahue, N. M., Kerminen, V. M., Kulmala, M., Ehn, M., and Worsnop, D. R.: Size-dependent influence of NO_x on the growth rates of organic aerosol particles, *Science Advances*, 6, 9, 10.1126/sciadv.aay4945, 2020.
- Zhao, D. F., Buchholz, A., Kortner, B., Schlag, P., Rubach, F., Kiendler-Scharr, A., Tillmann, R., Wahner, A., Flores, J. M., Rudich, Y., Watne, A. K., Hallquist, M., Wildt, J., and Mentel, T. F.: Size-dependent hygroscopicity parameter (κ) and chemical composition of secondary organic cloud condensation nuclei, *Geophys. Res. Lett.*, 42, 10920–10928, 10.1002/2015gl066497, 2015a.
- Zhao, D. F., Kaminski, M., Schlag, P., Fuchs, H., Acir, I. H., Bohn, B., Häsel, R., Kiendler-Scharr, A., Rohrer, F., Tillmann, R., Wang, M. J., Wegener, R., Wildt, J., Wahner, A., and Mentel, T. F.: Secondary organic aerosol formation from hydroxyl-radical oxidation and ozonolysis of monoterpenes, *Atmos. Chem. Phys.*, 15, 991–1012, 10.5194/acp-15-991-2015, 2015b.
- Zhao, D. F., Schmitt, S. H., Wang, M. J., Acir, I. H., Tillmann, R., Tan, Z. F., Novelli, A., Fuchs, H., Pullinen, I., Wegener, R., Rohrer, F., Wildt, J., Kiendler-Scharr, A., Wahner, A., and Mentel, T. F.: Effects of NO_x and SO₂ on the secondary organic aerosol formation from photooxidation of alpha-pinene and limonene, *Atmos. Chem. Phys.*, 18, 1611–1628, 10.5194/acp-18-1611-2018, 2018.

Ziemann, P. J., and Atkinson, R.: Kinetics, products, and mechanisms of secondary organic aerosol formation, *Chem. Soc. Rev.*, 41, 6582–6605, 10.1039/c2cs35122f, 2012.

1
2 **Supplement of**
3 **Highly oxygenated organic molecules (HOM) formation in the**
4 **isoprene oxidation by NO₃ radical**

4 Defeng Zhao^{1,2,3}, Iida Pullinen^{2, a}, Hendrik Fuchs², Stephanie Schrade², Rongrong Wu², Ismail-Hakki Acir^{2, b}, Ralf
5 Tillmann², Franz Rohrer², Jürgen Wildt², Yindong Guo¹, Astrid Kiendler-Scharr², Andreas Wahner², Sungah Kang², Luc
6 Vereecken², Thomas F. Mentel²

7 ¹Department of Atmospheric and Oceanic Sciences & Institute of Atmospheric Sciences, Fudan University, Shanghai,
8 200438, China;

9 ²Institute of Energy and Climate Research, IEK-8: Troposphere, Forschungszentrum Jülich, 52425, Jülich, Germany

10 ³Big Data Institute for Carbon Emission and Environmental Pollution, Fudan University, Shanghai, 200438,
11 China

12 ^aNow at: Department of Applied Physics, University of Eastern Finland, Kuopio, 7021, Finland.

13 ^bNow at: Institute of Nutrition and Food Sciences, University of Bonn, Bonn, 53115, Germany;

14 *Correspondence to:* Thomas F. Mentel (t.mentel@fz-juelich.de), Defeng Zhao (dfzhao@fudan.edu.cn)

15

16 In the supplement we describe the derivation of calibration coefficient of NO₃⁻-CIMS for H₂SO₄. In addition,
17 more tables and figures besides those in the main text are provided.

18 1 S1 Deriving calibration coefficient of H₂SO₄ in NO₃⁻-CIMS and HOM yield

19 In order to convert peak intensity in mass spectra to concentration, the calibration coefficient of H₂SO₄ is
20 derived. H₂SO₄ was produced in-situ in SAPHIR chamber by the oxidation SO₂ by OH. SO₂ (~15 ppb) was added
21 into the chamber and the roof was opened to initiate photo-oxidation. In SAPHIR chamber, OH radicals are mainly
22 formed by the photolysis of HONO (nitrous acid) directly coming off the chamber walls through a photolytic
23 process (Rohrer et al., 2005;Zhao et al., 2016). NO (~20 ppb) was added which can enhance OH production by
24 photochemical recycling. OH concentration was characterized by using laser induced fluorescence (LIF) with the
25 details described in (Fuchs et al., 2012). SO₂ concentrations was characterized using an SO₂ analyzer (Thermo
26 Systems 43i).

27 The concentration of H₂SO₄ in the chamber can be described by the following equation.

$$28 \frac{d[H_2SO_4]}{dt} = k[SO_2][OH] - (k_{wl} + k_{dil})[H_2SO_4] \quad (\text{Eq. 1})$$

29 where [H₂SO₄], [SO₂], [OH] are the concentration of these species, k is the rate constant for the reaction of SO₂
30 with OH, k_{wl} is the wall loss rate of H₂SO₄ (~6.0×10⁻⁴ s⁻¹ as characterized for low volatility compounds in our
31 previous publication (Zhao et al., 2018)) and k_{dil} is the dilution rate of H₂SO₄ (~1×10⁻⁵ s⁻¹).

$$32 [H_2SO_4]=C \times I \quad (\text{Eq. 2})$$

33 where C is the calibration coefficient of H₂SO₄, I is the peak intensity of H₂SO₄ determined by normalized peak
34 area of H₂SO₄ at time t, i.e., the peak area divided by total signal of mass spectrum (termed as normalized count
35 (nc)).

36 Substituting Eq.2 to Eq. 1, one can get

$$37 C \frac{dI}{dt} = k[SO_2][OH] - C(k_{wl} + k_{dil})I \quad (\text{Eq. 3})$$

38 Integrating Eq.3, one can get

$$39 C = \frac{k[SO_2][OH]}{\frac{I-I_0}{t} + (k_{wl} + k_{dil})I} \quad (\text{Eq. 4})$$

40 where I₀ is the peak intensity at time zero. C was determined to be 2.5×10¹⁰ molecules cm⁻³ nc⁻¹. The second term of
41 denominator in Eq. 4 is much lower the first term and can omitted. The uncertainty of C was estimated to -52%/+
42 101% from the uncertainty of SO₂ concentration (~7 %), OH concentration (~ 10 %), I (~ 10%) and k (Δlogk=±0.3)
43 using error propagation, which corresponds to (1.2-5.0)×10¹⁰ molecules cm⁻³ nc⁻¹. The C value is generally consistent
44 with the value of 3.7×10¹⁰ molecules cm⁻³ nc⁻¹ in our previous calibration (Pullinen et al., 2020).

45 HOM yield was calculated as

$$46 Y = \frac{[HOM]}{[VOC]_r} = \frac{I(HOM)C}{[VOC]_r} \quad (\text{Eq. 5})$$

47 where [HOM] is concentration of HOM and [VOC]_r is the concentration of VOC reacted. The uncertainty of HOM
48 yield was estimated to -55%/+ 103% from the uncertainty of HOM intensity (~10 %), VOC concentration (~ 15 %)
49 and C using error propagation.

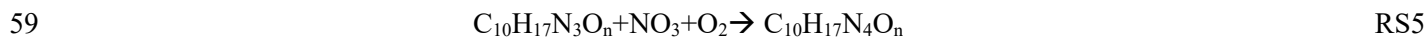
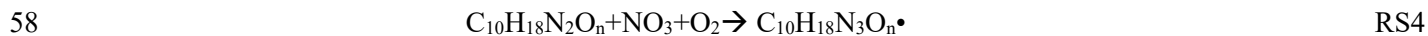
50
51

52 2 S2 Detailed mechanisms of trimer formation

53 The $C_{15}H_{25}N_5O_n$ series can be formed by the following reactions:



57 The $C_{10}H_{18}N_3O_n$ ($n=14-20$) and $C_{10}H_{17}N_4O_n$ can be formed by the dimers with NO_3 .

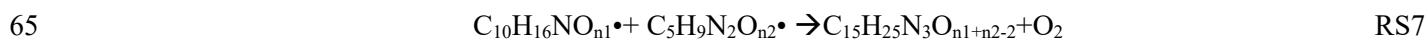


60 R21 is likely to be unimportant because both the abundance of $C_{10}H_{18}N_3O_n$ and $C_5H_7N_2O_n$ were low. Since

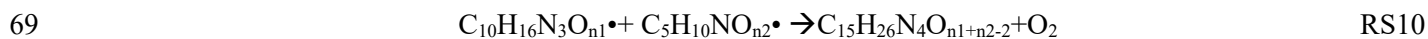
61 the peaks of $C_{10}H_{18}N_3O_n$ ($n=14-20$) series overlap with $C_{10}H_{16}N_2O_n$, we can only assign them with low confidence.

62 Similarly, $C_{10}H_{17}N_4O_n$ series overlap with $C_{10}H_{15}N_3O_n$ series (dimer 5).

63 The $C_{15}H_{25}N_3O_n$ series can be formed by the following reactions:



66 The $C_{15}H_{26}N_4O_n$ series can be formed by the following reactions:



70 R28 is likely to be unimportant because both the abundance of $C_{10}H_{16}N_3O_n$ and $C_5H_{10}NO_n$ were low.

71 The $C_{15}H_{24}N_2O_n$ series can be formed by the following reactions:



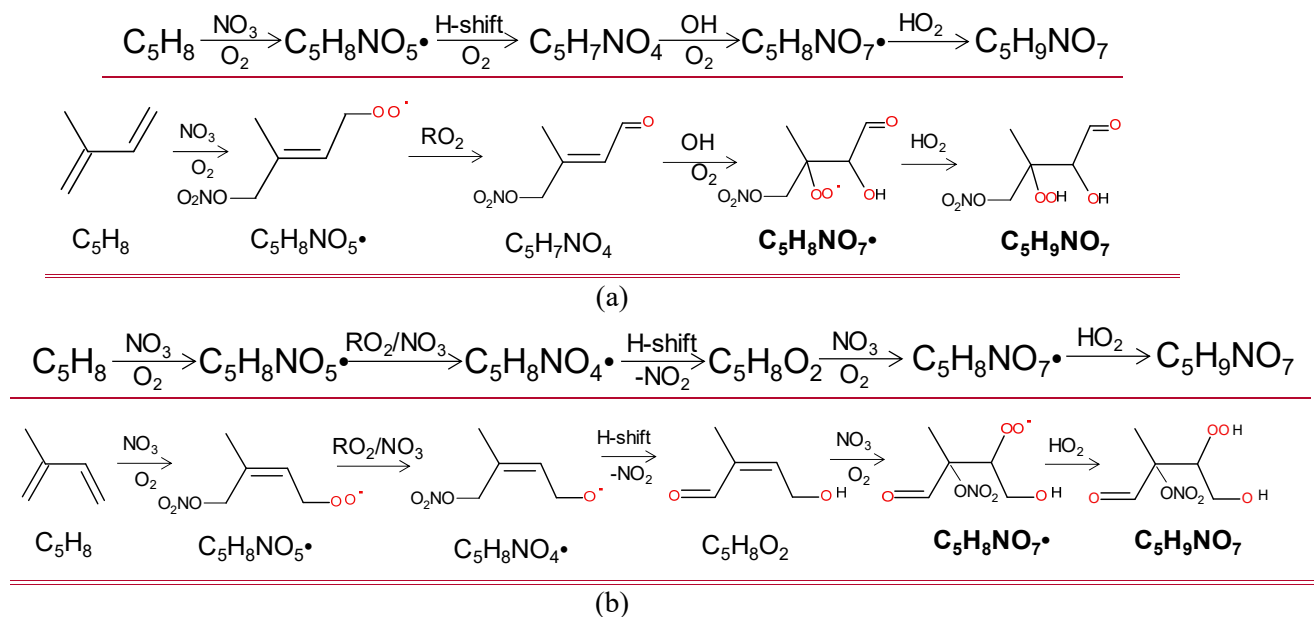
73 $C_{10}H_{16}NO_{n1}\bullet$ is formed via R15 as mentioned above.

74 References:

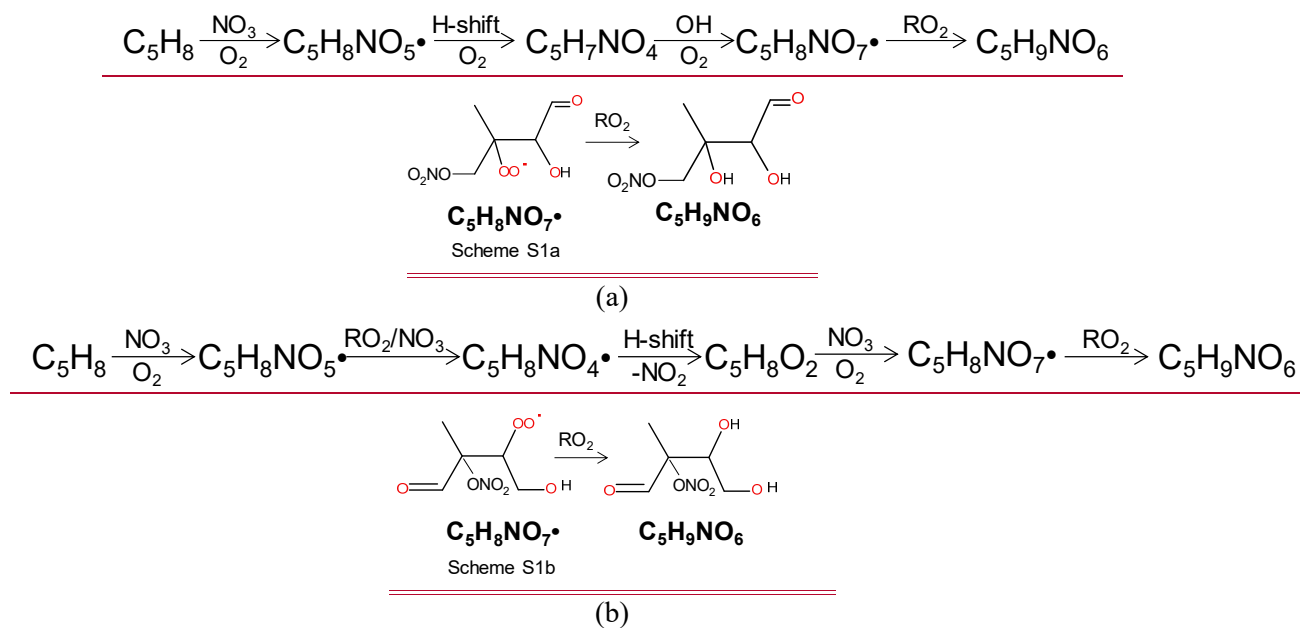
- 75 Fuchs, H., Dorn, H. P., Bachner, M., Bohn, B., Brauers, T., Gomm, S., Hofzumahaus, A., Holland, F., Nehr, S., Rohrer, F., Tillmann, R.,
76 and Wahner, A.: Comparison of OH concentration measurements by DOAS and LIF during SAPHIR chamber experiments at high OH
77 reactivity and low NO concentration, *Atmos. Meas. Tech.*, 5, 1611-1626, 10.5194/amt-5-1611-2012, 2012.
- 78 Pullinen, I., Schmitt, S., Kang, S., Sarrafzadeh, M., Schlag, P., Andres, S., Kleist, E., Mentel, T. F., Rohrer, F., Springer, M., Tillmann, R.,
79 Wildt, J., Wu, C., Zhao, D., Wahner, A., and Kiendler-Scharr, A.: Impact of NO_x on secondary organic aerosol (SOA) formation from α -
80 pinene and β -pinene photo-oxidation: the role of highly oxygenated organic nitrates, *Atmos. Chem. Phys. Discuss.*, 2020, 1-40, 10.5194/acp-
81 2019-1168, 2020.
- 82 Rohrer, F., Bohn, B., Brauers, T., Bruning, D., Johnen, F. J., Wahner, A., and Kleffmann, J.: Characterisation of the photolytic HONO-
83 source in the atmosphere simulation chamber SAPHIR, *Atmos. Chem. Phys.*, 5, 2189-2201, 2005.
- 84 Zhao, D. F., Buchholz, A., Kortner, B., Schlag, P., Rubach, F., Fuchs, H., Kiendler-Scharr, A., Tillmann, R., Wahner, A., Watne, Å. K.,
85 Hallquist, M., Flores, J. M., Rudich, Y., Kristensen, K., Hansen, A. M. K., Glasius, M., Kourtchev, I., Kalberer, M., and Mentel, T. F.: Cloud
86 condensation nuclei activity, droplet growth kinetics, and hygroscopicity of biogenic and anthropogenic secondary organic aerosol (SOA),
87 *Atmos. Chem. Phys.*, 16, 1105-1121, 10.5194/acp-16-1105-2016, 2016.
- 88 Zhao, D. F., Schmitt, S. H., Wang, M. J., Acir, I. H., Tillmann, R., Tan, Z. F., Novelli, A., Fuchs, H., Pullinen, I., Wegener, R., Rohrer, F.,
89 Wildt, J., Kiendler-Scharr, A., Wahner, A., and Mentel, T. F.: Effects of NO_x and SO₂ on the secondary organic aerosol formation from
90 photooxidation of alpha-pinene and limonene, *Atmos. Chem. Phys.*, 18, 1611-1628, 10.5194/acp-18-1611-2018, 2018.

91

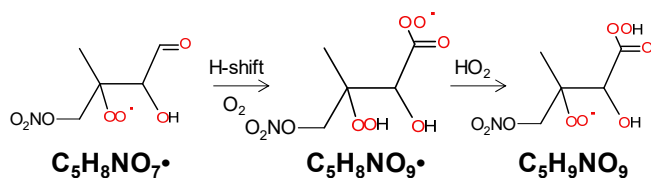
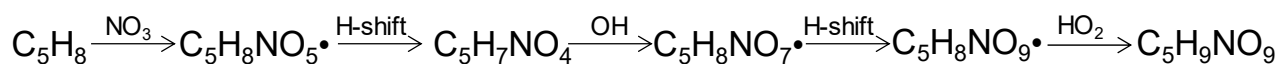
Supplement figures and tables



Scheme S1. The example pathway to form second-generation $\text{C}_5\text{H}_9\text{NO}_7$

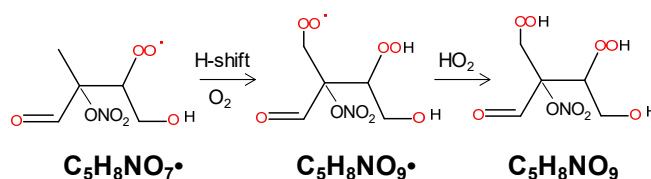
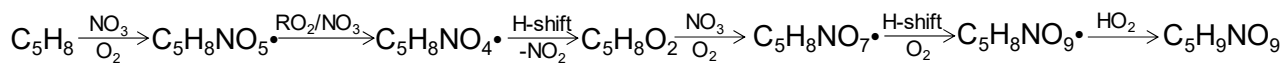


Scheme S2. The example pathway to form second-generation $\text{C}_5\text{H}_9\text{NO}_6$.



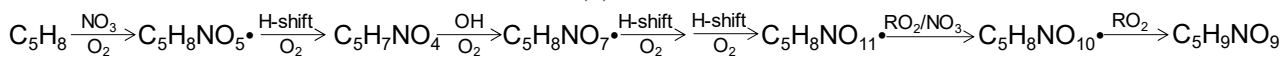
Scheme S1a

(a)

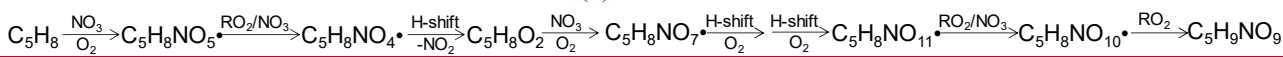


Scheme S1b

(b)

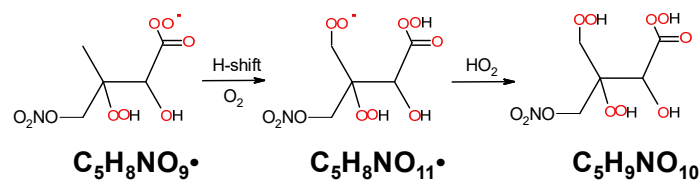
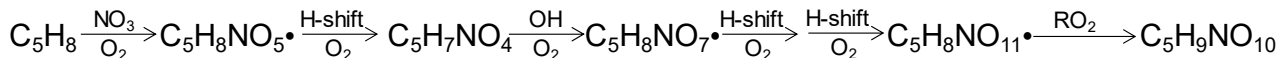


(e)



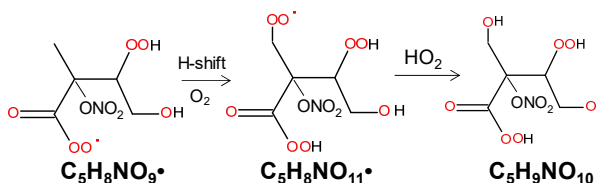
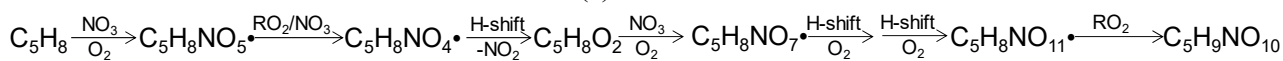
(d)

Scheme S3. The example pathway to form second-generation C₅H₉NO₉.



Scheme S3a

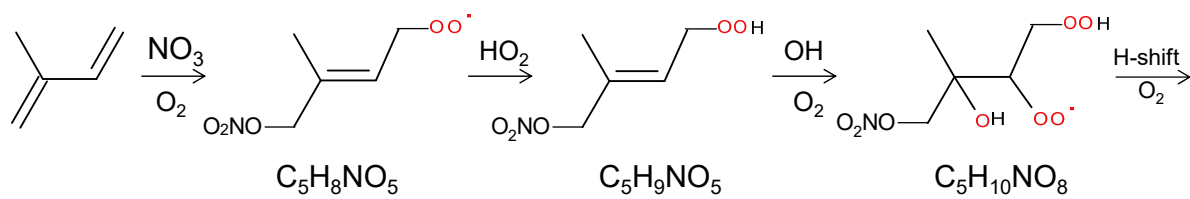
(a)



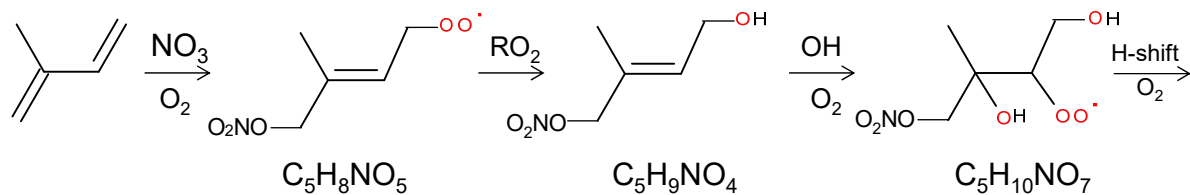
Scheme S3b

(b)

Scheme S4. The example pathway to form second-generation C₅H₉NO₁₀

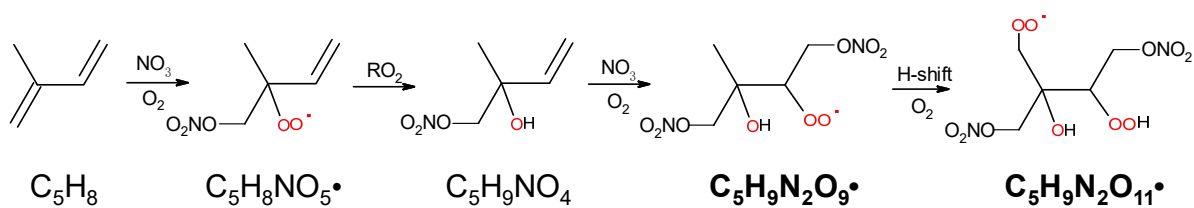


(a)

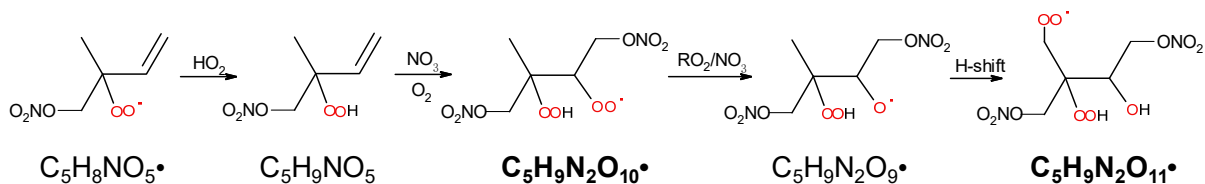


(b)

Scheme S5. The pathway to form $\text{C}_5\text{H}_{10}\text{NO}_{n(n \geq 7)} \cdot \text{RO}_2$ series with even (a) and odd (b) number of oxygen atoms.

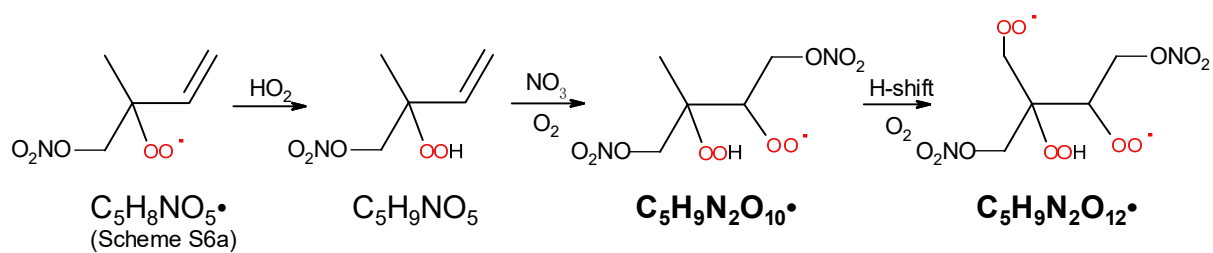


(a)

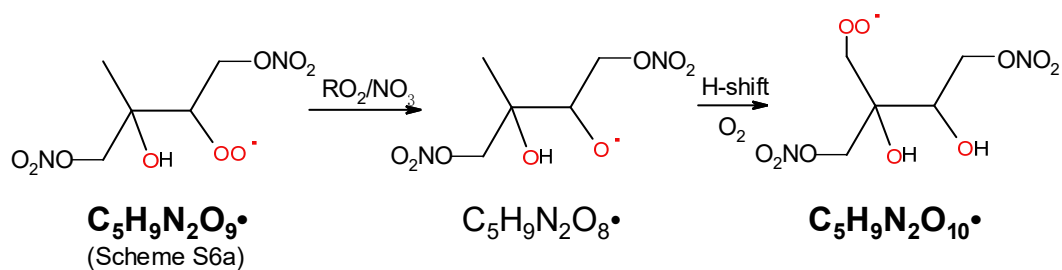


(b)

Scheme S6. The example pathway to form $\text{C}_5\text{H}_9\text{N}_2\text{O}_n$ ($n=9, 11$) HOM RO_2 series via 1- NO_3 -isoprene-2-OO RO_2 by RO_2 channel (a) and alkoxy-peroxy channel. The detected products are in bold.



(a)



(b)

Scheme S7. The example pathway to form $\text{C}_5\text{H}_9\text{N}_2\text{O}_n$ ($n=8, 10, 12$) HOM RO_2 series via 1- NO_3 -isoprene-2-OO RO_2 by RO_2 channel (a) and alkoxy-peroxy channel. The detected products are in **bold**.

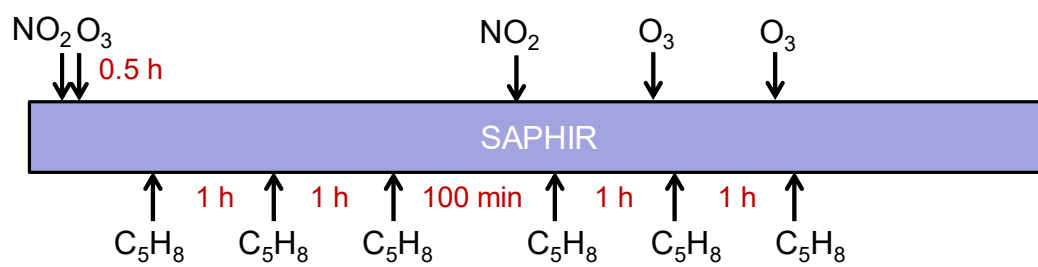


Figure S1. Schematic of the experimental procedure.

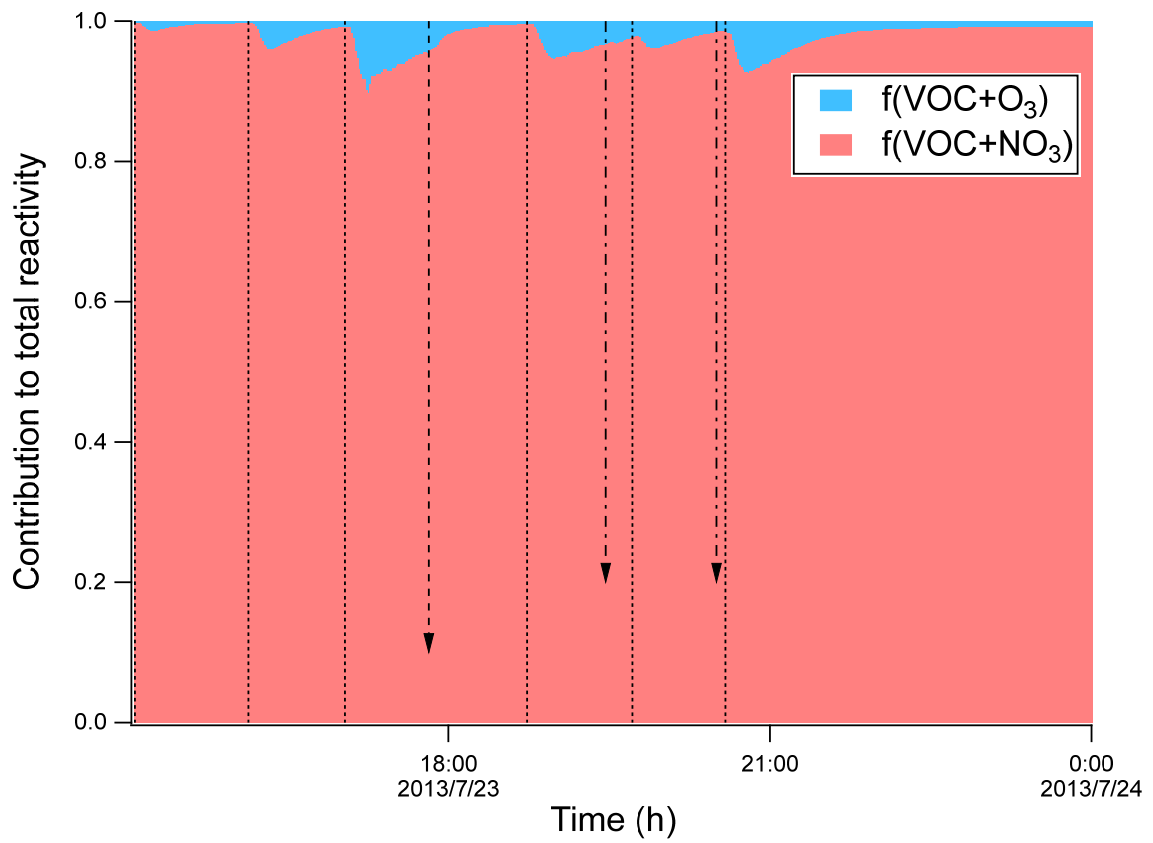
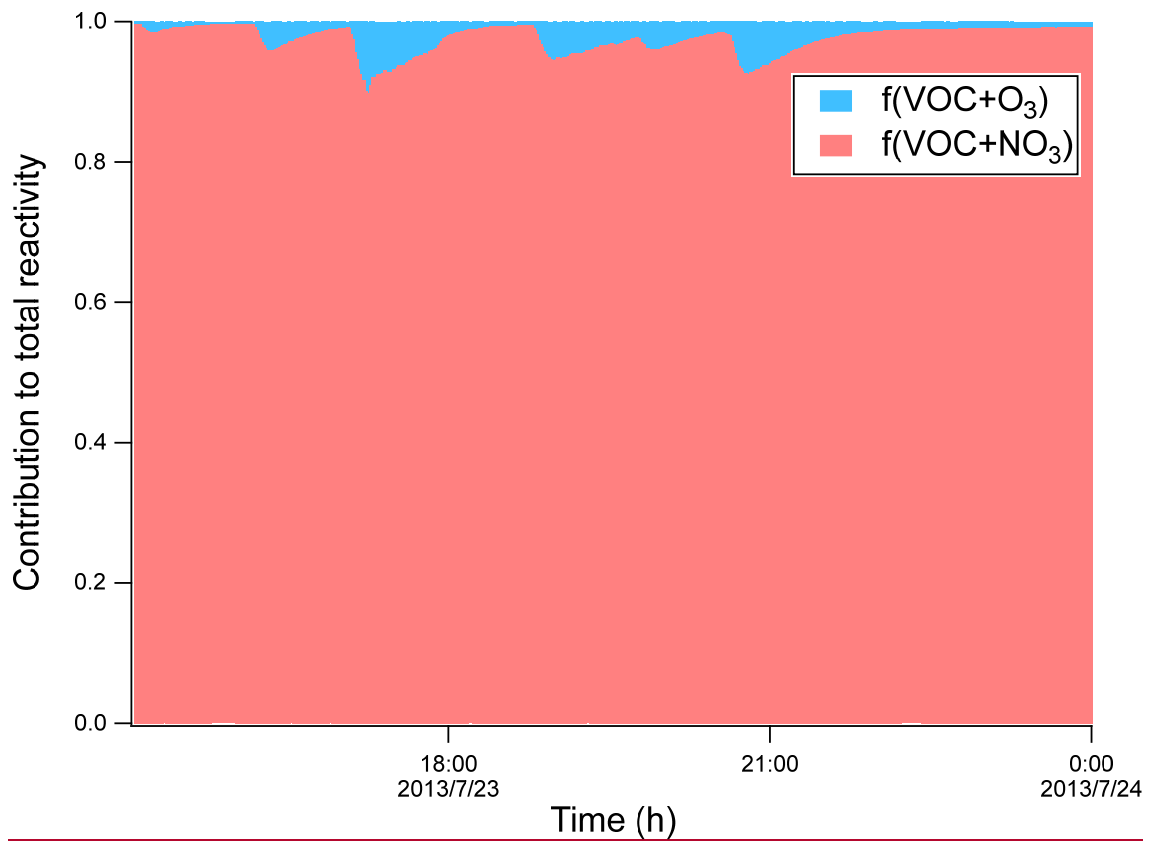
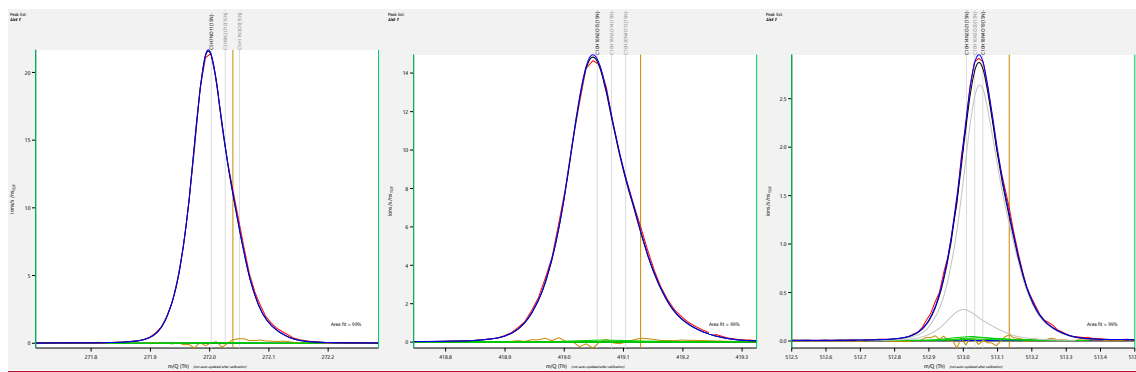


Figure S2. Relative contributions of the reaction rates of isoprene with NO_3 and with O_3 to the total isoprene loss. The dashed lines indicate the time of isoprene additions. The long-dashed arrow indicates the time of NO_2 addition. The dash-dotted arrows indicate the time of O_3 additions.



(a)

(b)

(c)

Figure S3. Examples of peak fitting. Formula in grey indicate compounds that have no noticeable effect on fitting residues and thus not included in the peak list.

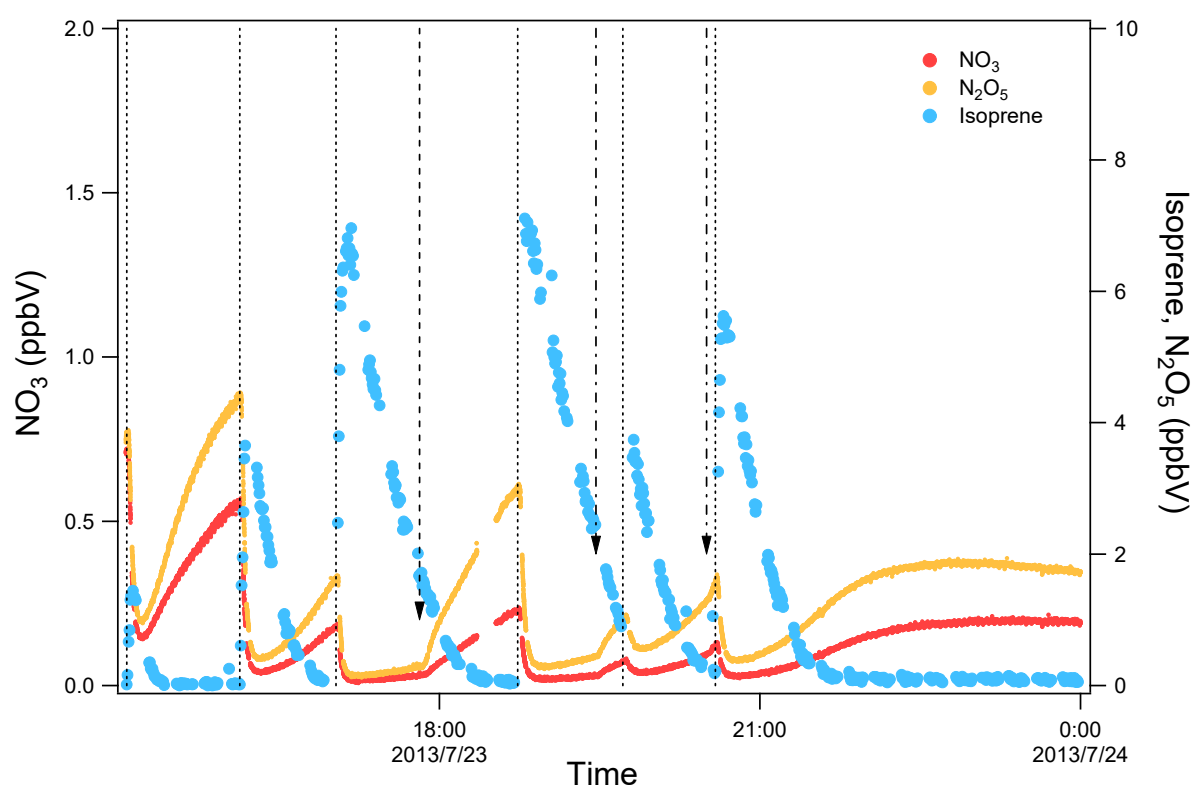
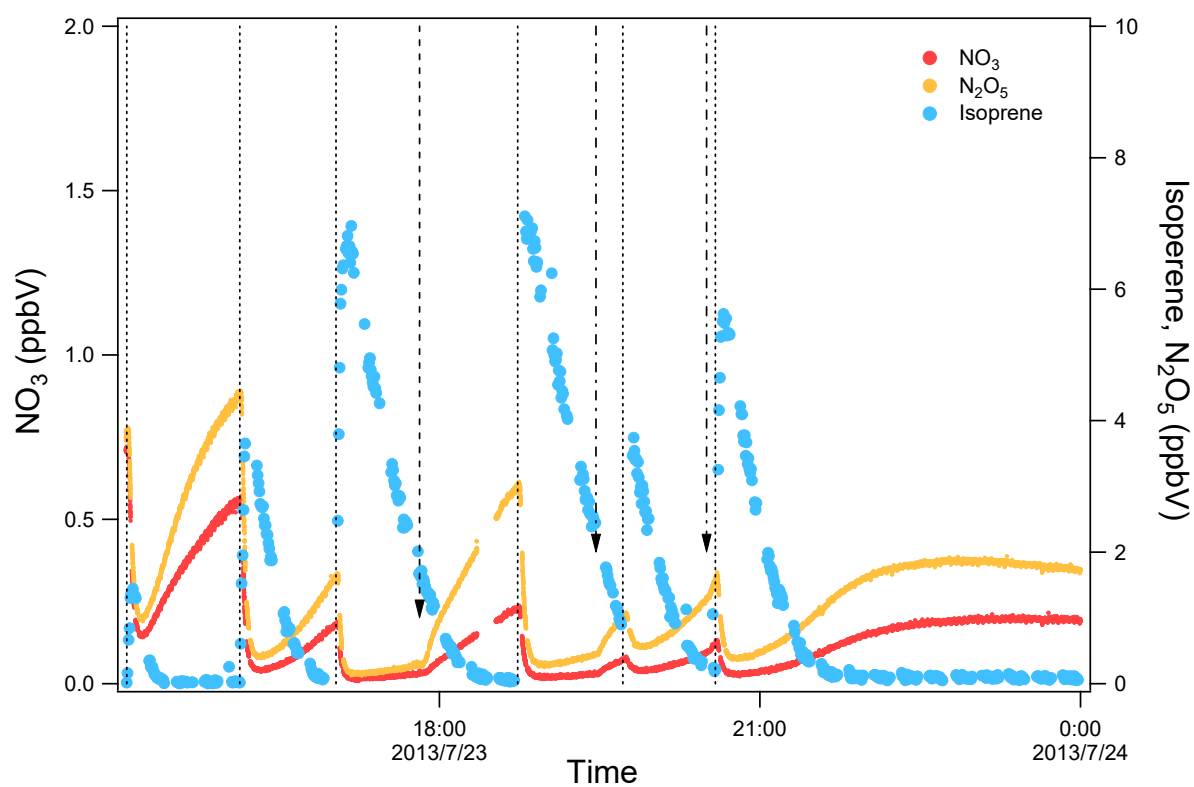


Figure S3S4. Time series of the of isoprene, NO_3 , and N_2O_5 concentration. The dashed lines indicate the time of isoprene additions. The long-dashed arrow indicates the time of NO_2 addition. The dash-dotted arrows indicate the time of O_3 additions.

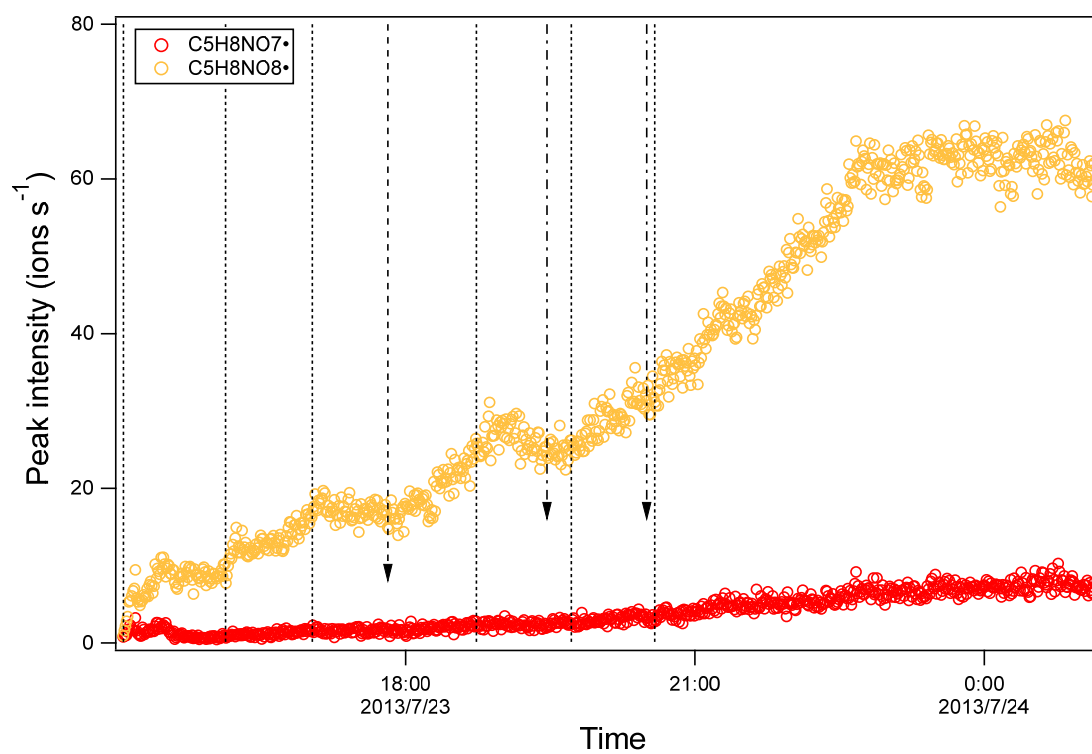


Figure S4S5. Time series of peak intensity of several HOM monomers of the $C_5H_8NO_n\bullet$ series. The dashed lines indicate the time of isoprene additions. The long-dashed arrow indicates the time of NO_2 addition. The dash-dotted arrows indicate the time of O_3 additions.

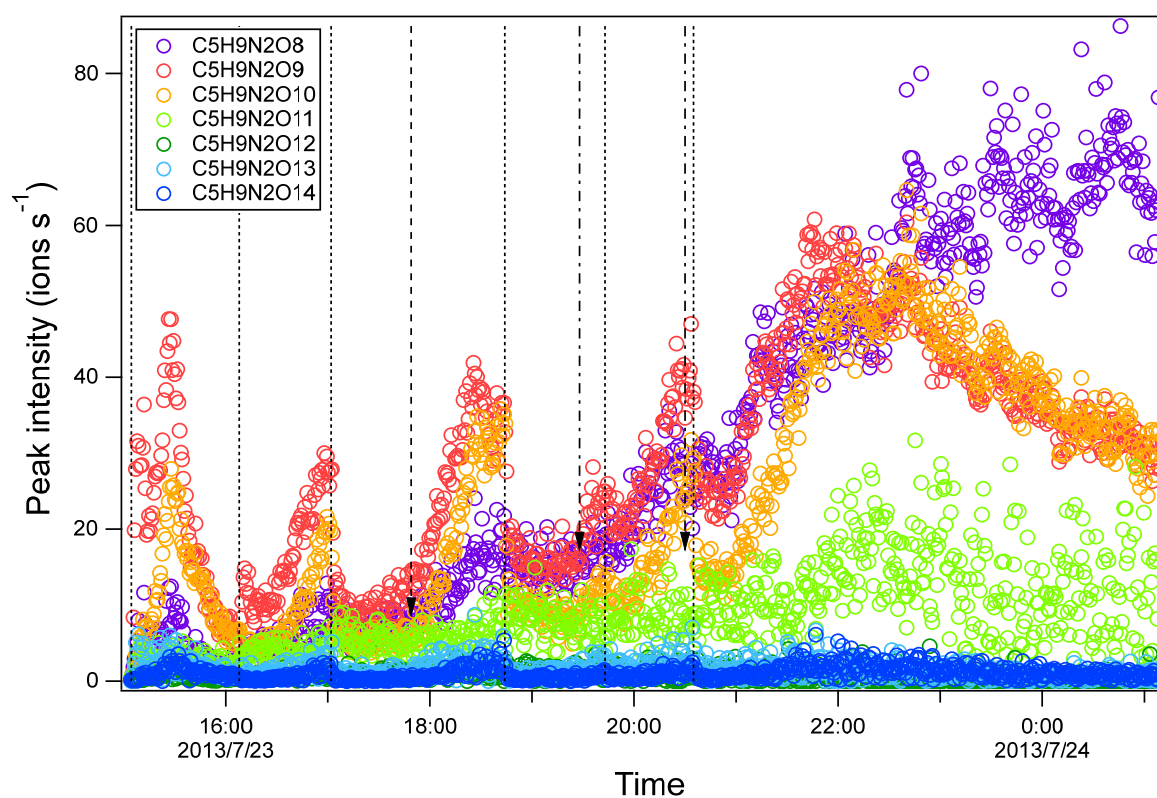
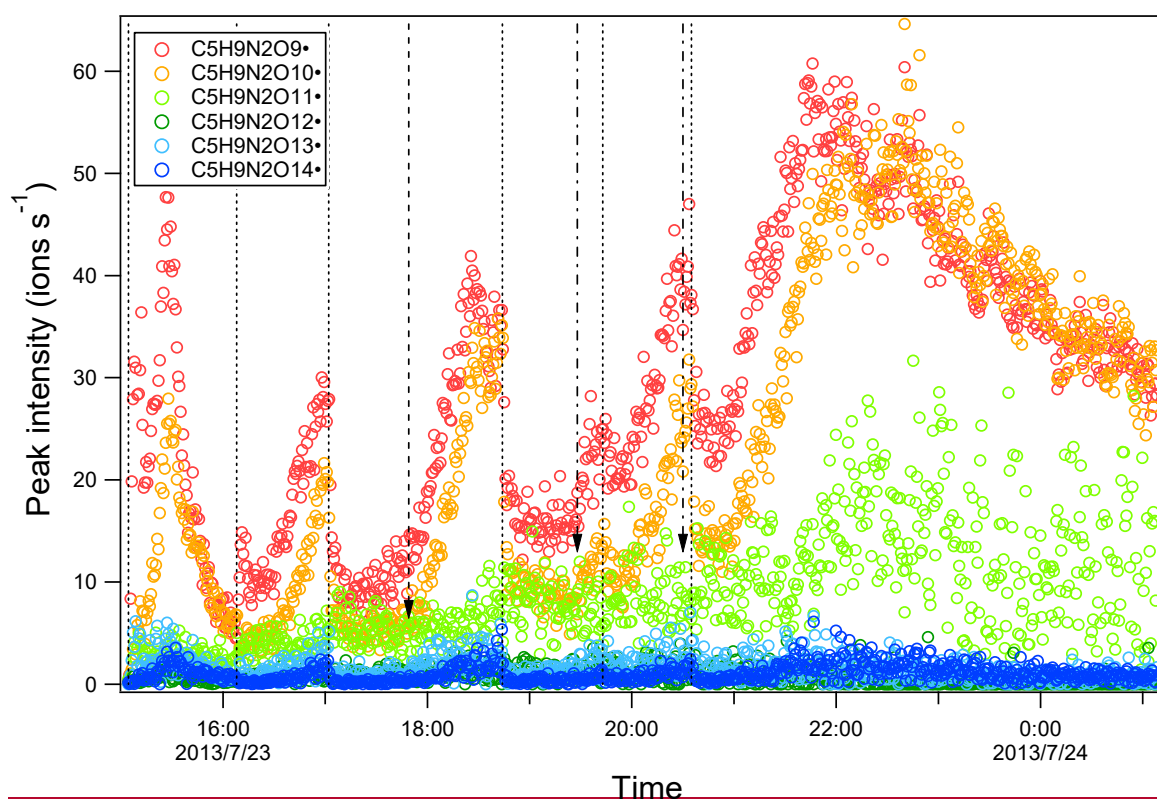


Figure S5S6. Time series of peak intensity of HOM monomers of the $C_5H_9N_2O_n\bullet$ series. The dashed lines indicate the time of isoprene additions. The long-dashed arrow indicates the time of NO_2 addition. The dash-dotted arrows indicate the time of O_3 additions.

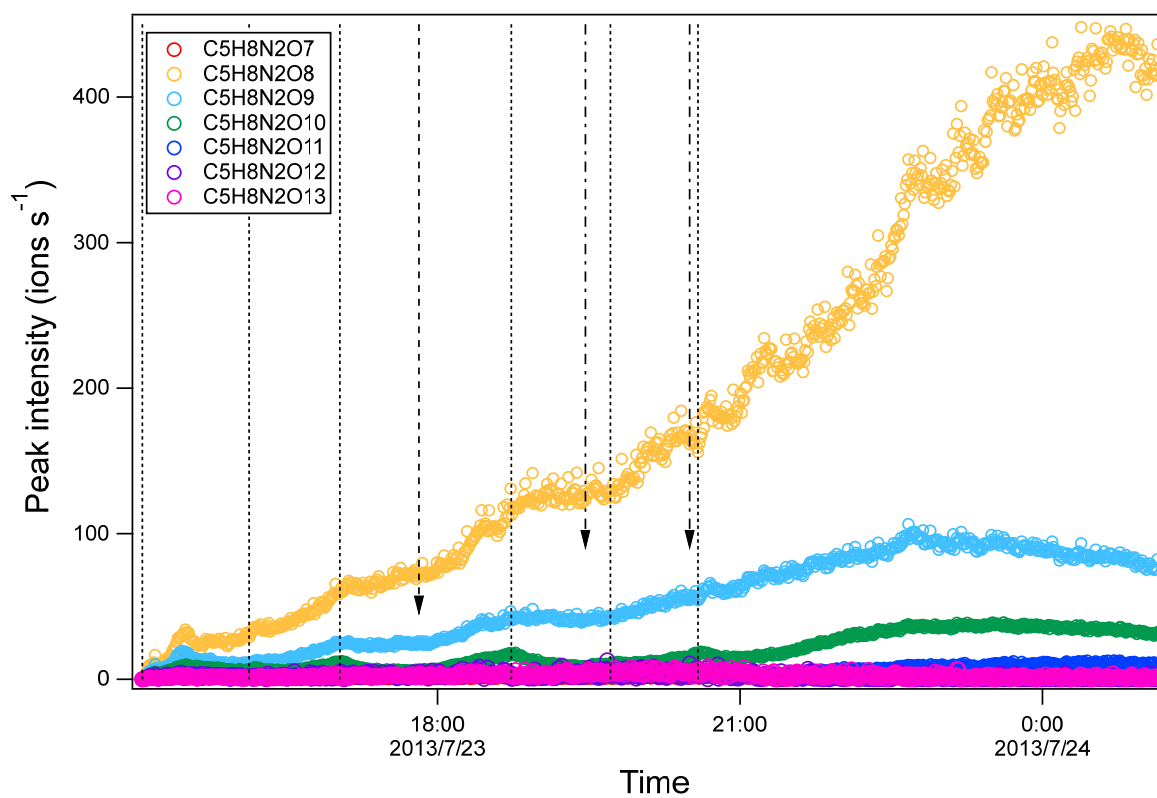


Figure S76. Time series of peak intensity of several HOM monomers of the $C_5H_8N_2O_n$ series (termination products of RO_2 $C_5H_9N_2O_n$). The dashed lines indicate the time of isoprene additions. The long-dashed arrow indicates the time of NO_2 addition. The dash-dotted arrows indicate the time of O_3 additions.

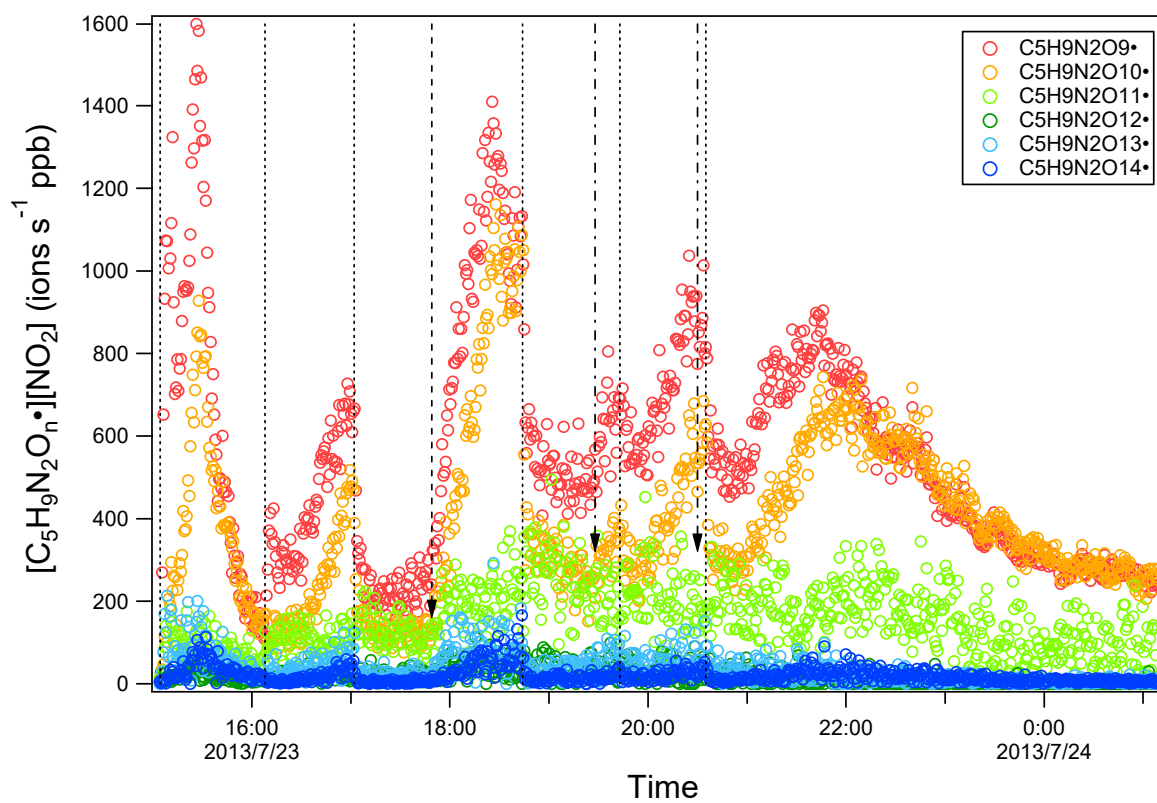
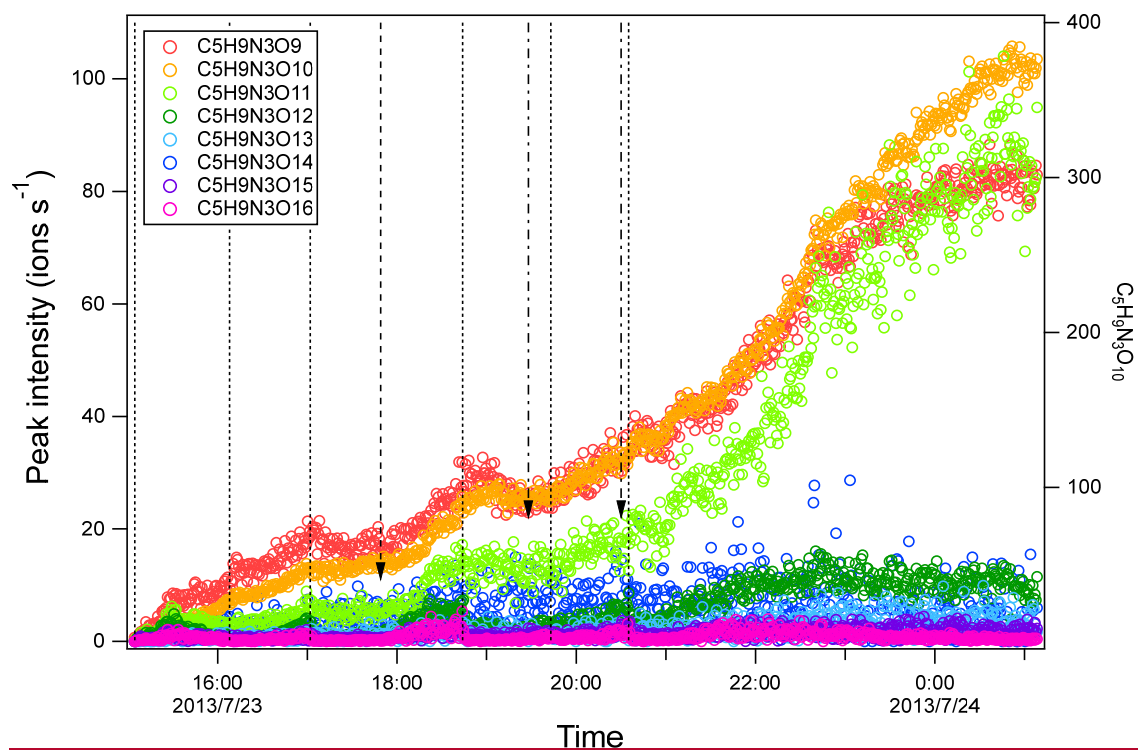


Figure S87. Time series of the product of the peak intensity of $C_5H_9N_2O_n\bullet$ and NO_2 concentration. The dashed lines indicate the time of isoprene additions. The long-dashed arrow indicates the time of NO_2 addition. The dash-dotted arrows indicate the time of O_3 additions.

|



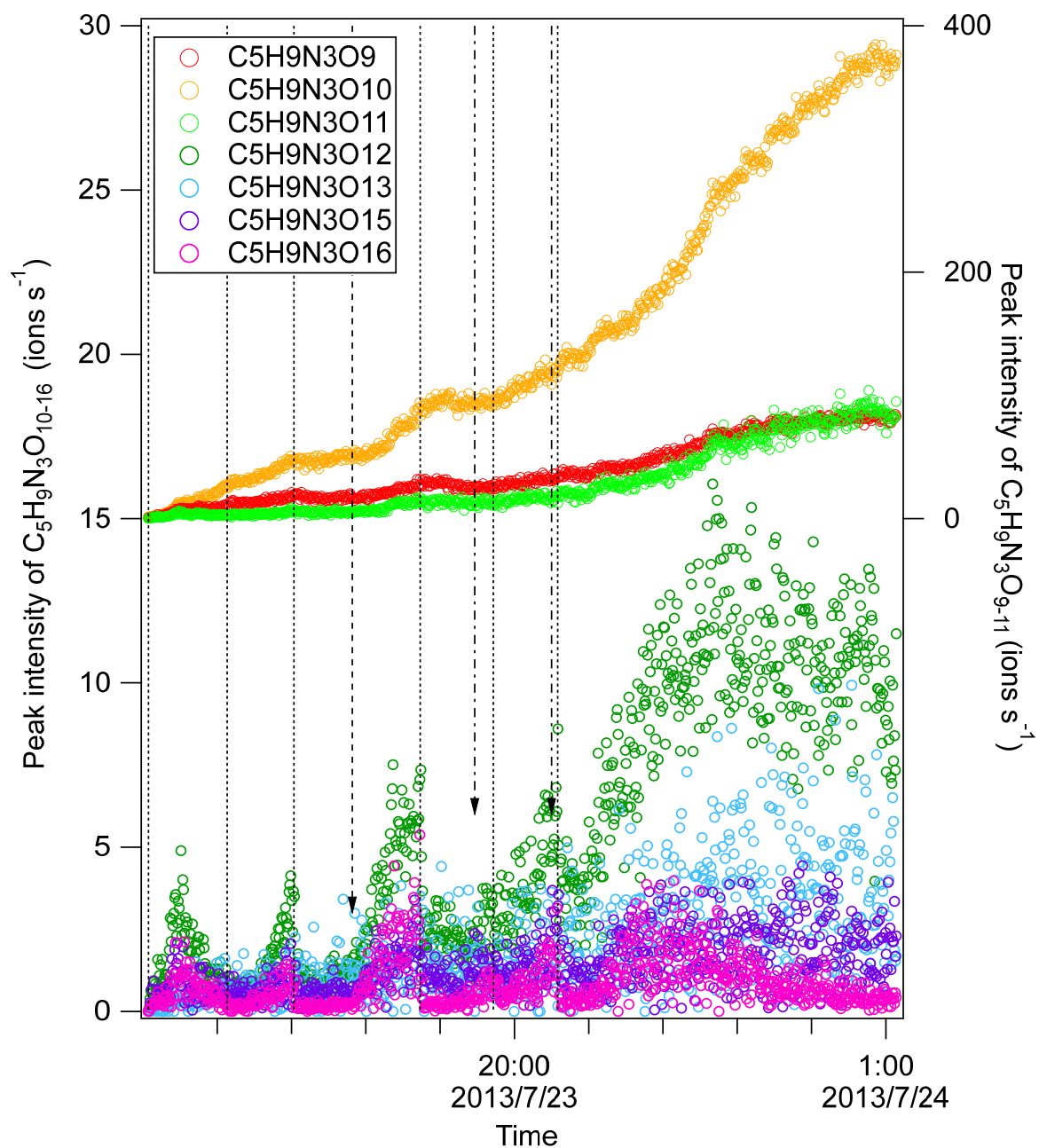
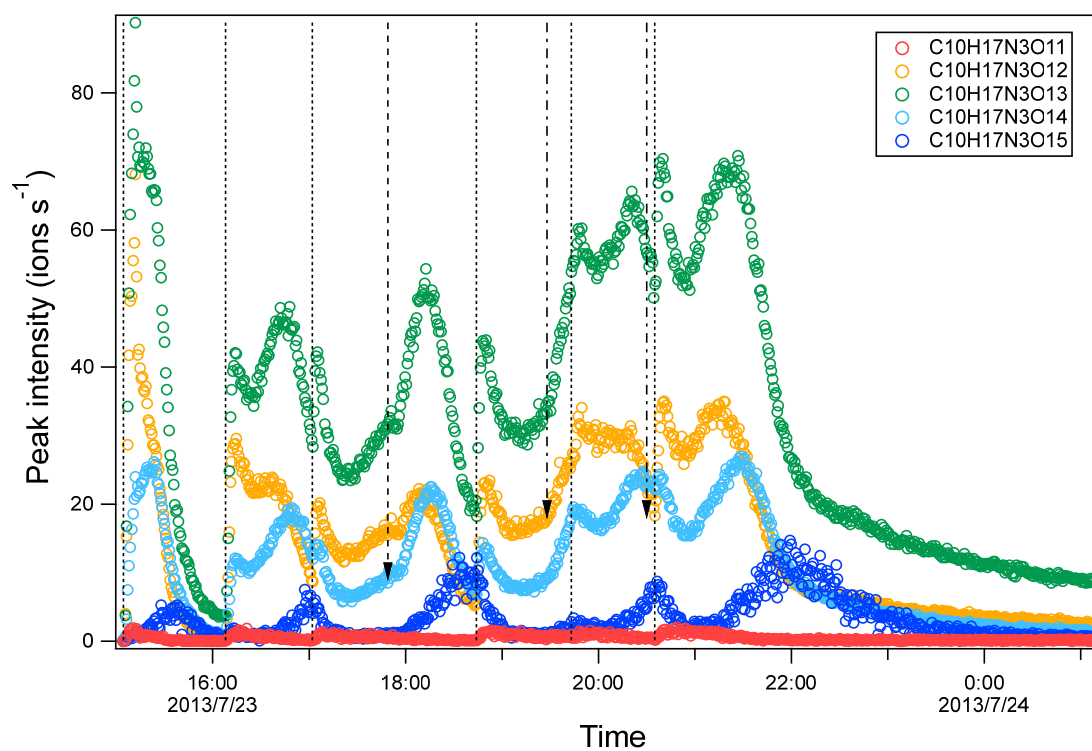
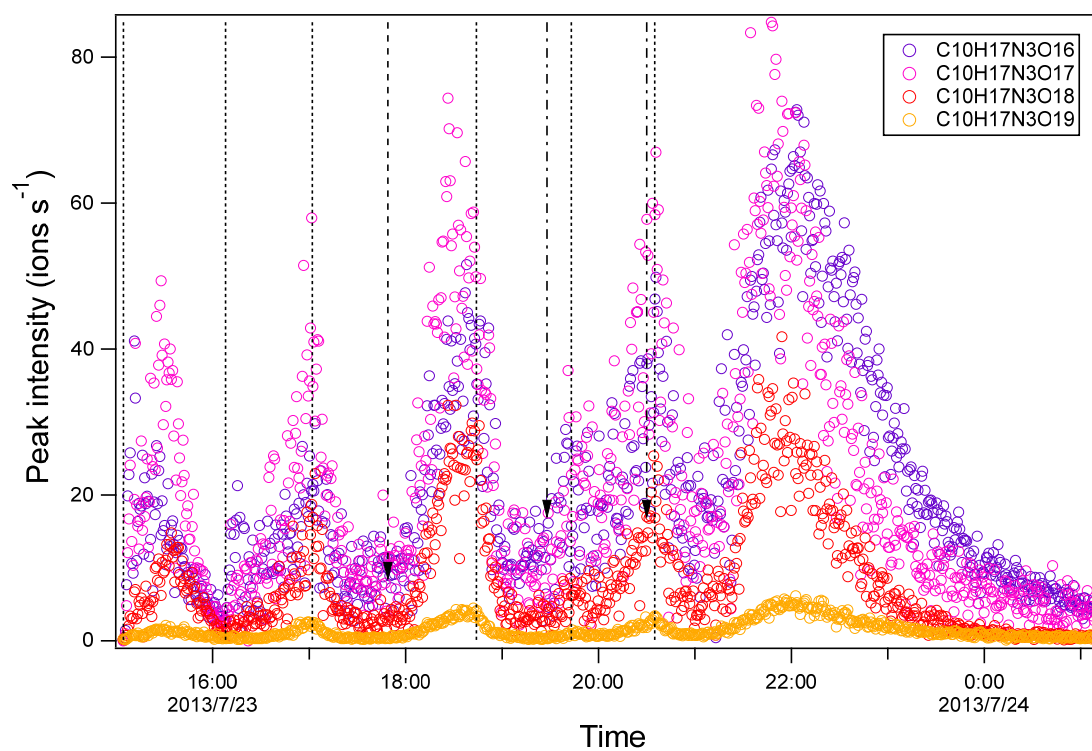


Figure S98. Time series of peak intensity of HOM monomers of the $C_5H_9N_3O_n$ series. The peak intensity of is shown on the left axis except for $C_5H_9N_3O_{10}$. The dashed lines indicate the time of isoprene additions. The long-dashed arrow indicates the time of NO_2 addition. The dash-dotted arrows indicate the time of O_3 additions.



(a)



(b)

Figure S9S10. Time series of peak intensity of several HOM dimers of the $C_{10}H_{17}N_3O_n$ series for $n=11-15$ (a) and $16-19$ (b). The dashed lines indicate the time of isoprene additions. The long-dashed arrow indicates the time of NO_2 addition. The dash-dotted arrows indicate the time of O_3 additions.

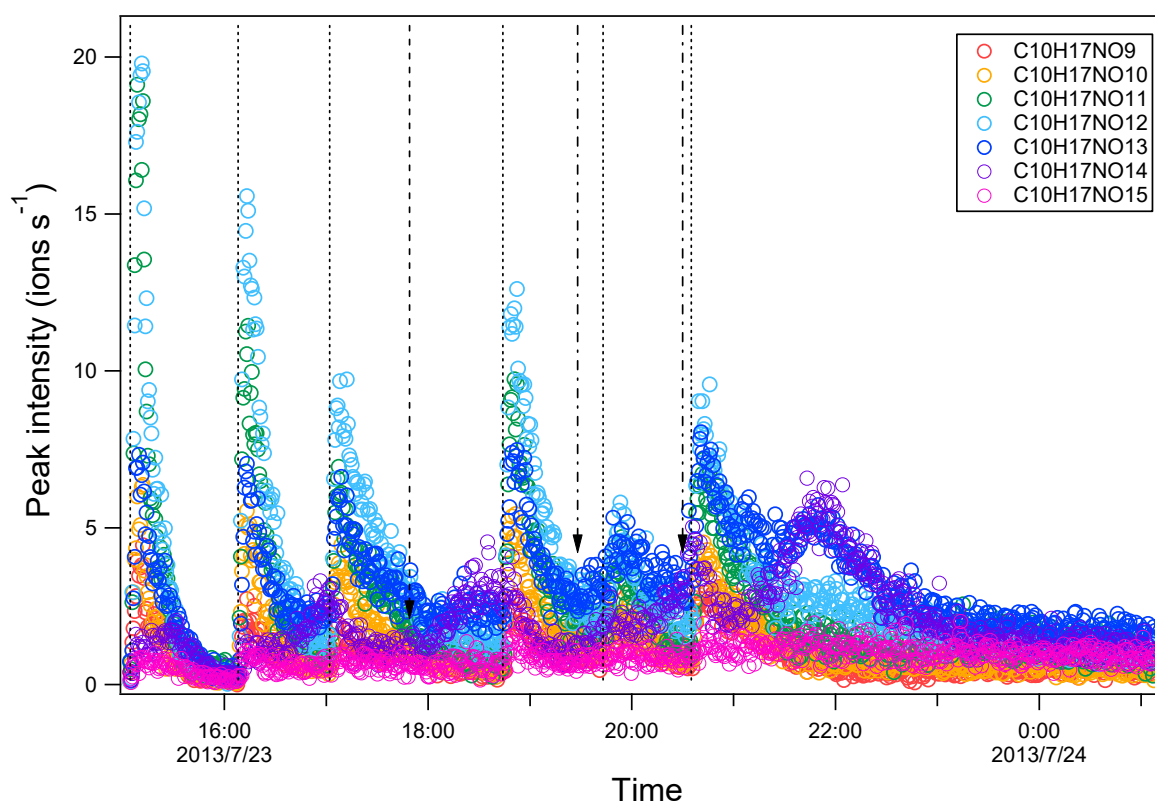


Figure S40S11. Time series of peak intensity of HOM monomers $C_{10}H_{17}NO_n$ series. The dashed lines indicate the time of isoprene additions. The long-dashed arrow indicates the time of NO_2 addition. The dash-dotted arrows indicate the time of O_3 additions.

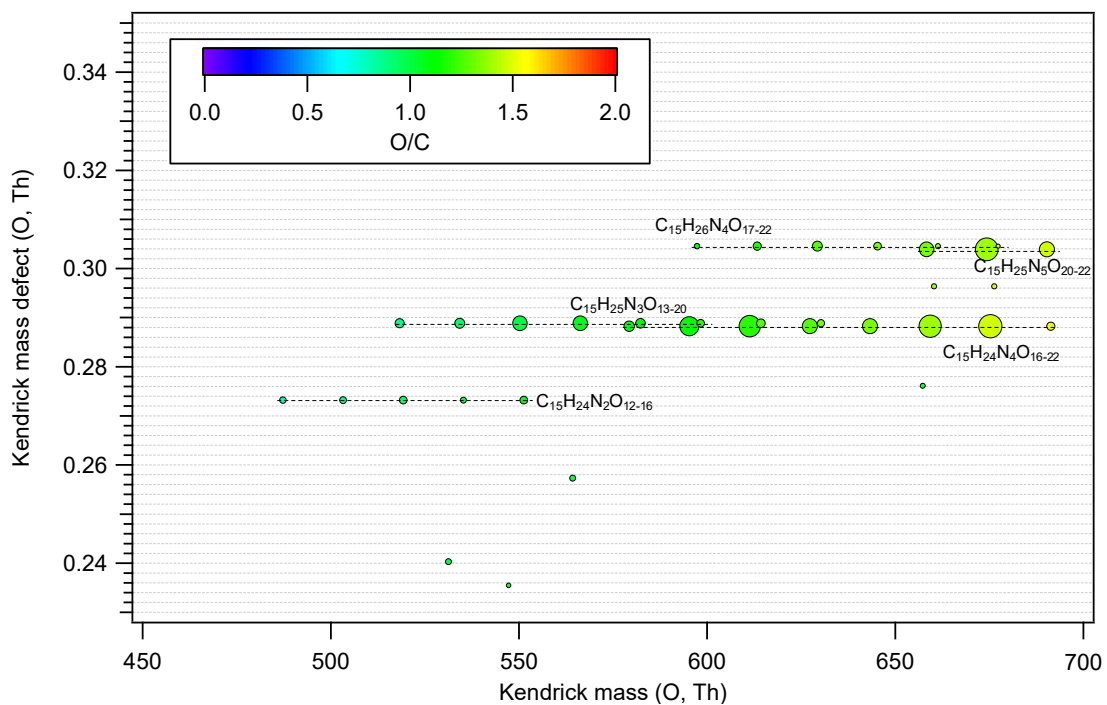


Figure S11+S12. Kendrick mass defect with Kendrick base O of HOM trimers formed in isoprene+NO₃. The area of the circles is set to be proportional to the average peak intensity of each molecular formula during the first isoprene addition period (P1).

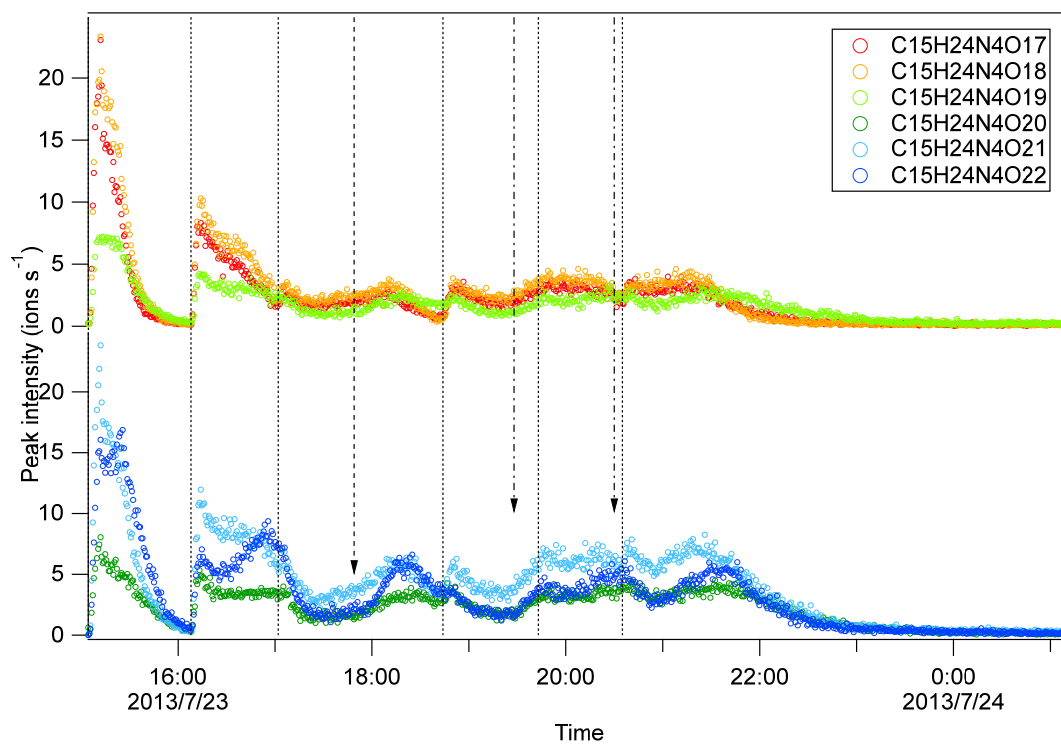
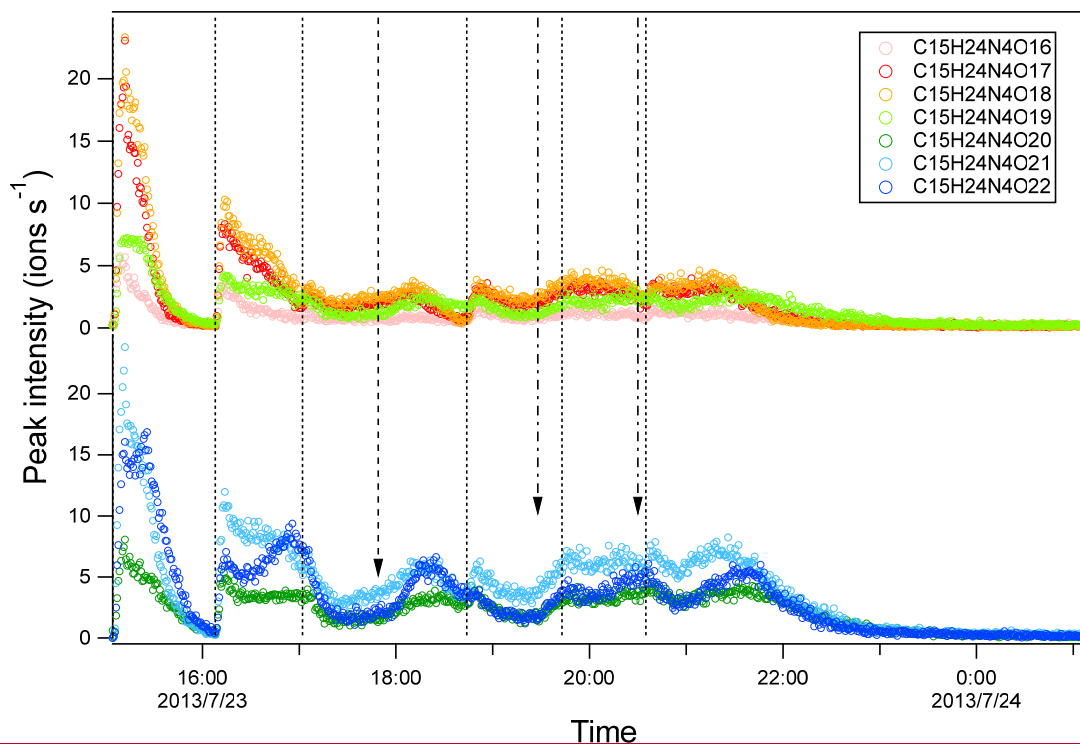


Figure S12S13. Time series of peak intensity of several HOM dimers of the $C_{15}H_{24}N_4O_n$ series. It is noted that the compounds are plotted in two panels for clarity. The dashed lines indicate the time of isoprene additions. The long-dashed arrow indicates the time of NO_2 addition. The dash-dotted arrows indicate the time of O_3 additions.

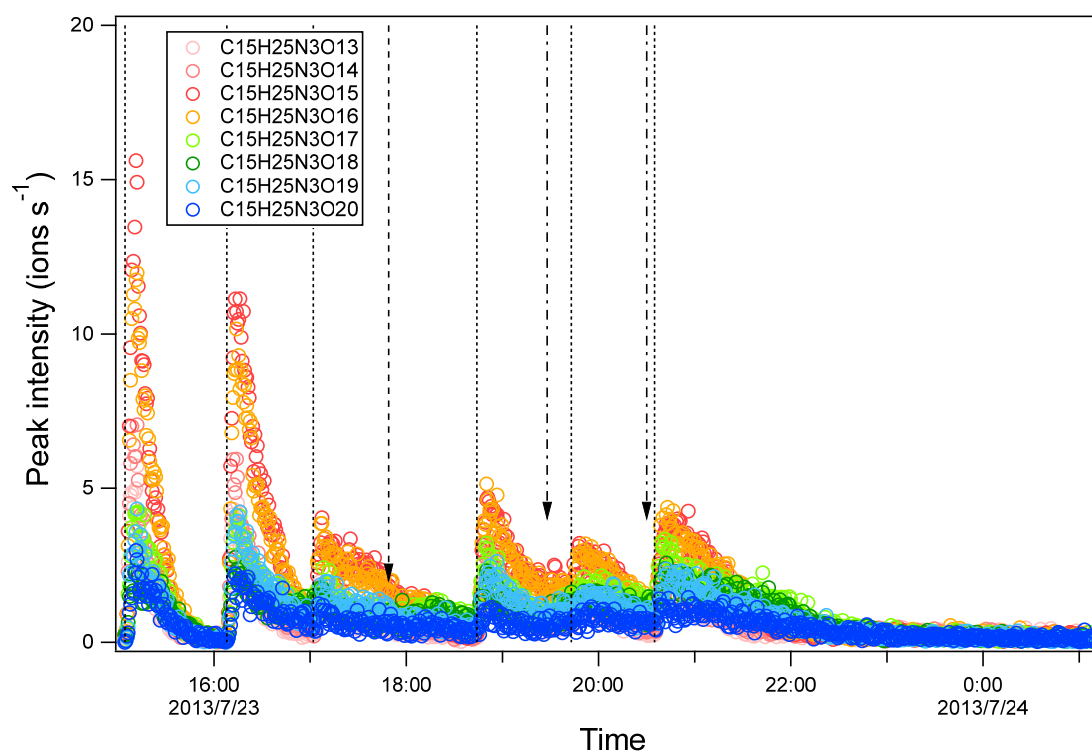
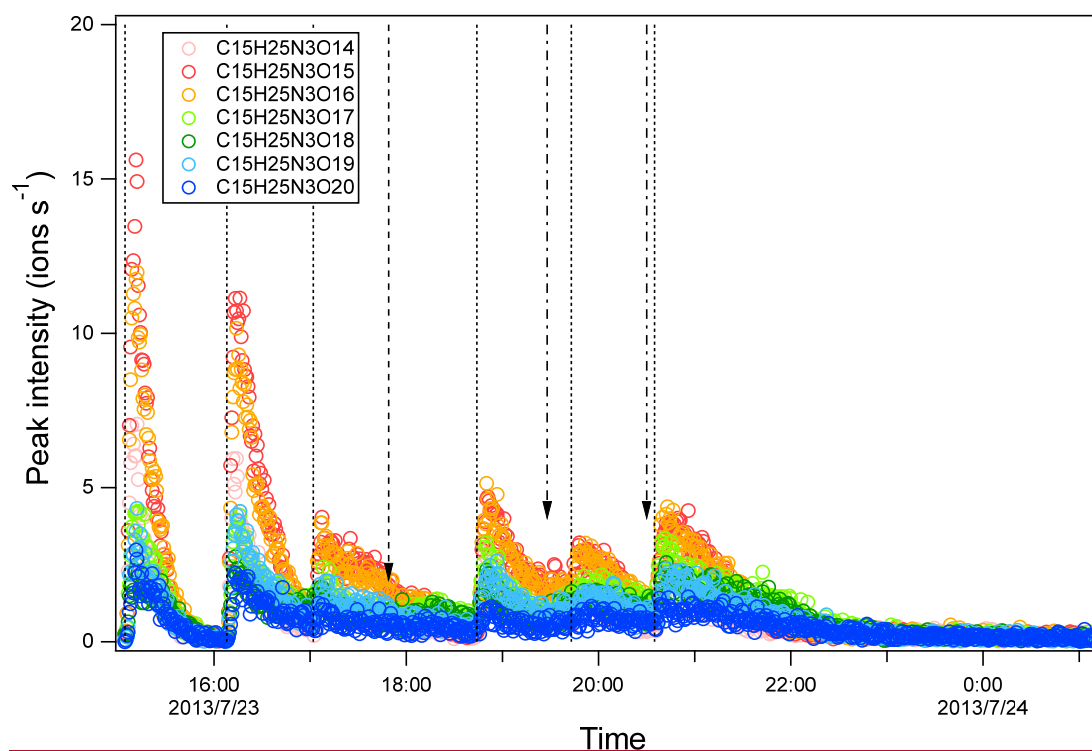


Figure S13S14. Time series of peak intensity of several HOM dimers of the $C_{15}H_{25}N_3O_n$ series. The dashed lines indicate the time of isoprene additions. The long-dashed arrow indicates the time of NO_2 addition. The dash-dotted arrows indicate the time of O_3 additions.

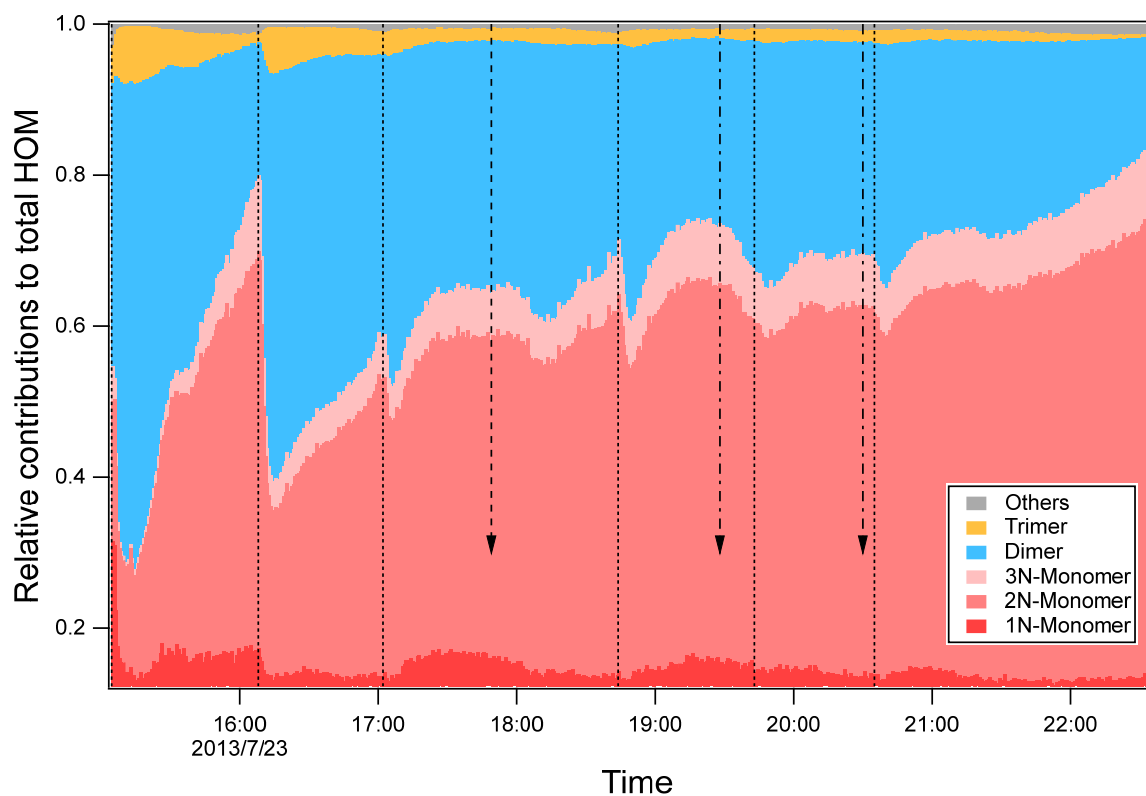


Figure S14S15. Relative contributions of HOM monomers, dimers, and trimers. Monomer 1-3N refers to the monomers containing 1-3 nitrogen atoms. The dashed lines indicate the time of isoprene additions. The long-dashed arrow indicates the time of NO_2 addition. The dash-dotted arrows indicate the time of O_3 additions.

Table S1. Intensity of HOM monomers C₅H₈NO_n and their corresponding termination products.

Series	Peroxy radical	Carbonyl	Hydroxyl ^c	Hydroperoxide ^c	Carbonyl /Hydroxyl
m/z	m	m-17	m-15	m+1	
M1a	C ₅ H ₈ NO ₇	C ₅ H ₇ NO ₆	C ₅ H ₉ NO ₆	C ₅ H ₉ NO ₇	
	257.016	240.013	242.028	258.023	
	1.5% ^a	4.5%	2.5%	13.9%	1.8
M1b	C ₅ H ₈ NO ₈	C ₅ H ₇ NO ₇	C ₅ H ₉ NO ₇	C ₅ H ₉ NO ₈	
	273.010	256.008	258.023	274.018	
	9.7%	8.1%	13.9%	24.9% ^c	0.6
M1a	C ₅ H ₈ NO ₉	C ₅ H ₇ NO ₈	C ₅ H ₉ NO ₈	C ₅ H ₉ NO ₉	
	289.0053	272.0026	274.0182	290.0131	
	11.9% ^b	34.0%	24.9%	28.5%	1.4
M1b	C ₅ H ₈ NO ₁₀	C ₅ H ₇ NO ₉	C ₅ H ₉ NO ₉	C ₅ H ₉ NO ₁₀	
	305.000	287.998	290.013	306.008	
	22.2% ^b	8.3%	28.5%	5.8%	0.3
M1a	C ₅ H ₈ NO ₁₁	C ₅ H ₇ NO ₁₀	C ₅ H ₉ NO ₁₀	C ₅ H ₉ NO ₁₁	
	320.995	303.992	306.008	322.003	
	2.3%	3.0%	5.8%	2.0%	0.5
M1b	C₅H₈NO₁₂	C₅H₇NO₁₁	C ₅ H ₉ NO ₁₁	C₅H₉NO₁₂	
	336.990	319.987	322.003	337.998	
	1.7%	3.0%	2.0%	2.0%	1.5

^a: The intensities are average intensity of each peak in MS during the first cycle (C1) normalized to the peak with the maximum intensity (C₁₀H₁₇N₃O₁₃).

^b: These intensities may be subject to higher uncertainties due to the overlap with C₅H₁₀N₂O₈ and C₅H₁₀N₂O₉.

^c: The relative contribution of HOM with hydroxyl or hydroperoxide cannot be differentiated and thus the total intensity is listed here.

Table S2. Intensity of HOM monomers $C_5H_9N_2O_n$ and their corresponding termination products.

Series	Peroxy radical	Carbonyl	Hydroxyl	Hydroperoxide	Carbonyl /Hydroxyl
m/z	m	m-17	m-15	m+1	
M2b	$C_5H_9N_2O_8$	$C_5H_8N_2O_7$	$C_5H_{10}N_2O_7$	$C_5H_{10}N_2O_8$	
	288.021	271.019	273.034	289.029	
	5.6% ^a	1.3%	0.8%	99.1%	1.6
M2a	$C_5H_9N_2O_9$	$C_5H_8N_2O_8$	$C_5H_{10}N_2O_8$	$C_5H_{10}N_2O_9$	
	304.0162	287.0135	289.0291	305.024	
	24.9%	57.9%	99.1%	82.3%	0.6
M2b	$C_5H_9N_2O_{10}$	$C_5H_8N_2O_9$	$C_5H_{10}N_2O_9$	$C_5H_{10}N_2O_{10}$	
	320.011	303.008	305.024	321.019	
	14.4%	29.7%	82.3%	9.3%	0.4
M2a	$C_5H_9N_2O_{11}$	$C_5H_8N_2O_{10}$	$C_5H_{10}N_2O_{10}$	$C_5H_{10}N_2O_{11}$	
	336.006	319.003	321.019	337.014	
	3.3%	18.3%	9.3%	0.4%	2.0
M2b	$C_5H_9N_2O_{12}$	$C_5H_8N_2O_{11}$	$C_5H_{10}N_2O_{11}$	$C_5H_{10}N_2O_{12}$	
	352.001	334.998	337.014	353.009	
	0.7%	2.5%	0.4%	4.3%	7.1

^a: The intensities are the average intensities of each peak in MS during the first cycle (C1) normalized to the peak with the maximum intensity ($C_{10}H_{17}N_3O_{13}$).

^b: The relative contribution of HOM with hydroxyl or hydroperoxide cannot be differentiated and thus the total intensity is listed here.

Table S3. Summary of the 50 major HOM productpeaks in the reaction of isoprene with NO₃

Molecular Formula	m/Q	HOM series[#]
C5H7NO5	224.017	Monomer-1
C5H7NO6	240.012	Monomer-1
C5H8NO10	241.020	Monomer-1
C5H9NO6	242.028	Monomer-1
C5H7NO7	256.007	Monomer-1
C5H8NO6	257.015	Monomer-1
C5H9NO7	258.023	Monomer-1
C5H11NO7	260.038	Monomer-4
C5H7NO8	272.002	Monomer-1
C5H8NO11	273.010	Monomer-1
C5H9NO8	274.018	Monomer-1
C5H10NO8	275.025	Monomer-4
C5H11NO8	276.033	Monomer-4
C5H8N2O8	287.013	Monomer-2
C5H7NO9	287.997	Monomer-1
C5H8NO7	289.005	Monomer-1
C5H10N2O8	289.029	Monomer-2
C5H9NO9	290.013	Monomer-1
C5H10NO9	291.020	Monomer-4
C5H11NO9	292.028	Monomer-4
C5H9N3O10	302.024	Monomer-2
C5H8N2O9	303.008	Monomer-2
C5H7NO10	303.992	Monomer-1
C5H9N2O9	304.016	Monomer-2
C5H8NO12	305.000	Monomer-1
C5H10N2O9	305.023	Monomer-2
C5H9NO10	306.007	Monomer-1
C5H11NO10	308.023	Monomer-4
C5H9N3O11	318.019	Monomer-2
C5H9N3O9	318.019	Monomer-2
C5H8N2O10	319.003	Monomer-2
C5H7NO11	319.987	Monomer-1
C5H9N2O10	320.011	Monomer-2
C5H8NO8	320.995	Monomer-1
C5H10N2O10	321.018	Monomer-2
C5H9NO11	322.002	Monomer-1
C5H11NO11	324.018	Monomer-4
C5H9N3O12	334.014	Monomer-2
C5H8N2O11	334.998	Monomer-2
C5H7NO12	335.982	Monomer-1
C5H9N2O11	336.005	Monomer-2
C5H10N2O11	337.013	Monomer-2
C5H9NO12	337.997	Monomer-1
C5H9N3O13	350.009	Monomer-2
C5H9N2O12	352.000	Monomer-2

C5H8NO9	352.984	Monomer-1
C5H10N2O12	353.008	Monomer-2
C5H9N3O14	366.003	Monomer-2
C5H9N2O13	367.995	Monomer-2
C5H10N2O13	369.003	Monomer-2
C5H9N3O15	381.998	Monomer-2
C5H9N2O14	383.990	Monomer-2
C10H16N2O10	387.065	Dimer-1
C10H18N2O10	389.081	Dimer-4
C10H16N2O11	403.060	Dimer-1
C10H17N2O11	404.069	Dimer-R2
C10H18N2O11	405.076	Dimer-4
C10H17N3O11	418.071	Dimer-2
C10H16N2O12	419.055	Dimer-1
C10H17N2O12	420.064	Dimer-R2
C10H18N2O12	421.071	Dimer-4
C10H16N3O12	433.059	Dimer-R1
C10H17N3O12	434.066	Dimer-2
C10H16N2O13	435.050	Dimer-1
C10H18N2O13	437.066	Dimer-4
C10H15N3O13	448.045	Dimer-5
C10H16N3O13	449.054	Dimer-R1
C10H17N3O13	450.061	Dimer-2
C10H16N2O14	451.045	Dimer-1
C10H18N2O14	453.061	Dimer-4
C10H15N3O14	464.040	Dimer-5
C10H16N3O14	465.049	Dimer-R1
C10H17N3O14	466.056	Dimer-2
C10H16N2O15	467.040	Dimer-1
C10H18N2O15	469.056	Dimer-4
C10H15N3O15	480.035	Dimer-5
C10H16N3O15	481.044	Dimer-R1
C10H17N3O15	482.051	Dimer-2
C10H16N2O16	483.035	Dimer-1
C10H18N2O16	485.050	Dimer-4
C10H15N3O16	496.030	Dimer-5
C10H16N3O16	497.038	Dimer-R1
C10H18N4O15	497.062	Dimer-3
C10H17N3O16	498.046	Dimer-2
C10H16N2O17	499.030	Dimer-1
C15H25N3O12	502.129	Trimer-3
C10H15N3O17	512.025	Dimer-5
C10H17N4O16	512.049	Dimer-R3
C10H18N4O16	513.057	Dimer-3
C10H17N3O17	514.041	Dimer-2
C15H25N3O13	518.124	Trimer-3
C10H17N4O17	528.044	Dimer-R3
C10H18N4O17	529.052	Dimer-3

C10H17N3O18	530.036	Dimer 2
C15H25N3O14	534.119	Trimer 3
C10H17N4O18	544.039	Dimer R3
C10H18N4O18	545.046	Dimer 3
C10H17N3O19	546.031	Dimer 2
C15H25N3O15	550.114	Trimer 3
C15H25N3O16	566.109	Trimer 3
C15H25N3O17	582.104	Trimer 3
C15H24N4O17	595.099	Trimer 1
C15H26N4O17	597.115	Trimer 4
C15H25N3O18	598.099	Trimer 3
C15H24N4O18	611.094	Trimer 1
C15H26N4O18	613.110	Trimer 4
C15H25N3O19	614.094	Trimer 3
C15H24N4O19	627.089	Trimer 1
C15H26N4O19	629.105	Trimer 4
C15H25N3O20	630.089	Trimer 3
C15H24N4O20	643.084	Trimer 1
C15H26N4O20	645.099	Trimer 4
C15H25N5O20	658.095	Trimer 2
C15H24N4O21	659.079	Trimer 1
C15H26N4O21	661.094	Trimer 4
C15H25N5O21	674.090	Trimer 2
C15H24N4O22	675.074	Trimer 1
C15H25N5O22	690.085	Trimer 2

<u>Detected mass</u> <u>(m/Q)</u>	<u>HOM mass (Da)</u>	<u>HOM</u> <u>Formula</u>
<u>256.008</u>	<u>193.022</u>	<u>C5H7NO7</u>
<u>258.023</u>	<u>195.038</u>	<u>C5H9NO7</u>
<u>272.003</u>	<u>209.017</u>	<u>C5H7NO8</u>
<u>273.010</u>	<u>210.025</u>	<u>C5H8NO8</u>
<u>274.018</u>	<u>211.033</u>	<u>C5H9NO8</u>
<u>287.013</u>	<u>224.028</u>	<u>C5H8N2O8</u>
<u>287.997</u>	<u>225.012</u>	<u>C5H7NO9</u>
<u>289.005</u>	<u>226.020</u>	<u>C5H8NO9</u>
<u>289.029</u>	<u>226.044</u>	<u>C5H10N2O8</u>
<u>290.013</u>	<u>227.028</u>	<u>C5H9NO9</u>
<u>303.008</u>	<u>240.023</u>	<u>C5H8N2O9</u>
<u>304.016</u>	<u>241.031</u>	<u>C5H9N2O9</u>
<u>305.000</u>	<u>242.015</u>	<u>C5H8NO10</u>
<u>305.024</u>	<u>242.039</u>	<u>C5H10N2O9</u>
<u>306.008</u>	<u>243.023</u>	<u>C5H9NO10</u>
<u>318.019</u>	<u>255.034</u>	<u>C5H9N3O9</u>
<u>319.003</u>	<u>256.018</u>	<u>C5H8N2O10</u>
<u>320.011</u>	<u>257.026</u>	<u>C5H9N2O10</u>
<u>321.019</u>	<u>258.034</u>	<u>C5H10N2O10</u>
<u>334.014</u>	<u>271.029</u>	<u>C5H9N3O10</u>
<u>351.006</u>	<u>224.028</u>	<u>C5H8N2O8</u>

<u>353.022</u>	<u>226.044</u>	<u>C5H10N2O8</u>
<u>367.001</u>	<u>240.023</u>	<u>C5H8N2O9</u>
<u>368.009</u>	<u>241.031</u>	<u>C5H9N2O9</u>
<u>369.017</u>	<u>242.039</u>	<u>C5H10N2O9</u>
<u>372.055</u>	<u>309.070</u>	<u>C10H15NO10</u>
<u>403.061</u>	<u>340.075</u>	<u>C10H16N2O11</u>
<u>405.076</u>	<u>342.091</u>	<u>C10H18N2O11</u>
<u>419.056</u>	<u>356.070</u>	<u>C10H16N2O12</u>
<u>434.067</u>	<u>371.081</u>	<u>C10H17N3O12</u>
<u>434.067</u>	<u>371.081</u>	<u>C10H17N3O12</u>
<u>435.051</u>	<u>372.065</u>	<u>C10H16N2O13</u>
<u>450.062</u>	<u>387.076</u>	<u>C10H17N3O13</u>
<u>451.046</u>	<u>388.060</u>	<u>C10H16N2O14</u>
<u>464.041</u>	<u>401.055</u>	<u>C10H15N3O14</u>
<u>466.056</u>	<u>403.071</u>	<u>C10H17N3O14</u>
<u>467.040</u>	<u>404.055</u>	<u>C10H16N2O15</u>
<u>482.051</u>	<u>419.066</u>	<u>C10H17N3O15</u>
<u>498.046</u>	<u>435.061</u>	<u>C10H17N3O16</u>
<u>498.059</u>	<u>371.081</u>	<u>C10H17N3O12</u>
<u>499.030</u>	<u>436.045</u>	<u>C10H16N2O17</u>
<u>513.057</u>	<u>450.072</u>	<u>C10H18N4O16</u>
<u>514.041</u>	<u>451.056</u>	<u>C10H17N3O17</u>
<u>514.054</u>	<u>387.076</u>	<u>C10H13N3O13</u>
<u>529.052</u>	<u>466.067</u>	<u>C10H18N4O17</u>
<u>530.036</u>	<u>467.051</u>	<u>C10H17N3O18</u>
<u>611.094</u>	<u>548.109</u>	<u>C15H24N4O18</u>
<u>659.079</u>	<u>596.093</u>	<u>C15H24N4O21</u>
<u>674.090</u>	<u>611.104</u>	<u>C15H25N5O21</u>
<u>675.074</u>	<u>612.088</u>	<u>C15H24N4O22</u>

^a: ~~The numbering of HOM series is referred to the main text.~~